**JOINT TRANSPORTATION RESEARCH PROGRAM**

INDIANA DEPARTMENT OF TRANSPORTATION
AND PURDUE UNIVERSITY

# Truck Traffic and Load Spectra of Indiana Roadways for the Mechanistic-Empirical Pavement Design Guide


Jieyi Bao, Xiaoqiang Hu, Cheng Peng, Yi Jiang,
Shuo Li, Tommy Nantung

SPR-4231 • Report Number: FHWA/IN/JTRP-2020/21 • DOI: 10.5703/1288284317227

## RECOMMENDED CITATION

Bao, J., Hu, X., Peng, C., Jiang, Y., Li, S., & Nantung, T. (2020). *Truck traffic and load spectra of Indiana roadways for the mechanistic-empirical pavement design guide* (Joint Transportation Research Program Publication No. FHWA/IN/JTRP-2020/21). West Lafayette, IN: Purdue University. https://doi.org/10.5703/1288284317227

## AUTHORS

**Jieyi Bao**
**Xiaoqiang Hu**
**Cheng Peng**
Graduate Research Asssistants
School of Construction Management Technology
Purdue University

**Yi Jiang, PhD, PE**
Professor and Chair of Graduate Program
School of Construction Management Technology
(765) 494-5602
jiang2@purdue.edu
*Corresponding Author*

**Tommy Nantung, PhD, PE**
Section Manager
Division of Research and Development
Indiana Department of Transportation

**Shuo Li, PhD, PE**
Research Engineer
Division of Research and Development
Indiana Department of Transportation

## AKNOWLEDGMENT

This research project was sponsored by the Indiana Department of Transportation (INDOT) in cooperation with the Federal Highway Administration (FHWA) through the Joint Transportation Research Program (JTRP). The authors would like to thank the study advisory committee members, Kumar Dave, Greg Katter, and Nick Cosenza of INDOT, and Tom Duncan of FHWA Indiana Division, for their valuable assistance, data collection, and technical guidance. Special appreciations are extended to Mr. Greg Katter of INDOT for his help and support for providing the traffic data from INDOT's weigh-in-motion (WIM) and automatic traffic recorder (ATR) stations, and to Mr. Wayne Bunnell of INDOT for his effort to obtain the traffic video files and to match video records with the WIM data. The authors recognize the assistance provided by Dr. Karen Zhu of INDOT for traffic data and GIS maps. The authors appreciate Mr. Tim Wells of INDOT for his help in transferring the video files to us. The authors especially want to thank Mr. Tom Duncan of FHWA Indiana Division for his careful review and helpful edit of this report.

## JOINT TRANSPORTATION RESEARCH PROGRAM

The Joint Transportation Research Program serves as a vehicle for INDOT collaboration with higher education institutions and industry in Indiana to facilitate innovation that results in continuous improvement in the planning, design, construction, operation, management and economic efficiency of the Indiana transportation infrastructure. https://engineering.purdue.edu/JTRP/index_html

Published reports of the Joint Transportation Research Program are available at http://docs.lib.purdue.edu/jtrp/.

## NOTICE

# TECHNICAL REPORT DOCUMENTATION PAGE

<table>
<tr><td>1. Report No.<br>FHWA/IN/JTRP-2020/21</td><td>2. Government Accession No.</td><td>3. Recipient's Catalog No.</td></tr>
<tr><td colspan="2" rowspan="2">4. Title and Subtitle<br>Truck Traffic and Load Spectra of Indiana Roadways for the Mechanistic-Empirical Pavement Design Guide</td><td>5. Report Date<br>September 2020</td></tr>
<tr><td>6. Performing Organization Code</td></tr>
<tr><td colspan="2">7. Author(s)<br>Jieyi Bao, Xiaoqiang Hu, Cheng Peng, Yi Jiang, Shuo Li, and Tommy Nantung</td><td>8. Performing Organization Report No.<br>FHWA/IN/JTRP-2020/21</td></tr>
<tr><td colspan="2" rowspan="2">9. Performing Organization Name and Address<br>Joint Transportation Research Program (SPR)<br>Hall for Discovery and Learning Research (DLR), Suite 204<br>207 S. Martin Jischke Drive<br>West Lafayette, IN 47907</td><td>10. Work Unit No.</td></tr>
<tr><td>11. Contract or Grant No.<br>SPR-4231</td></tr>
<tr><td colspan="2" rowspan="2">12. Sponsoring Agency Name and Address<br>Indiana Department of Transportation<br>State Office Building<br>100 North Senate Avenue<br>Indianapolis, IN 46204</td><td>13. Type of Report and Period Covered<br>Final Report</td></tr>
<tr><td>14. Sponsoring Agency Code</td></tr>
<tr><td colspan="3">15. Supplementary Notes<br>Conducted in cooperation with the U.S. Department of Transportation, Federal Highway Administration.</td></tr>
<tr><td colspan="3">16. Abstract<br>The Mechanistic-Empirical Pavement Design Guide (MEPDG) has been employed for pavement design by the Indiana Department of Transportation (INDOT) since 2009 and has generated efficient pavement designs with a lower cost. It has been demonstrated that the success of MEPDG implementation depends largely on a high level of accuracy associated with the information supplied as design inputs. Vehicular traffic loading is one of the key factors that may cause not only pavement structural failures, such as fatigue cracking and rutting, but also functional surface distresses, including friction and smoothness. In particular, truck load spectra play a critical role in all aspects of the pavement structure design. Inaccurate traffic information will yield an incorrect estimate of pavement thickness, which can either make the pavement fail prematurely in the case of under-designed thickness or increase construction cost in the case of over-designed thickness. The primary objective of this study was to update the traffic design input module, and thus to improve the current INDOT pavement design procedures. Efforts were made to reclassify truck traffic categories to accurately account for the specific axle load spectra on two-lane roads with low truck traffic and interstate routes with very high truck traffic. The traffic input module was updated with the most recent data to better reflect the axle load spectra for pavement design. Vehicle platoons were analyzed to better understand the truck traffic characteristics. The unclassified vehicles by traffic recording devices were examined and analyzed to identify possible causes of the inaccurate data collection. Bus traffic in the Indiana urban areas was investigated to provide additional information for highway engineers with respect to city streets as well as highway sections passing through urban areas. New equivalent single axle load (ESAL) values were determined based on the updated traffic data. In addition, a truck traffic data repository and visualization model and a TABLEAU interactive visualization dashboard model were developed for easy access, view, storage, and analysis of MEPDG related traffic data.</td></tr>
<tr><td colspan="2">17. Key Words<br>truck traffic, axle load spectra, pavement design, MEPDG, vehicle platoon, ESAL, visualization, weigh-in-motion, vehicle classification, automatic traffic recorder, AADTT, AADT, truck volume distribution</td><td>18. Distribution Statement<br>No restrictions. This document is available through the National Technical Information Service, Springfield, VA 22161.</td></tr>
<tr><td>19. Security Classif. (of this report)<br>Unclassified</td><td>20. Security Classif. (of this page)<br>Unclassified</td><td>21. No. of Pages<br>94 including appendices<br><br>22. Price</td></tr>
</table>

Form DOT F 1700.7 (8-72) Reproduction of completed page authorized

# EXECUTIVE SUMMARY

## Introduction

*The Mechanistic-Empirical Pavement Design Guide* (MEPDG) has been employed for pavement design by the Indiana Department of Transportation (INDOT) since 2009 and has generated efficient, lower cost pavement designs. The MEPDG is capable of analyzing the impacts of varying traffic loads on a pavement structure and providing a more realistic design for the pavement structure of interest. However, it has been demonstrated that the success of MEPDG implementation depends largely on a high level of accuracy associated with the information supplied as design inputs. Truck traffic volume distribution and axle load spectra play a critical role in all respects of the pavement structure design. Inaccurate traffic information will yield an incorrect estimate of pavement thickness, which can either make the pavement fail prematurely, in the case of under-designed thickness, or increase construction cost, in the case of over-designed thickness. The traffic input module in the current INDOT MEPDG pavement design procedures was developed with traffic data collected through weigh-in-motion stations between 2000 to 2004. Over the past 10 years, the Indiana highway network has changed significantly through new construction, roadway expansion projects, data collection improvement, and safety enhancement. Consequently, these changes have impacted the statewide traffic in every respects, such as traffic volume, speed, class distribution, truck percentage, lane distribution, and growth rate. However, the current traffic design input module does not reflect the impact of these improvements and changes. The primary objective of this study was to update the traffic design input module, therefore improving the current INDOT pavement design procedures.

## Results and Findings

### *Truck Traffic Distributions and Axle Load Spectra*

The traffic data recorded at 143 ATR and WIM stations over the past 3 years and annual traffic data maintained by INDOT were utilized in the analysis. The current truck traffic and the truck traffic in 2008 were compared, and it was found that traffic volumes and truck traffic volumes had mostly increased, considerably, on the Indiana highway network. Truck traffic data in terms of Average Annual Daily Truck Traffic (AADTT) and axle load spectra were compiled and stored for MEPDG pavement design. Bus traffic data on traffic volumes and axle load distributions were obtained through WIM and public transportation information. The equivalent single axle load (ESAL) values were calculated based on the updated truck volumes and truck axle load data at WIM sites. Analysis was performed to evaluate the shifts in truck traffic and axle load spectra for low and high truck volume roadways, and more reasonable subcategories were determined. All results and findings were combined to update the traffic variables in the current traffic design input module, including average annual daily truck traffic; truck volume monthly adjustment factors; truck volume lane distribution factors; truck volume directional distribution factors; truck volume class distributions; traffic volume hourly distribution factors; distributions of single-, tandem-, tridem-, and quad-axle loads; average axle weight; average axle spacing; and average number of axle types.

### *Vehicle/Truck Platoon Analysis*

Analysis was performed to better understand the traffic characteristics when vehicles travel in groups with relatively short headways between vehicles. The critical intervals were established to define vehicle platoons. Various types of platoons and their features were analyzed in terms of platoon lengths, leading vehicle types, and composition of vehicles.

### *Unclassified Vehicles*

Analysis of unclassified vehicles was performed with the ATR/WIM recorded data. A neural network model was established to determine the appropriate allocations of unclassified vehicles to truck classes. Since the number of unclassified vehicles is often fairly high at some ATR or WIM stations, the allocations will help to improve the accuracy of truck traffic data and thus improve pavement design. Video records of traffic on an interstate section and traffic data from a nearby WIM station were utilized to identify some causes for vehicle misclassifications.

### *Traffic Database Repository and Visualization*

A truck traffic data repository and visualization model and a Tableau interactive visualization dashboard model were developed for easy access, view, storage, and analysis of the updated MEPDG related traffic data.

## Implementation

The following recommendations are provided for future implementation of the research results:

- The updated truck traffic information should be used to replace the information produced from the last study for MEPDG pavement design. The information includes average annual daily truck traffic; truck volume monthly adjustment factors; truck volume lane distribution factors; truck volume directional distribution factors; truck volume class distributions; traffic volume hourly distribution factors; distributions of for single-, tandem-, tridem-, and quad-axle loads; average axle weight; average axle spacing; and average number of axle types.
- The subcategories for low truck volume roads (Group A) and high truck volume roads (Group D) should be utilized for pavement design to reflect more realistic traffic situations.
- Unclassified vehicles should not be discarded or arbitrarily assigned to truck classes. The developed allocation proportions should be applied to appropriately allocate unclassified vehicles to vehicle classes for pavement design.
- The updated ESAL values should be adopted for INDOT applications in areas such as pavement asset management and construction cost estimate.
- The truck traffic data repository and visualization model and a Tableau interactive visualization dashboard model can be used for easy access and analysis and for a visualized view of the MEPDG related traffic data.

CONTENTS

# LIST OF TABLES

# LIST OF FIGURES

# 1. INTRODUCTION AND LITERATURE REVIEW

## 1.1 Background

*The Mechanistic-Empirical Pavement Design Guide* (MEPDG) has been employed for pavement design by the Indiana Department of Transportation (INDOT) since 2009 and has generated efficient pavement designs with a lower cost (Nantung, 2010). The MEPDG is capable of analyzing the impacts of varying traffic loads on a pavement structure and providing a more realistic design for the pavement structure of interest. However, it has been demonstrated that the success of MEPDG implementation depends largely on a high level of accuracy associated with the information supplied as design inputs (Jiang, Nantung, Mangold, et al., 2008; Li et al., 2005). Vehicular traffic loading is one of the key factors that may cause not only pavement structural failures such as fatigue cracking and rutting, but also functional surface distresses, including friction and smoothness. In particular, truck load spectra play a critical role in all aspects of the pavement structure design. Inaccurate traffic information will yield an incorrect estimate of pavement thickness, which can either make the pavement fail prematurely in the case of under-designed thickness or increase construction cost in the case of over-designed thickness.

The traffic input module in the current INDOT MEPDG pavement design procedures was developed from traffic data collected solely at 47 weigh-in-motion (WIM) stations over a time period of 2000 to 2004 (Jiang, Nantung, & Chen, 2008). Several major issues have been raised about the traffic input module by INDOT pavement engineers over the past years. First, the current truck traffic volume categories (A, B, C, D) could not characterize the real truck traffic on INDOT roadways accurately in many cases. Second, the MEPDG requires FHWA Class 4 (bus) and above for the analysis of the impact of truck traffic. However, there is a serious lack of information on bus traffic in the current traffic design input module, particularly in urban areas. This is because INDOT WIM stations were mostly installed on roads in rural areas. Consequently, the current traffic design input module cannot accurately reflect the characteristics of bus traffic in urban areas, particularly on downtown streets.

Over the past 10 years, great efforts such as I-69 expansion project, Hoosier Heartland project, and "Major Moves" projects have been made to significantly improve and expand Indiana's highway infrastructure. In 2006, the oversight responsibility of Indiana Toll Road (ITR) was turned over to the ITR Concession Company LLC (ITRCC). There is no doubt that all of the above efforts can have diverse impacts on regional traffic, such as traffic volume, speed, class distribution, truck percentage, lane distribution, and growth rate. However, the current traffic design input module does not reflect the impact of these improvements and changes. In addition, traffic data collected by permanently installed automatic traffic recorder (ATR) systems is also readily available across the entire state. It was necessary to assess and utilize the ATR traffic data to improve the traffic input module for two-lane roads carrying low truck traffic volume and urban streets. Evidently, there was an urgent need to review the traffic data in the recent years and to update the traffic characteristics for the purpose of accuracy in designing pavement using the MEPDG.

The primary objective of this study was to update the traffic design input module, and thus to improve the current INDOT pavement design procedures. Efforts were made to reclassify truck traffic categories to accurately account for the specific axle load spectra on two-lane roads and interstate routes with very high truck traffic volume. The traffic input module was updated with the most recent data to better reflect the axle load spectra for pavement design. Vehicle platoons were analyzed to better understand the truck traffic characteristics. The unclassified vehicles by WIM/ATR devices were examined and analyzed to identify possible causes of the inaccuracy of data collection. Bus traffic in the Indiana urban areas was investigated to provide additional information for highway engineers with respect to city streets as well as highway sections passing through urban areas. New equivalent single axle load (ESAL) values were determined based on the updated traffic data. In addition, a truck traffic data repository and visualization model and a Tableau interactive visualization dashboard model were developed for easy access, view, storage, and analysis of MEPDG related traffic data.

## 1.2 Literature Review

Since the MEPDG was developed and utilized by highway agencies, much research has been conducted in many aspects related to the pavement design method. Weigh-in-Motion (WIM) systems, are widely applied on US highways to record real-time traffic data, including time, lane, vehicle class, speed and axle features (Jiang, Nantung, & Chen, 2008). Classification results of vehicle types from the WIM sensors are determined from screening vehicles in traffic streams and recording traffic patterns (Nichols & Bullock, 2004). However, the WIM devices have failed to produce completely accurate vehicle classification data due to various causes including system malfunction, traffic conjunction, and adverse weather conditions. Error reduction of vehicle classification record in WIM traffic data will affect prediction of pavement longitudinal cracking in pavement design. The bias of predicted cracking based on inaccurate vehicle class distribution lead to overestimation or underestimation of pavement thickness (Tarefder & Rodriguez-Ruiz, 2013).

The Federal Highway Administration (FHWA) schema on highway vehicle classification is based on the number of vehicle axles and vehicle units (FHWA, 2016). Computer vision techniques have been employed to process images and videos for visual detection and inspection on civil infrastructure systems (Spencer et al., 2019). Convolution neural networks (CNNs) have been rapidly growth and wildly applied on automation on data recognition (Ng et al., 2015). Li et al. (2014) analyzed and compared four clustering approaches to generate traffic load inputs. A Wisconsin study (Titi et al., 2018) used the MEPDG to evaluate pavement damage and deterioration caused by overload heavy truck traffic. Papagiannakis et al. (2006) used clustering techniques to establish similarities in vehicle classification and axle load distributions between traffic data collection sites. Cluster analysis methodologies were also utilized by Wang et al. (2011) to identify truck loading groups in order to ease the preparation of the traffic load spectra inputs for the MEPDG procedure.

Ziedan et al. (2017) compared the design output using site-specific traffic input data to the design output using national default values. It was found in the study that the national input values overestimated the pavement distresses. Yang et al. (2017) explored the correlations between distress predictions and various potential temperature indices and verified the effects of temperature indices on pavement designs. Various types of theories and methodologies were applied in the MEPDG related research, including the finite element analysis (Gungor, et al., 2017), statistical analysis (TaghaviGhalesari & Chang-Albitres, 2019; Yang & Wu, 2012), and support vector regression (SVR) method (Castro-Neto et al., 2009).

Generally, traffic vehicle platoon can be defined as a group of vehicles that drive closely with one another and virtually linked as a whole, either voluntarily or involuntarily (Bhoopalam et al., 2018; Karim et al., 2014). The reason of the formation and separation of platoons varies and can be influenced by different factors and targets of research, such as the benefits on traffic congestion, fuel/time save, and driving safety (Zhao et al., 2018). Many studies have been focused on modeling vehicle platoons, especially truck only platoons. In order to group vehicles into platoons, time headway is the most wildly used threshold factors (Karim et al., 2014). The autonomous truck platoon behaviors were analyzed in highway exits by Mesa-Arango and Fabregas (2017). Jiang et al. (2006) developed an algorithm of traffic signal timing in terms of real time platoon detections.

### 1.3 Main Tasks

The following tasks were accomplished in this study:

1. Review of the existing INDOT's traffic classification practices. This included a review of the existing ATR/WIM databases maintained by INDOT, previous studies related to the accuracy and reliability of INDOT's ATR/WIM data, INDOT annual traffic volume reports by ATR and WIM system, and Indiana Average Annual Daily Traffic (AADT) data and related GIS maps.
2. Extracting traffic information from the binary ATR/WIM data files and transferring the data into a format for data analysis and validation. A computer program was developed to extract the necessary information from the huge amount of ASCII raw ATR/WIM data for the purpose of data validation and MEPDG requirements.
3. Analysis of INDOT's ATR/WIM traffic data. ATR/WIM and AADT data maintained by INDOT were compiled, examined, and analyzed. The data collected over the most recent 3 years were utilized in the analysis.
4. Determination of possible subcategories for low and high truck traffic volume roads. An in-depth analysis was performed on ATR/WIM data and more reasonable subcategories were determined. Analysis was performed to evaluate the shifts in truck traffic and axle load spectra for low and high truck volume roadways.
5. Examination of truck traffic and load conditions. The truck traffic data in terms of Average Annual Daily Truck Traffic (AADTT) and axle load spectra were compiled and illustrated.
6. Creation of bus traffic data. Bus traffic data with respect of traffic volumes and axle load distributions were obtained through WIM and public transportation information.
7. Vehicle/Truck platoon analysis: Analysis was performed to define the characteristics of vehicle/truck platoons on Indiana roadways.
8. Analysis of unclassified vehicles in ATR/WIM recorded data. A neural network model was established to determine the appropriate allocations of unclassified vehicles to truck classes. Since the number of unclassified vehicles is often fairly high at some ATR or WIM stations, the allocations will help to improve the accuracy of truck traffic data and thus improve pavement design.
9. Update on traffic design input module. All results and findings were included and combined to update the traffic variables in the current traffic design input module, including average annual daily truck traffic, truck volume monthly adjustment factors, truck volume lane distribution factors, truck volume directional distribution factors, truck volume class distributions, traffic volume hourly distribution factors, distributions of for single-, tandem-, tridem-, and quad-axle loads, average axle weight, average axle spacing, and average number of axle types.
10. Determination of ESAL categories. The updated truck axle load data at WIM sites were utilized to calculate ESALs at all WIM stations.
11. Traffic database with the most recent WIM/AVC data. A truck traffic data repository and visualization model and a Tableau interactive visualization dashboard model were developed for easy access, view, storage, and analysis of MEPDG related traffic data.

## 2. DATABASE AND TRAFFIC VOLUME DISTRIBUTION

### 2.1 WIM and ATR Database

Two types of automatic traffic data recording devices, weigh-in-motion (WIM) and automatic traffic recorder (ATR), have been employed on Indiana roadways. In 2018, there were 95 ATR stations and 63 WIM stations in Indiana. Figure 2.1 illustrates the distribution of the 158 ATR and WIM stations in Indiana in 2018, where ATR stations are denoted by blue triangles and WIM stations are denoted by red squares.

The ATR and WIM data from 2016 to 2018 was retrieved for data analysis in this study. ATR and WIM devices are designed to record traffic data continuously.

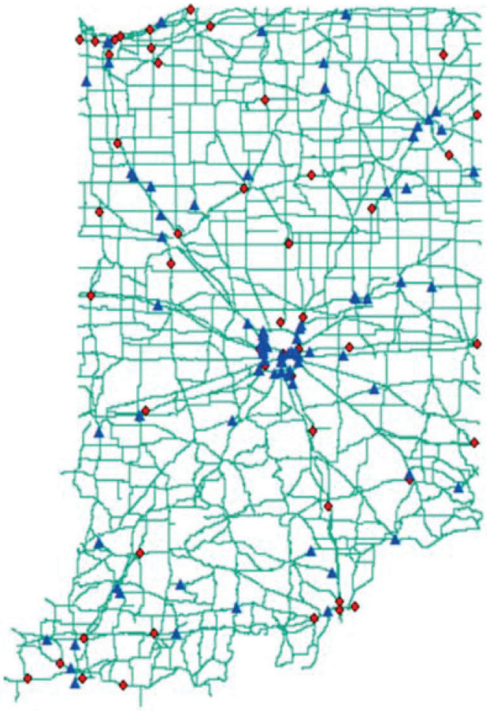

**Figure 2.1** Distribution of ATR/WIM stations in Indiana.

Ideally, an ATR and WIM station would provide complete traffic data of every vehicle passing the station at any time. However, it was found during the data retrieving that the traffic data in many stations were not complete due to either device problems or road constructions. In some stations, the ATR or WIM devices failed to record traffic data for a long period of time, even as long as a few months. Tables 2.1 and 2.2 display the number of sites with complete and incomplete data and sites without data during the 3 years for ATR and WIM respectively. Figure 2.2 shows the percent of the ATR and WIM stations with complete traffic data within the 3 years. Therefore, only minority of the ATR and WIM stations recorded complete data within the 3-year period.

## 2.2 Statewide Traffic Volume Distributions

The first step of data processing was to download traffic data of the 3 years—2016, 2017, and 2018—from the ATR and WIM systems. The ATR and WIM data were stored in binary format. In order to read the traffic data from the binary files, iAnalyze software was utilized to decode and to convert the binary data into the American Standard Code for Information Interchange (ASCII) data. The generated output through iAnalyze is in the form of Comma-Separated Values (CSV) files, which includes traffic information on vehicle passing time, speed, axle weight, axle spacing, and air temperature. A computer program in Python was developed and utilized to extract the necessary information for analyzing traffic data with respect to volume distribution, axle load spectra, and vehicle classifications. The retrieved traffic data were stored in Excel format.

Vehicles are classified as 13 classes by the Federal Highway Administration (FHWA), as shown in Figure 2.3. In the 13 classes of vehicles, traffic volumes of Classes 4 through 13 vehicles, including buses and various types of trucks, are denoted as truck traffic volumes. Truck traffic volumes are the primary input for pavement design since the vehicles in the group exert a significant impact on pavement structure and are the main forces causing pavement structure damages and distresses.

In addition to ATR and WIM database, a base map of Indiana traffic volumes is available. The base map is updated annually based on INDOT's statewide traffic data collection mechanism. It contains traffic volumes on the roadway network in Indiana in terms of AADT and AADTT. The base map traffic data can be processed

TABLE 2.1
**Status of ATR sites**

| Data Availability | Number of Sites |
|---|---|
| Sites with complete 3 years of data (2016, 2017, 2018) | 21 |
| Sites with incomplete data (2016, 2017, 2018) | 71 |
| Sites without data (2016, 2017, 2018) | 3 |
| *Total* | *95* |

TABLE 2.2
**Status of WIM sites**

| Data Availability | Number of Sites |
|---|---|
| Sites with complete 3 years of data (2016, 2017, 2018) | 8 |
| Sites with incomplete data (2016, 2017, 2018) | 43 |
| Sites without data (2016, 2017, 2018) | 6 |
| Sites with ZIP/CSV format data (unreadable) | 6 |
| *Total* | *63* |

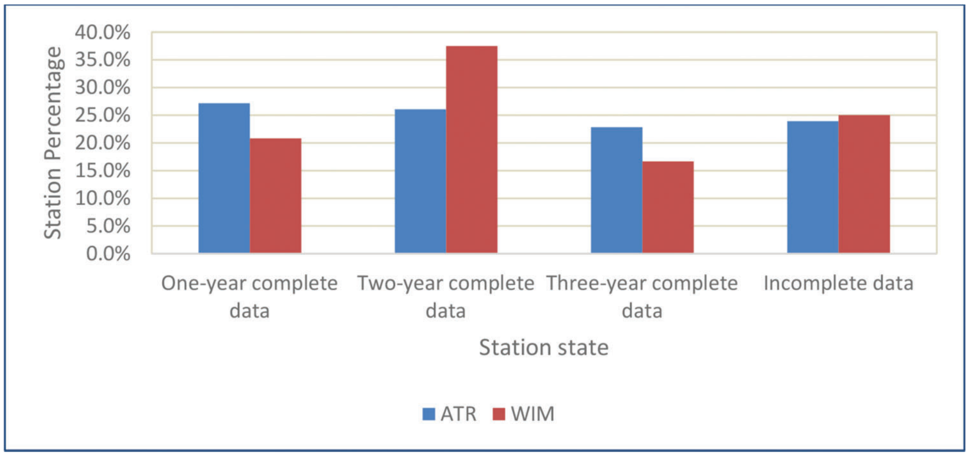


**Figure 2.2** Proportions of ATR/WIM stations with complete traffic data.

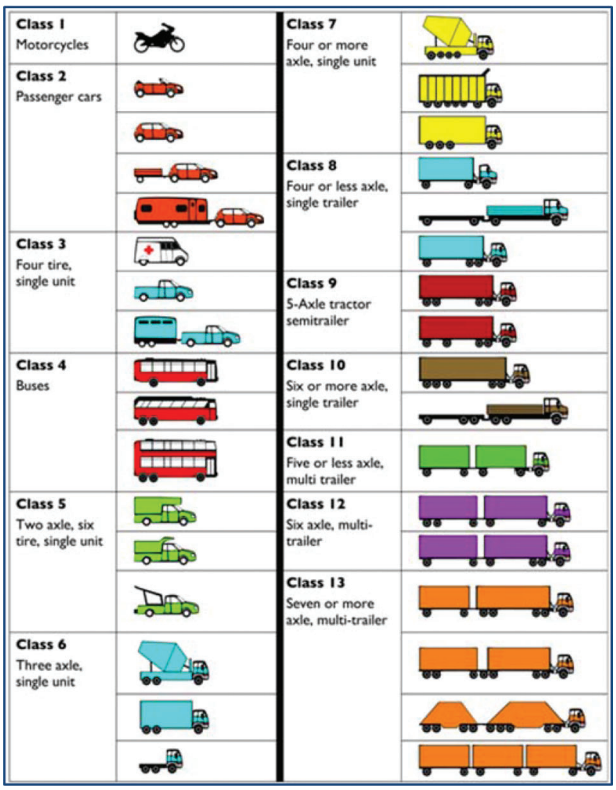


**Figure 2.3** FHWA vehicle classification (FHWA, 2016).

with GIS software to show statewide traffic volume distributions in 2D or 3D graphs. Using the base map in 2017, the AADT distributions were obtained as exhibited in Figure 2.4 and Figure 2.5. The 2D and 3D graphs in the two figures present a clear illustration of the statewide AADT distribution. The areas, locations, and roadways with different levels of traffic volumes can be visually identified by using the two graphs together. Similar to traffic volume distributions, the statewide truck traffic distributions in terms of AADTT are plotted in Figure 2.6 and Figure 2.7. In these two figures, the relative magnitudes of truck traffic volumes are visualized in both 2D and 3D imagines.

In Figure 2.4 and Figure 2.6, the GIS maps include and display all values of AADT and AADTT, respectively. In order to show different levels of AADT or AADTT, a GIS map can be divided into a number of maps with different levels (layers). The individual layer GIS maps for AADT are shown in Figure 2.8 and those for AADTT are shown in Figure 2.9. These GIS maps exhibit more detailed visual information on the statewide traffic and truck traffic distributions in various levels.

### 2.3 Traffic Volume Changes

The current truck traffic input for INDOT's mechanistic-empirical pavement design is based on the previous study (Jiang, Li, Nantung, & Chen, 2008) with 5-year WIM data up to 2004. It was expected that the traffic volumes should have changed significantly since then. Therefore, the WIM data in 2004 were compared to the WIM data in 2016, 2017, and 2018. There were 26 common WIM stations that existed in 2004 as well as in 2018. The recorded traffic volumes at these WIM sites in 2004 and 2018 are listed in Table 2.3. As shown in the table, the traffic volumes (AADT) increased at 17 out of the 26 WIM sites, ranging from 1% to 162%. The truck traffic volumes (AADTT) increased at 19 out of the 26 WIM sites, ranging from 3% to 130%. During the period of 15 years, the average increases in AADT and AADTT are 15% and 17%, respectively. The magnitudes of the increases in traffic volumes, especially in truck traffic volumes, indicate that there was a significant need to update the statewide traffic for appropriate pavement design in Indiana.

To further illustrate the changes in traffic conditions, the traffic data in Table 2.3 are presented in graphs. The AADT volumes in 2004 and 2018 at the 26 WIM sites are plotted in Figure 2.10. The corresponding percentages of AADT changes are shown in Figure 2.11. Similarly, the comparisons of truck traffic volumes (AADTT) in 2004 and 2018 are displayed in Figures 2.12 and 2.13. These figures indicate that traffic volumes and truck traffic volumes increased in the

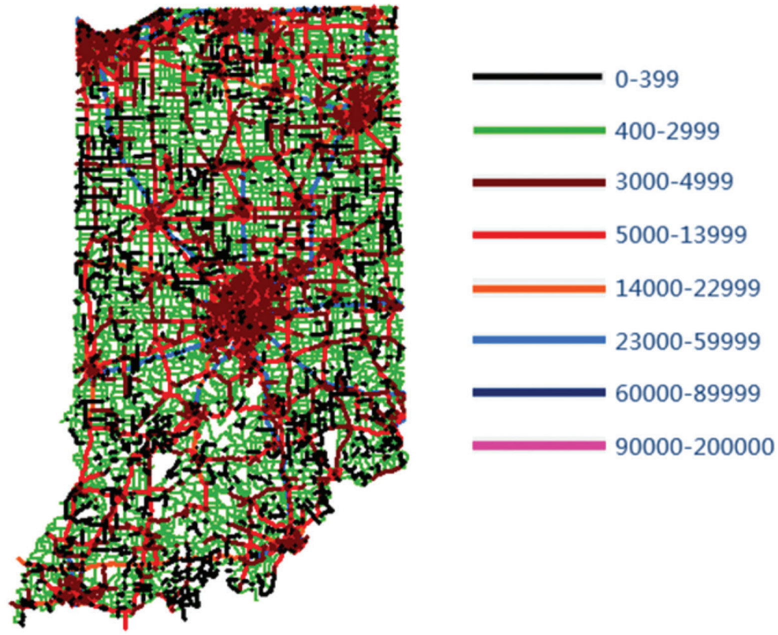


**Figure 2.4** Average annual daily traffic (AADT) distribution map (2017).

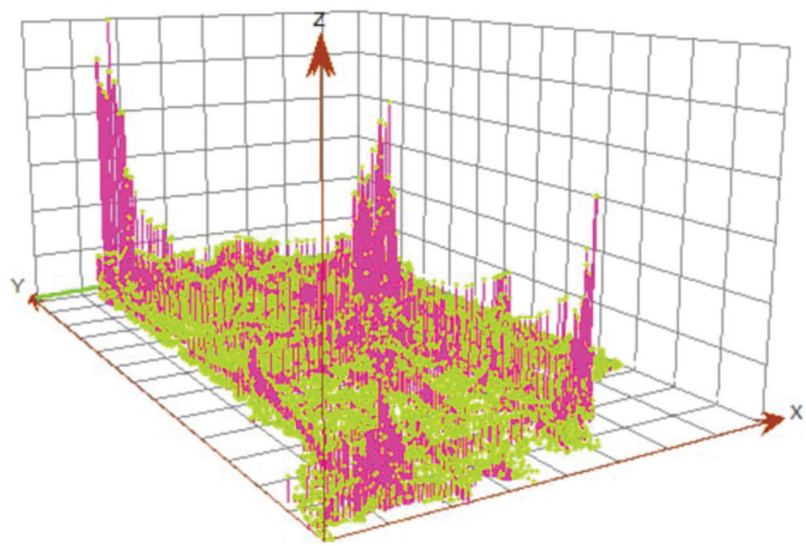


**Figure 2.5** Average annual daily traffic (AADT) distribution in 3D (2017).

15 years at most of the WIM sites. At some of the WIM sites, the traffic volumes or truck traffic volumes decreased. However, the magnitudes of the increases are much greater that those of the decreases as shown in Figures 2.11 and 2.13. It is interesting to notice in Table 2.3 and in the figures that there were a few cases that the traffic volume increased while the truck traffic volume decreased and vise versa at same WIM site.

The distributions of traffic volumes and truck traffic volumes in 2004 were compared with those in 2016, 2017. An example of such a comparison is demonstrated in Figures 2.14 and 2.15 with the traffic data at WIM Site 351 on I-465 in Indianapolis. The differences are clearly shown in terms of the average hourly traffic volumes and the average hourly truck traffic volumes between 2004 and 2016 through 2018. Not only the hourly volumes had increased significantly since 2004, but also the volume distributions had changed, as reflected in the relative volume proportions and the time periods of peak volumes along the 24 hours.

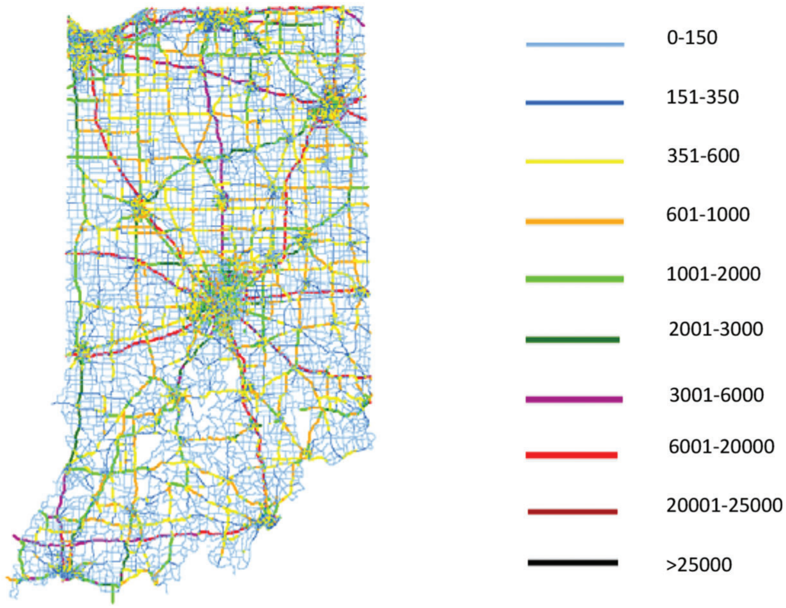


**Figure 2.6** Average annual daily truck traffic (AADTT) distribution map (2017).

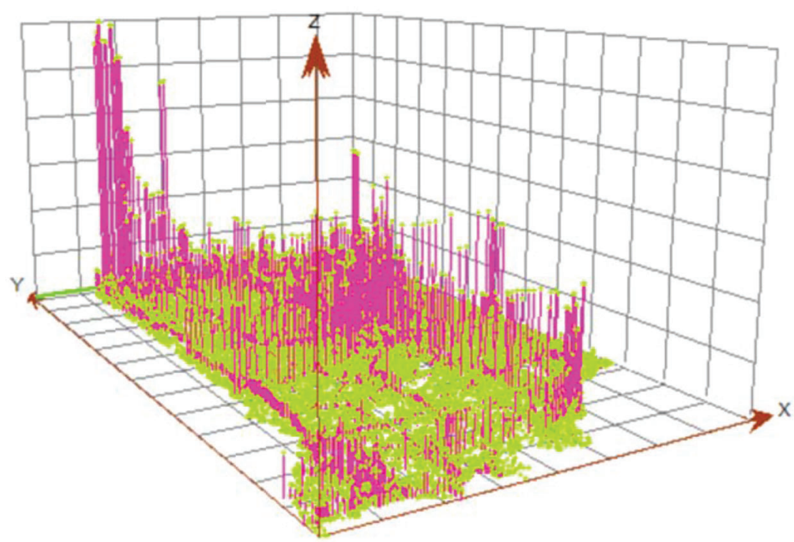


**Figure 2.7** Average annual daily truck traffic (AADTT) distribution in 3D (2017).

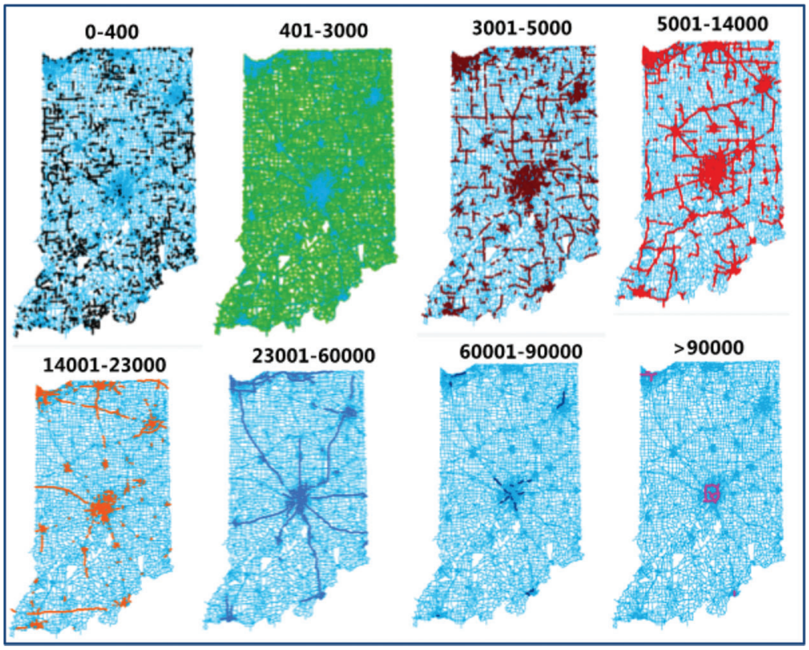


**Figure 2.8** AADT range maps (2017).

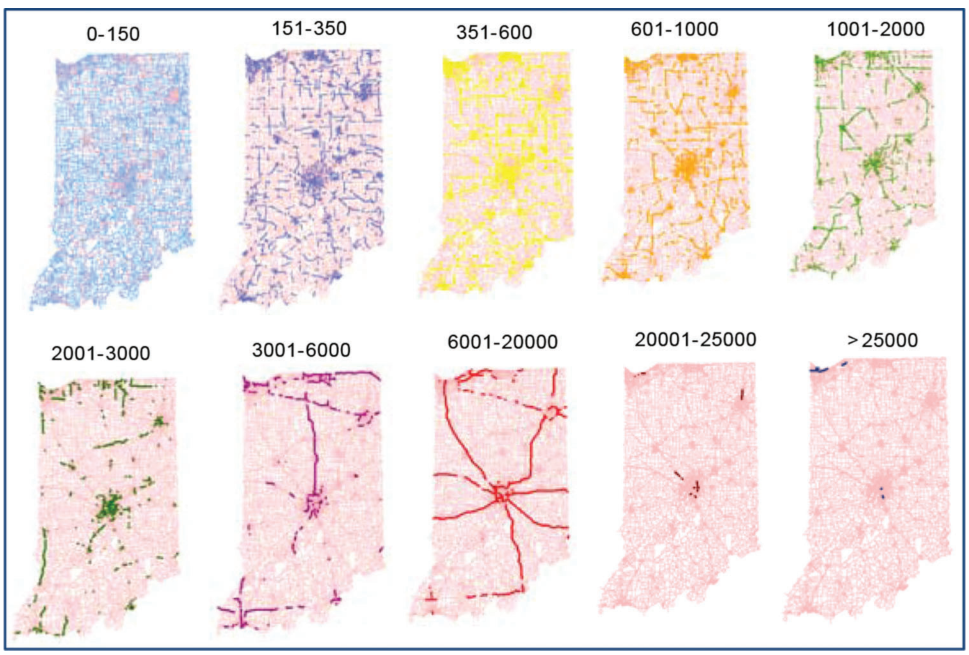


**Figure 2.9** AADTT range maps (2017).

TABLE 2.3
**Comparison of traffic volumes in 2004 and 2018**

| | AADT | | | AADTT | | |
|---|---|---|---|---|---|---|
| **Site Number** | **2004** | **2018** | **Change** | **2004** | **2018** | **Change** |
| 100 | 1,863 | 3,537 | 90% | 659 | 1,258 | 91% |
| 120 | 16,507 | 18,144 | 10% | 5,257 | 3,671 | -30% |
| 200 | 30,121 | 26,952 | -11% | 7,654 | 8,156 | 7% |
| 210 | 7,379 | 10,080 | 37% | 1,587 | 2,133 | 34% |
| 220 | 10,112 | 10,955 | 8% | 1,914 | 1,794 | -6% |
| 230 | 24,340 | 30,054 | 23% | 7,676 | 9,036 | 18% |
| 310 | 35,479 | 34,881 | -2% | 3,055 | 2,067 | -32% |
| 340 | 88,704 | 48,957 | -45% | 14,948 | 9,109 | -39% |
| 351 | 43,427 | 94,294 | 117% | 5,638 | 11,302 | 100% |
| 352 | 36,067 | 83,206 | 131% | 4,109 | 9,461 | 130% |
| 360 | 37,536 | 41,996 | 12% | 11,797 | 16,235 | 38% |
| 370 | 39,655 | 33,743 | -15% | 11,942 | 14,112 | 18% |
| 420 | 38,780 | 101,761 | 162% | 8,383 | 14,730 | 76% |
| 430 | 45,302 | 15,028 | -67% | 11,952 | 12,558 | 5% |
| 450 | 8,800 | 6,634 | -25% | 1,052 | 1,012 | -4% |
| 470 | 23,584 | 32,298 | 37% | 3,455 | 4,963 | 44% |
| 520 | 4,511 | 3,219 | -29% | 1,003 | 725 | -28% |
| 530 | 31,217 | 35,605 | 14% | 7,957 | 7,522 | -5% |
| 540 | 29,514 | 32,562 | 10% | 4,900 | 6,835 | 40% |
| 600 | 9,191 | 9,033 | -2% | 1,643 | 2,054 | 25% |
| 610 | 16,609 | 16,516 | -1% | 5,095 | 5,838 | 15% |
| 620 | 6,824 | 7,647 | 12% | 2,168 | 2,564 | 18% |
| 630 | 13,903 | 9,202 | -34% | 1,429 | 1,388 | -3% |
| 640 | 7,664 | 9,297 | 21% | 519 | 695 | 34% |
| 650 | 23,764 | 25,829 | 9% | 2,284 | 2,577 | 13% |
| 660 | 20,995 | 10,254 | -51% | 2,641 | 871 | -67% |

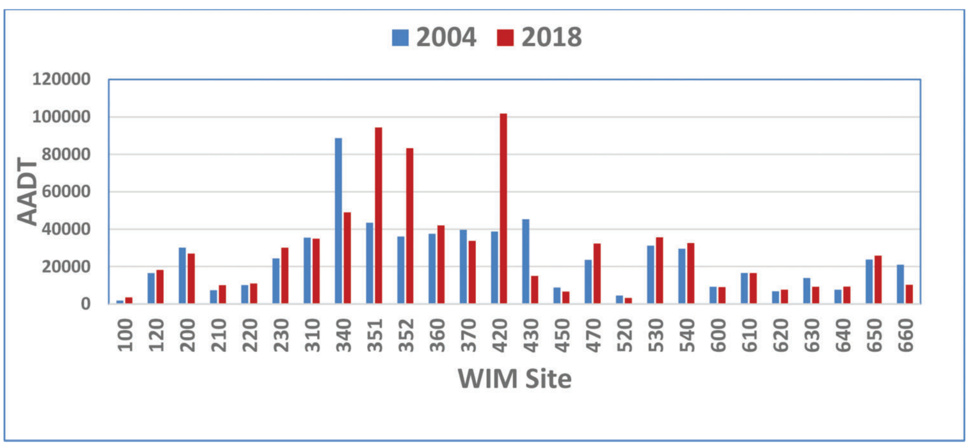


**Figure 2.10** Traffic volumes in 2004 and 2018.

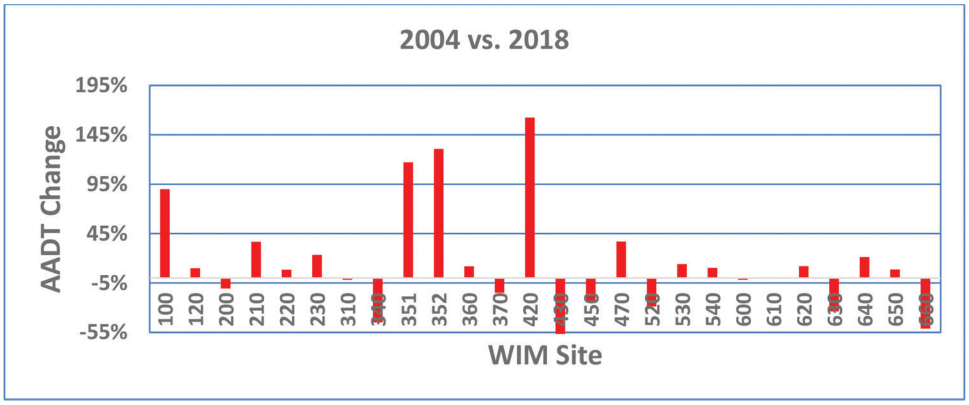


**Figure 2.11** Traffic volume changes (2004 vs. 2018).

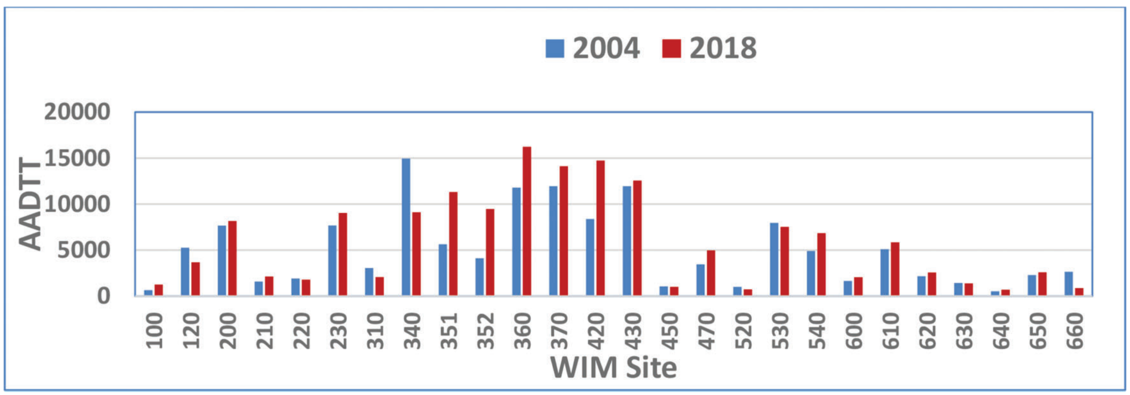


**Figure 2.12** Truck traffic volumes in 2004 and 2018.

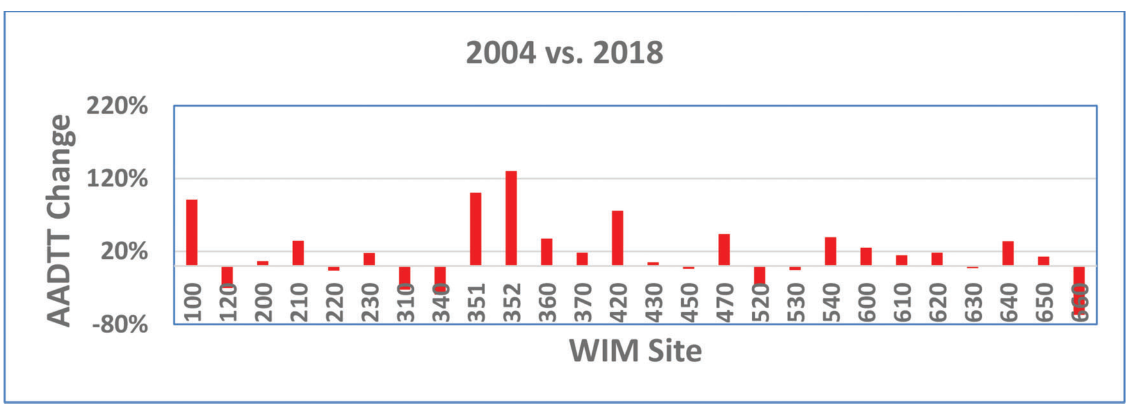


**Figure 2.13** Truck traffic volume changes (2004 vs. 2018).

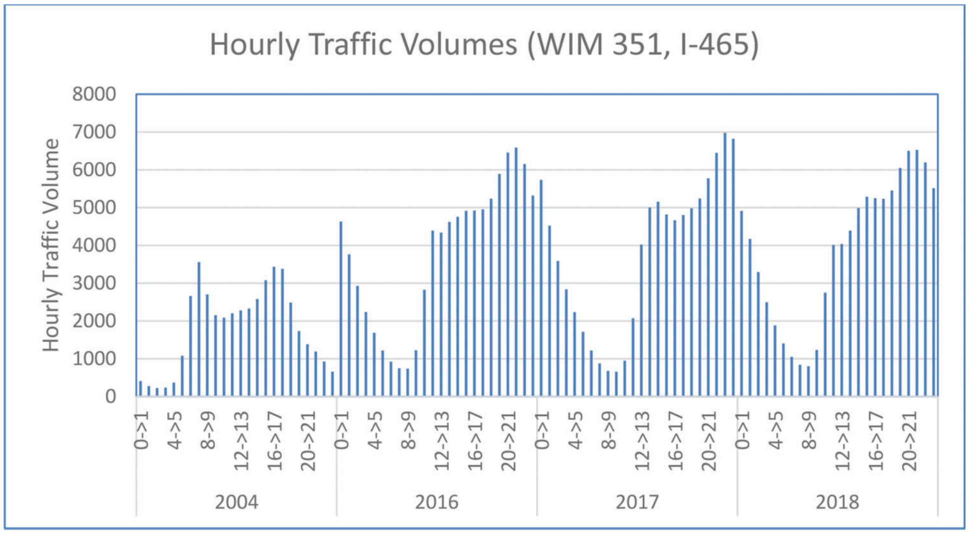


**Figure 2.14** Average hourly traffic volumes (2004 vs. 2016, 2017, and 2018).

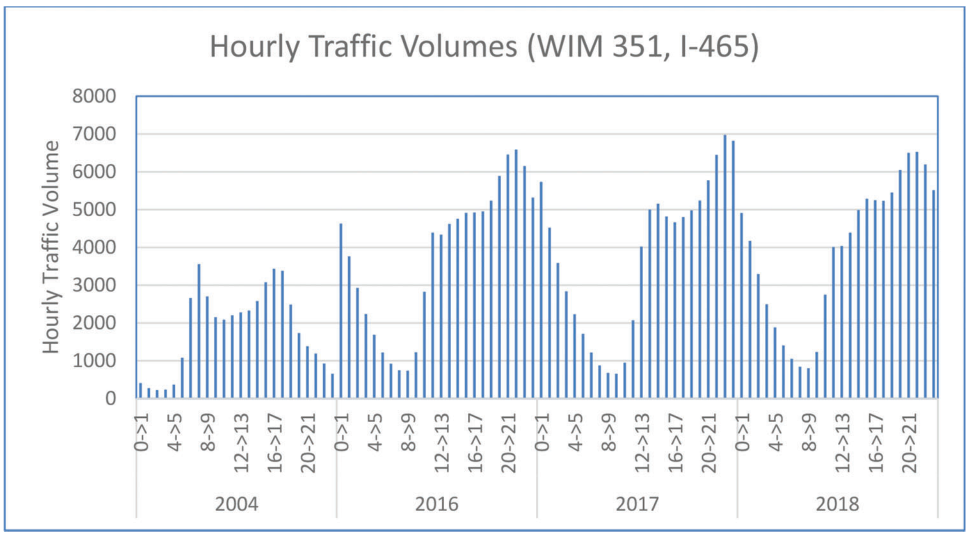


**Figure 2.15** Average hourly truck traffic volumes (2004 vs. 2016, 2017, and 2018).

# 3. TRUCK TRAFFIC AND AXLE LOAD SPECTRA

## 3.1 Truck Traffic Volumes

In the 13 classes of vehicles in the FHWA classification system (FHWA, 2016), Class 4 through Class 13 vehicles are denoted as trucks. It should be noted that the buses (Class 4) are included in the truck traffic. Truck traffic volumes are the primary input for pavement design since the vehicles in the group exert a significant impact on pavement structure and are the main forces causing pavement structure damages and distresses.

Box plots are utilized to illustrate the truck traffic distribution patterns on different types of roadways. A box plot, also known as box-and-whisker plot, is often used to study the distribution of data and to visualize the spread and skew of the data (Subramanian, 2020). A box plot uses the following values to depict the distribution of a dataset: minimum, first quartile, median, third quartile, and maximum. As shown in the diagram in Figure 3.1, the box plot contains a box and some horizontal and vertical lines. The box represents the range from the first quartile to the third quartile. Fifty percent of the data points are contained inside of the box. The horizontal line inside the box represents the median of the data. If the median is not in the middle of the box, then the distribution is skewed. The distribution is positively skewed if the median is closer to the bottom. If the median is closer to the top, then the distribution is negatively skewed. The first quartile (Q1) is the 25th percentile value of the data. It is also called the lower quartile. The third quartile (Q3) is the 75th percentile of the data. It is also called the upper quartile. Quartiles are a special case of a type of

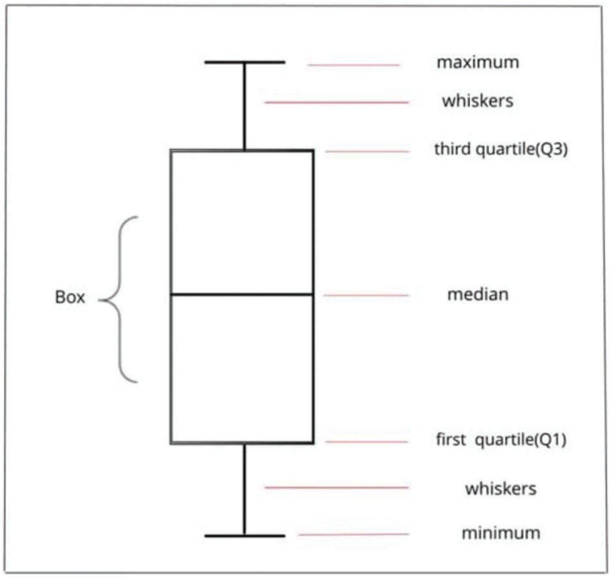


**Figure 3.1** Box and whiskers plot (Subramanian, 2020).

statistics called quantiles, which are numbers dividing data into quantities of equal size. Extending from both the ends of the box plot are called whiskers, which extends till the adjacent values. The lower adjacent value is the furthest data point that is within 1.5 times of the interquartile range (IQR) of the lower end of the box, and the upper adjacent value is the furthest data that is within 1.5 times of the IQR of the upper end of the box. The interquartile range is calculated as $IQR = Q_3 - Q_1$. Any data points past the whisker ends are considered as outliers and represented with circles or diamonds.

The recorded ATR and WIM data in 2016, 2017, and 2018 were retrieved, compiled, and analyzed to examine the characteristics of truck traffic in Indiana. The truck traffic distributions were analyzed for interstate highways, US routes, and state roads. The box plots for the interstate highways with four to twelve lanes are depicted in Figure 3.2 for the period of 3 years. As shown in the figure, on four-lane interstate highways, the truck traffic changed from a relatively symmetric distribution in 2016 to positively skewed (skewed toward the bottom) distributions in 2017 and 2018. In addition, the sizes of the boxes and ranges (distances between minimum to maximum) of the four-lane interstate highways experienced only minor changes during the 3 years. The median values of the truck traffic volumes remained relatively stable on four-lane, six-lane, and eight-lane interstates, while the median values on ten-lane and twelve-lane sections experienced a decreasing trend in the 3 years. The distributions of the truck traffic volumes are negatively skewed for the eight-lane and twelve-lane interstates. It should be noted that the truck traffic distribution on ten-lane interstate highways changed from a negatively distribution in 2016 to symmetric distributions in 2017 and 2018. In terms of the distribution medians, the truck traffic volumes on the four-lane, six-lane, and eight-lane interstate highways remained consistent, while those on the ten-lane and twelve-lane interstate highways moved downward in the 3 years.

The box plots for the US routes and state roads are displayed in Figure 3.3 and 3.4, respectively. The box plots in Figure 3.3 indicate that the truck traffic distributions in 2016 and 2017 are similar for both two-lane and four-lane US routes. However, the truck traffic volume distributions shifted up with increased maximum values on two-lane US routes and shifted down with decreased median and maximum values on four-lane US routes in 2018.

As shown in Figure 3.4, the medians for two-lane and four-lane state roads remained in the same levels during the 3 years. The maximum values, however, experienced apparent changes for two-lane state roads.

The 3-year ATR and WIM data of 2016, 2017, and 2018 were used for the data processing and analysis to update the required traffic inputs for the MEPDG. All of the required traffic inputs for the MEPDG were obtained from all the ATR and WIM stations. To illustrate the truck traffic and axle load spectra, a WIM station on I-70 (WIM Site 315) was utilized in this report to present the processed traffic data. The WIM station was located on I-70 in Indianapolis as shown in Figure 3.5. The WIM device recorded traffic data of five eastbound lanes at this location where the lanes were numbered with the driving lane as Line 1 and the lane adjacent to the highway median as Line 5. The traffic inputs for the MEPDG include the following:

- average annual daily truck traffic,
- truck volume monthly adjustment factors,
- truck volume lane distribution factors,
- truck volume directional distribution factors,
- truck volume class distributions, and
- traffic volume hourly distribution factors.

Truck traffic can be expressed in different forms, including average annual daily truck traffic (AADTT), average monthly daily truck traffic (AMDTT), and average hourly truck traffic (AHTT). The obtained values of the truck traffic are in the forms of average monthly daily truck traffic (AMDTT) and average hourly truck traffic (AHTT) of a year. Table 3.1 presents the monthly AMDTT values at the I-70 WIM station. It should be noted that the average values shown in the last row of Table 3.1 are the values of AADTT of the corresponding lanes. With the AMDTT values, the monthly adjustment factors (MAF) can be calculated by the following equation (ARA, 2004):

$$MAF_i = \frac{AMDTT_i}{\sum_{i=1}^{12} AMDTT_i} \times 12 \qquad \text{(Eq. 3.1)}$$

Where:

$MAF_i$: monthly adjustment factor for month i.

$AMDTT_i$: average monthly daily truck traffic for month i.

The monthly adjustment factors calculated with the data in Table 3.1 are plotted in Figure 3.6. The MAF values reflect the monthly as well as seasonal impact of truck traffic on pavement structures.

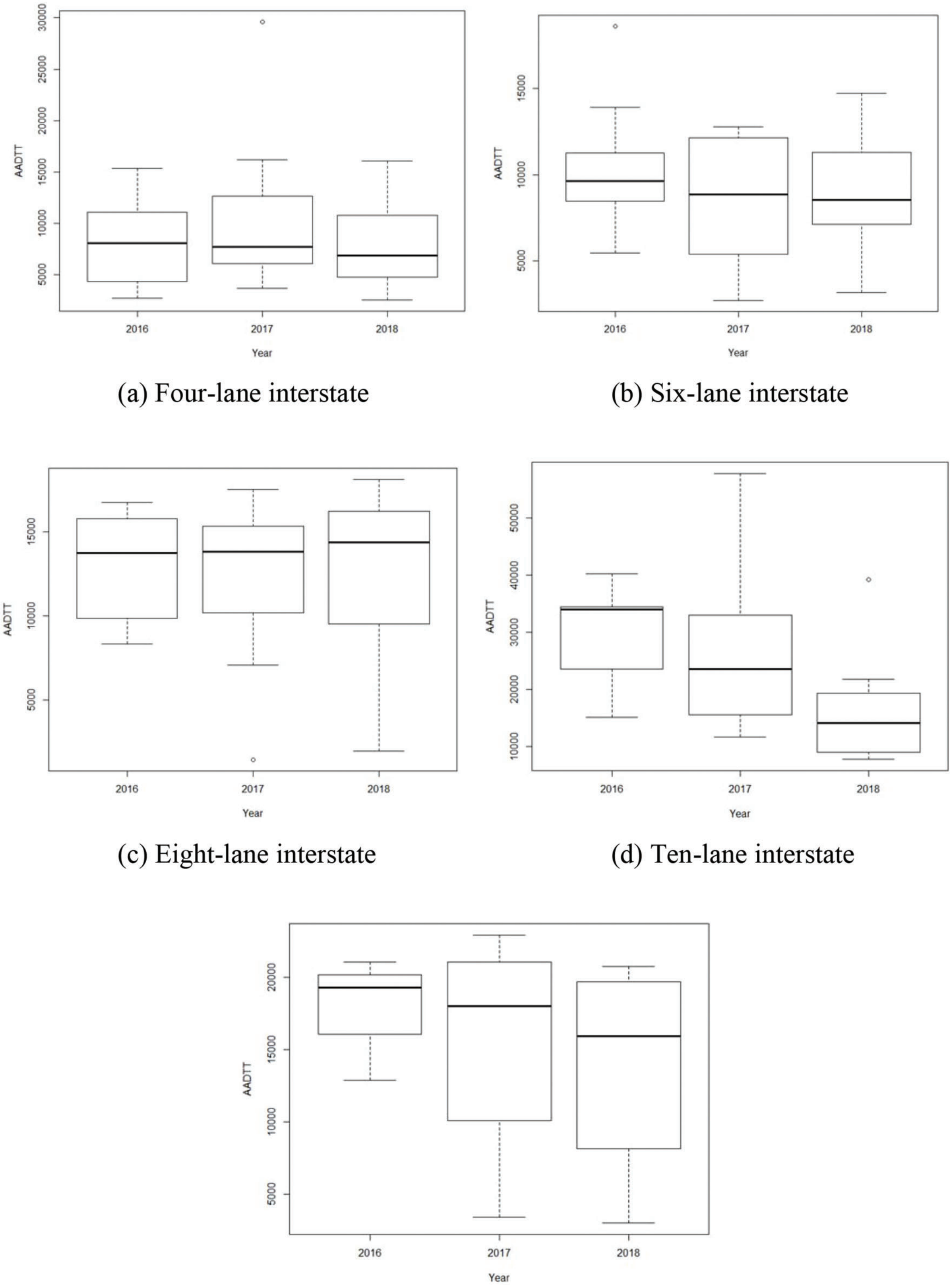


(a) Four-lane interstate

(b) Six-lane interstate

(c) Eight-lane interstate

(d) Ten-lane interstate

(e) Twelve-lane interstate

**Figure 3.2** Truck traffic distributions on interstate highways.

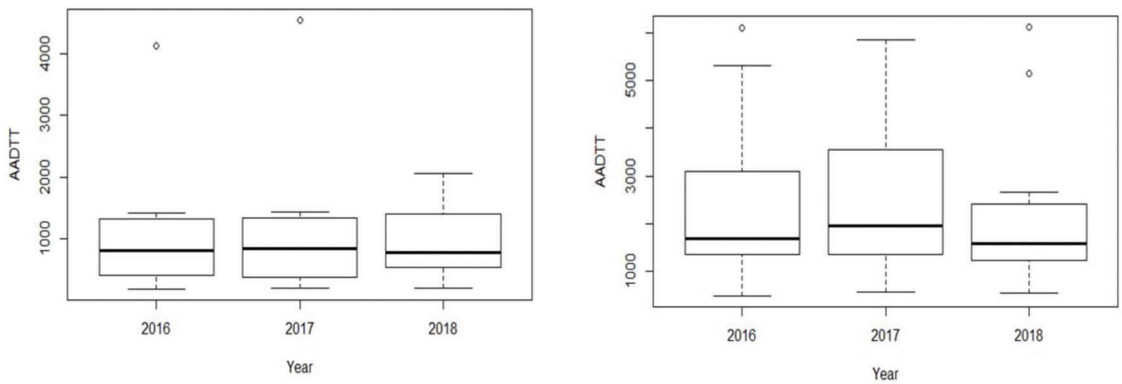


(a) Two-lane US routes (b) Four-lane US routes

**Figure 3.3** Truck traffic distributions on US routes.

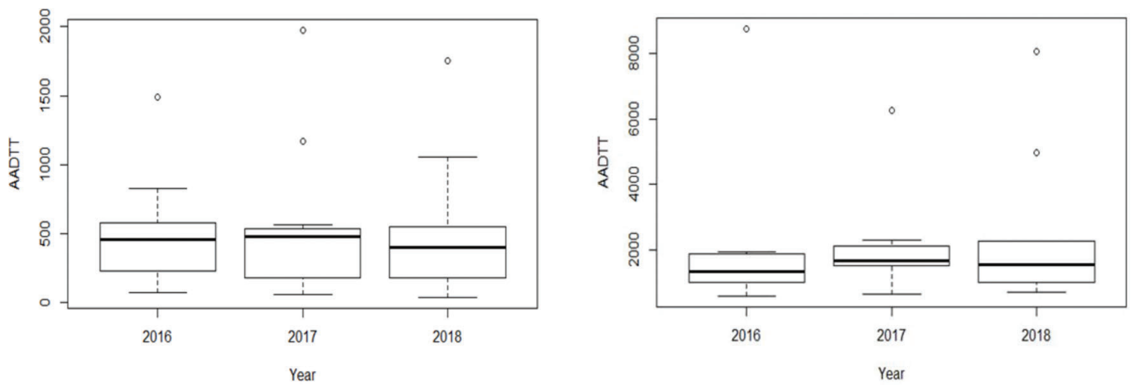


(a) Two-lane state roads (b) Four-lane state roads

**Figure 3.4** Truck traffic distributions on state roads.

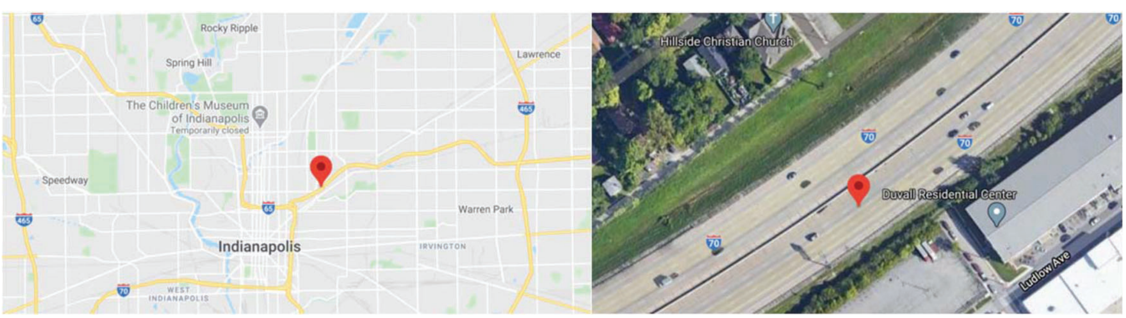


**Figure 3.5** WIM Station 315 on I-70 (Google, n.d.).

Through processing the WIM data, the average hourly truck volumes at the I-70 WIM station were obtained as graphically illustrated in Figure 3.7. The variations of the hourly truck volumes during the 24 hours at the site are clearly shown in the graph. Using the average hourly truck volumes, the hourly distributions factors can be calculated. Figure 3.8 displays the hourly distribution factors. The hourly distribution factors are the percentages of truck traffic at each hour out of the total truck volume during the 24-hour period. Thus, the sum of the 24 hourly distribution factors should be equal to 100%.

The truck traffic contains ten types of trucks, Classes 4 through 13, as defined by the FHWA vehicle classifications (FHWA, 2016). The truck volumes of the vehicle types are of interest to highway engineers for MEPDG pavement design. The truck volumes of the ten vehicle types in each month at the WIM station are presented in Table 3.2. In order to visually illustrate the distribution of the truck traffic, the truck volumes by truck classes are drawn in Figure 3.9. The truck volumes in the figure indicate that most of the trucks at this location were Class 5 vehicles, followed by Class 9 vehicles. It is interesting to note that in most cases

Class 9 truck volume would be higher than Class 5 truck volume on freeways. The reason for the higher Class 5 truck volume at this location is probably that the WIM site is inside Indianapolis where Class 5 trucks, including delivery and construction trucks, are more active for urban commercial and residential services.

TABLE 3.1
**Average monthly truck traffic at the I-70 WIM site**

| Month | Lane 1 | Lane 2 | Lane 3 | Lane 4 | Lane 5 | $AMDTT_i$ |
|---|---|---|---|---|---|---|
| January | 1,807 | 3,424 | 2,280 | 1,439 | 1,336 | *10,286* |
| February | 1,400 | 2,985 | 2,123 | 1,210 | 1,440 | *9,158* |
| March | 967 | 2,621 | 1,665 | 1,637 | 1,097 | *7,987* |
| April | 971 | 1,955 | 2,866 | 1,527 | 1,568 | *8,887* |
| May | 1,053 | 1,614 | 2,346 | 431 | 971 | *6,415* |
| June | 1,126 | 2,077 | 2,622 | 591 | 1,159 | *7,575* |
| July | 900 | 2,860 | 2,050 | 333 | 544 | *6,687* |
| August | 1,142 | 3,102 | 2,321 | 1,078 | 1,398 | *9,041* |
| September | 971 | 3,430 | 3,107 | 1,923 | 1,429 | *10,860* |
| October | 1,033 | 3,239 | 3,544 | 2,318 | 1,435 | *11,569* |
| November | 941 | 3,291 | 2,574 | 2,268 | 1,573 | *10,647* |
| December | 1,013 | 3,028 | 3,261 | 1,948 | 1,813 | *11,063* |
| *Average* | *1,110* | *2,802* | *2,563* | *1,392* | *1,314* | — |

Distributions of truck traffic on roadway lanes at this WIM site were obtained. Figure 3.10 presents the average daily truck volumes in each month. Based on the data in Figure 3.10, the lane distribution factors of truck traffic can be computed as shown in Figure 3.11.

The lane distribution factors in Figure 3.11 are the proportions of all trucks (Class 4 through Class 13) on the five lanes. It is of interest to highway engineers to know the lane distributions of individual classes of trucks. Figure 3.12 and Figure 3.13 display the lane distributions of individual truck classes in two different ways. Apparently, the lane distributions of different vehicle classes are notably different.

The lane distribution factors for the individual vehicle types are displayed in Figures 3.14 through 3.23. These lane distribution factors provide specified information on the impact of individual types of vehicles on roadway lanes. The lane distribution factors reveal that Lane 2 and Lane 3 carried most of the truck traffic for almost

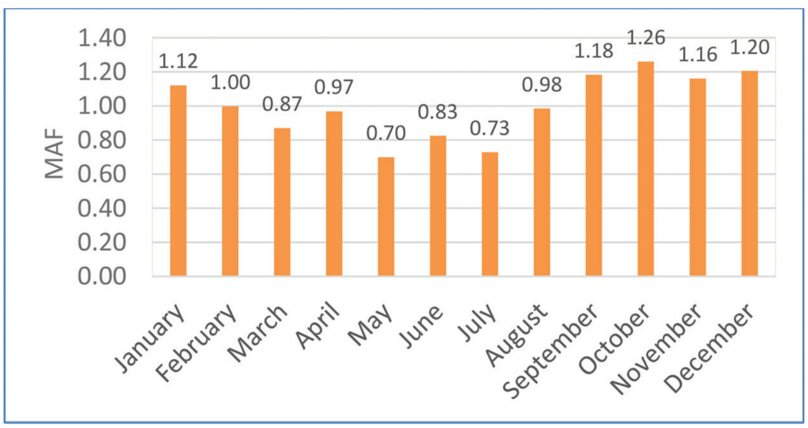


**Figure 3.6** Monthly adjustment factors.

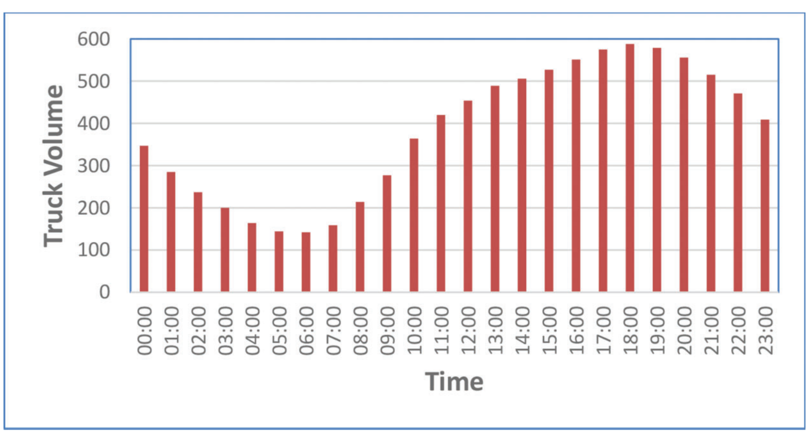


**Figure 3.7** Average hourly truck traffic.

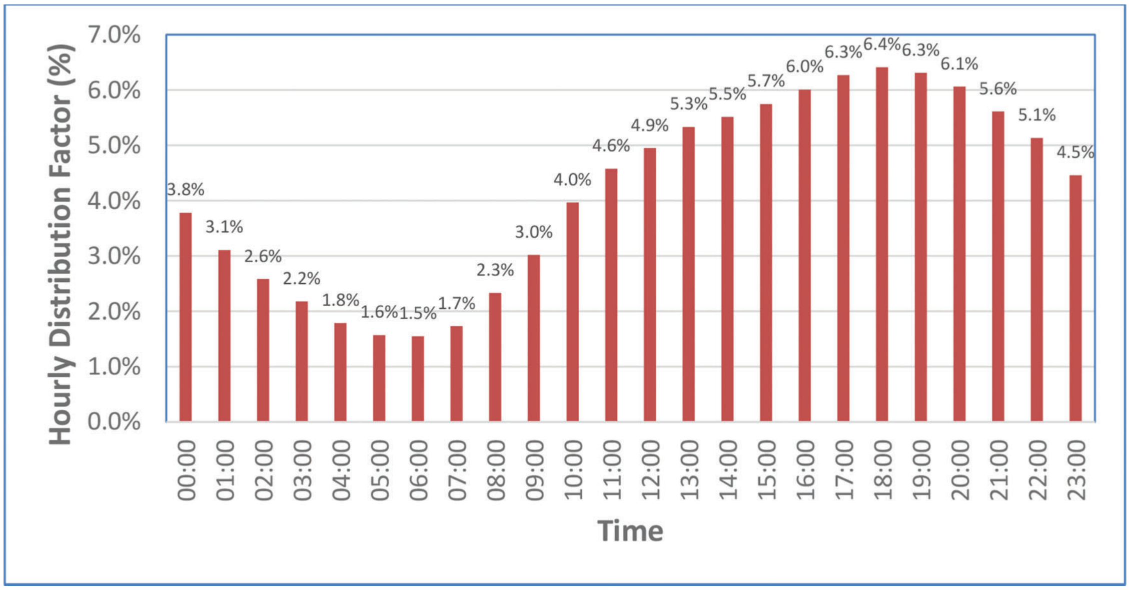


**Figure 3.8** Hourly distribution factors of truck traffic.

TABLE 3.2
**Average monthly daily truck volumes of different vehicle classes**

| | Vehicle Class | | | | | | | | | |
|---|---|---|---|---|---|---|---|---|---|---|
| **Month** | **C4** | **C5** | **C6** | **C7** | **C8** | **C9** | **C10** | **C11** | **C12** | **C13** |
| January | 271 | 6,205 | 221 | 39 | 568 | 2,787 | 22 | 105 | 57 | 13 |
| February | 262 | 5,270 | 209 | 32 | 561 | 2,664 | 16 | 89 | 52 | 5 |
| March | 231 | 4,380 | 214 | 43 | 550 | 2,418 | 16 | 77 | 49 | 10 |
| April | 272 | 4,839 | 235 | 50 | 703 | 2,604 | 13 | 107 | 56 | 9 |
| May | 199 | 3,668 | 167 | 35 | 503 | 1,697 | 8 | 72 | 37 | 30 |
| June | 232 | 3,983 | 211 | 46 | 678 | 2,264 | 8 | 88 | 44 | 22 |
| July | 221 | 3,011 | 216 | 59 | 602 | 2,428 | 9 | 76 | 41 | 25 |
| August | 281 | 4,412 | 281 | 67 | 570 | 2,923 | 16 | 94 | 55 | 50 |
| September | 348 | 4,839 | 376 | 84 | 608 | 4,233 | 30 | 131 | 81 | 131 |
| October | 395 | 4,802 | 438 | 100 | 649 | 4,654 | 33 | 156 | 93 | 249 |
| November | 308 | 4,680 | 347 | 84 | 454 | 3,525 | 19 | 105 | 79 | 1,046 |
| December | 243 | 4,685 | 235 | 51 | 316 | 2,541 | 10 | 62 | 56 | 2,863 |
| *Average* | *272* | *4,564* | *262* | *57* | *563* | *2,895* | *17* | *97* | *58* | *371* |

all of the truck classes. A unique case is that the majority of Class 13 trucks traveled on Lane 3 (83%) and Lane 5 (15%) (Figure 3.23).

Similarly, the directional distributions can be obtained as shown in Figure 3.24. A directional distribution factor represents the higher proportion of a given vehicle type among the two travel directions of the roadway. For example, in Figure 3.24 the directional distribution factor for C9 is 0.58 because 0.58 is greater than 0.42 among the two proportions of 0.58 (westbound) and 0.42 (eastbound). At this WIM site, for all of the vehicle classes, except for C13, the westbound truck proportions are the directional distribution factors as they are greater than the eastbound proportions. Using the higher values of the directional proportions, the directional distribution factors for all classes of trucks are shown in Figure 3.25. The lane and directional distribution factors are essential for highway engineers to design appropriate pavement structures.

## 3.2 Axle Load Spectra

In addition to truck traffic volumes, truck axle loads are also part of the key requirements for MEPDG. The truck axle load data for MEPDG, often denoted as axle load spectra, include the following:

- single-axle load distributions,
- tandem-axle load distributions,
- tridem-axle load distributions,
- quad-axle load distributions,
- all-axle load distributions,
- average axle weight (kips) and average axle spacing (feet); (note: 1.0 kip = 1,000 pounds), and
- average number of axle types.

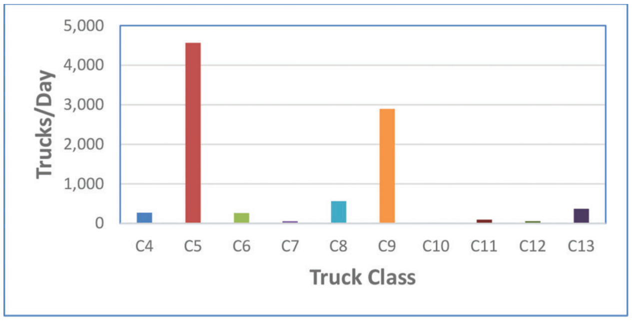


**Figure 3.9** Truck volume distribution by vehicle classes.

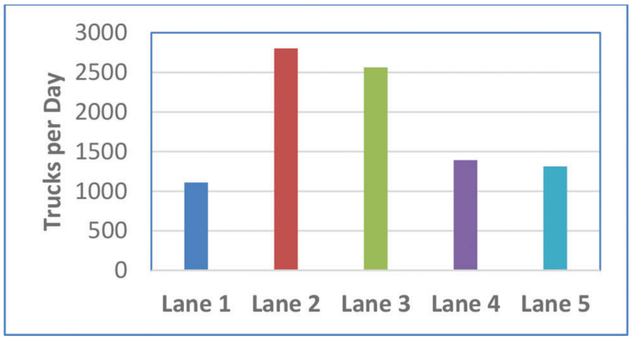


**Figure 3.10** Truck traffic distribution on roadway lanes.

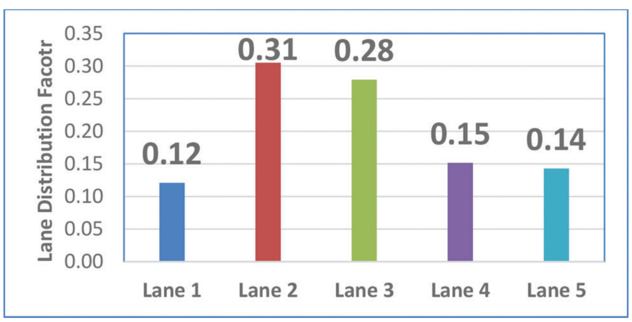


**Figure 3.11** Lane distribution factors.

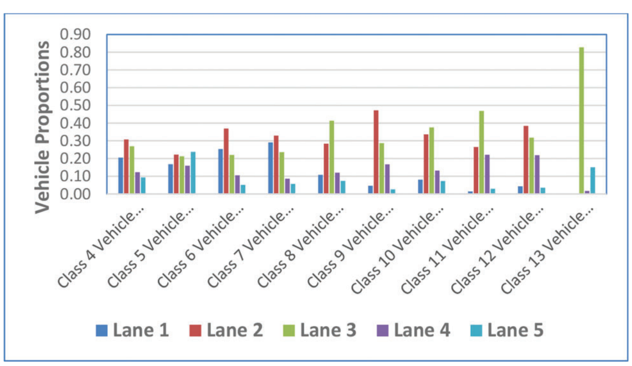


**Figure 3.12** Lane distribution of vehicle classes.

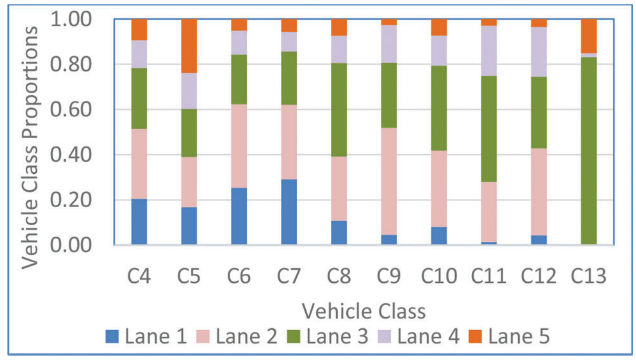


**Figure 3.13** Proportions of vehicle classes on roadway lanes.

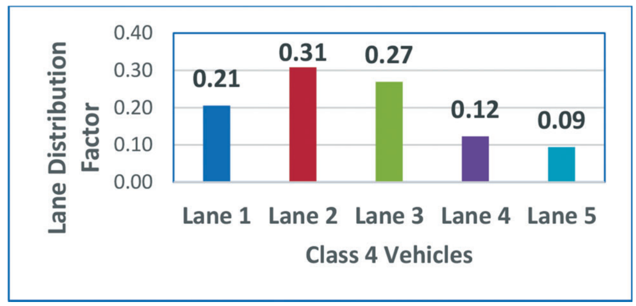


**Figure 3.14** Lane distribution factors of Class 4 vehicles.

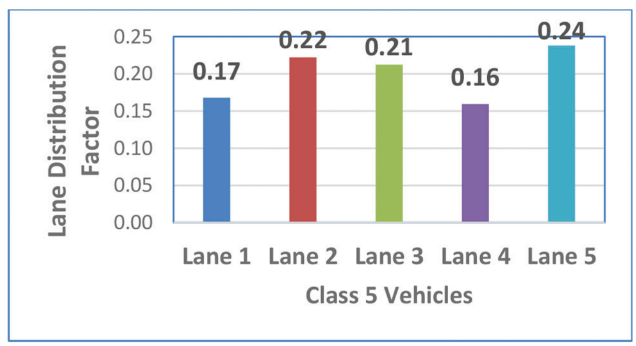


**Figure 3.15** Lane distribution factors of Class 5 vehicles.

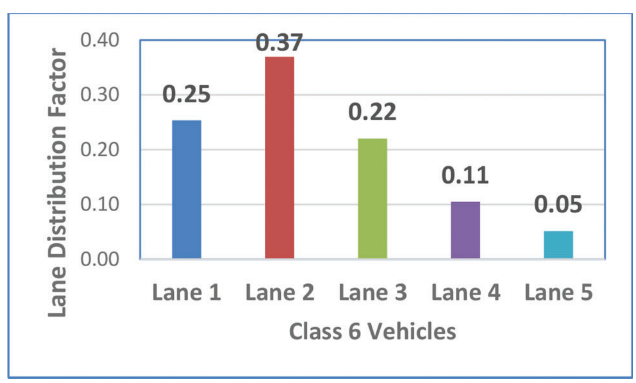


**Figure 3.16** Lane distribution factors of Class 6 vehicles.

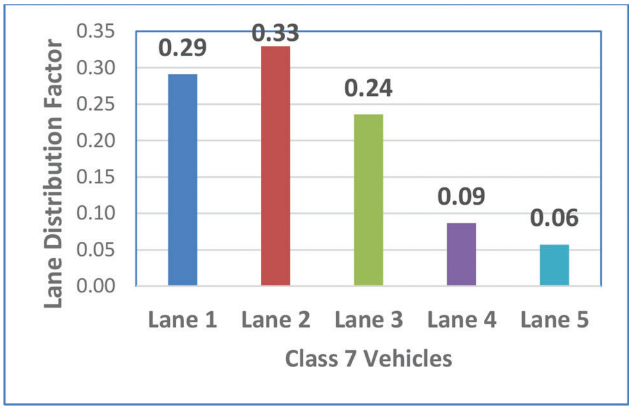


**Figure 3.17** Lane distribution factors of Class 7 vehicles.

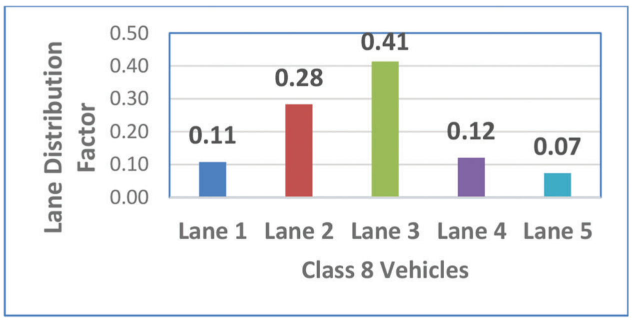


**Figure 3.18** Lane distribution factors of Class 8 vehicles.

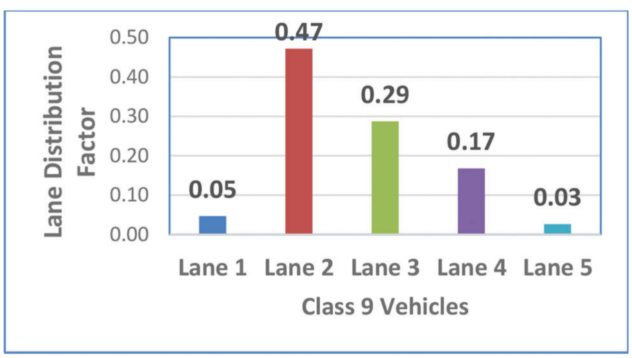


**Figure 3.19** Lane distribution factors of Class 9 vehicles.

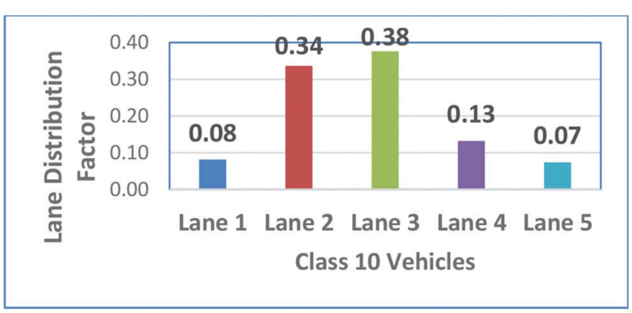


**Figure 3.20** Lane distribution factors of Class 10 vehicles.

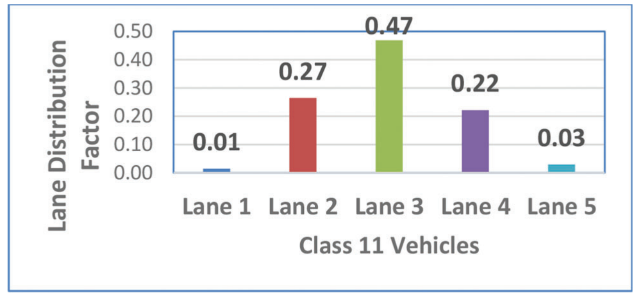


**Figure 3.21** Lane distribution factors of Class 11 vehicles.

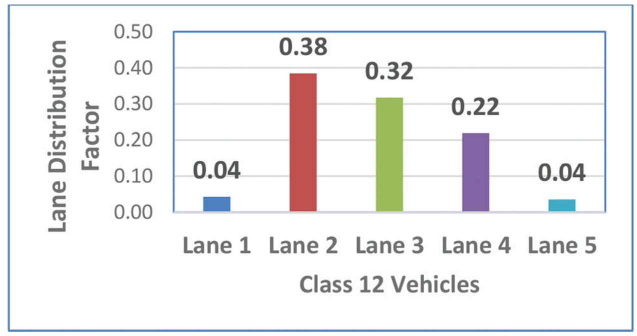


**Figure 3.22** Lane distribution factors of Class 12 vehicles.


**Figure 3.23** Lane distribution factors of Class 13 vehicles.

Same as in the previous section, WIM Site 315 on I-70 was also selected to demonstrate axle load spectra. Through processing the WIM data files, the values of average axle weights, average axle spacing, and average numbers of axle types were obtained as listed in Table 3.3 for the I-70 WIM station. In the table, Wi denotes the average weight of the ith axle of the vehicle class, Si-j is the average spacing between the ith and jth axles, and the low part of the table shows the average numbers of a particular type of axles (single, tandem, etc.) per vehicle. For example, from Table 3.3 the following values can be seen for the vehicles in Class 6:

- There are three axles with average weights of 12.50 kips (W1), 8.40 kips (W2), and 7.82 kips (W3).

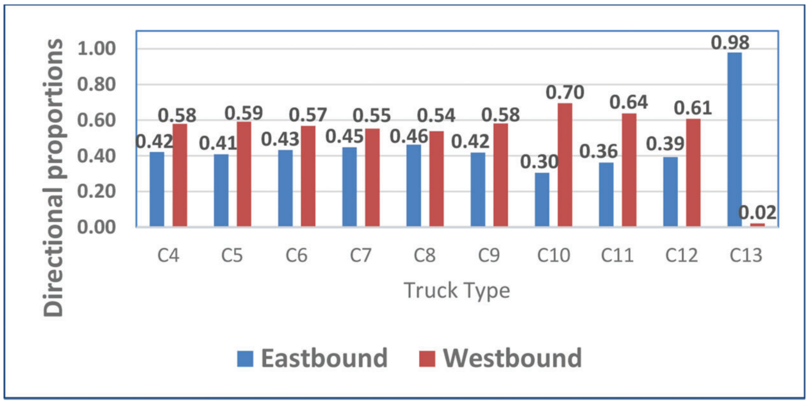


**Figure 3.24** Directional distributions.

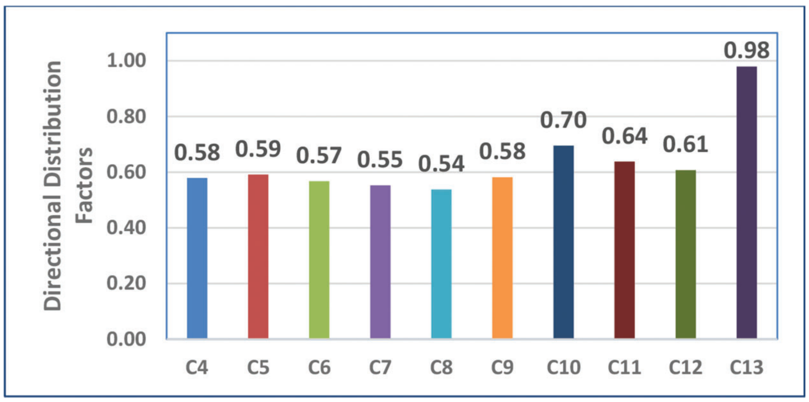


**Figure 3.25** Directional distribution factors.

- The average axle spacing is 16.83 feet between the first and second axles (S1-2) and 4.34 feet between the second and third axles (S2-3).
- The average number of single axles is 1.0 per vehicle, the average number of tandem axles is 2.0 per vehicle, and the average numbers of tridem and quad axles are both 0.

The number of average axle weights in the table implies the maximum number of axles in each class of trucks. As indicated in Table 3.3, the maximum number of axles of Class 6 vehicles is three because there are three weights (W1, W2, and W3), while the maximum number of axles of Class 13 vehicles is twelve because there are twelve weights (W1 through W12).

The magnitudes of axle loads are a major parameter for pavement design. To quantify axle loads, the MEPDG requires the axle load distributions for all classes of trucks. The axle load distributions are the percentages of axle loads in specified weight intervals, such as zero to three kips, three to four kips, and four to five kips. The axle load distributions include the axle weights for all-axle loads, single-axle loads, tandem-axle loads, tridem-axle load, and quad-axle loads. The values of the all-axle load distributions are shown in Tables A.1. The values in the table are the percentages of the vehicle classes with axle loads within the given load ranges. For example, in Table A.1, the value corresponding to vehicle class C4 and axle load range 0–3 kips is 3.98; meaning that 3.98% of Class 4 vehicles have axle loads less than 3 kips. The value 1.71 (corresponding to C4 and axle load 3–4 kips) indicates that 1.71% of Class 4 vehicles have axle load between 3 kips and 4 kips.

Similarly, the values of the single-axle load distributions, tandem-axle load distributions, and tridem-axle load distributions are presented in Tables A.2. A.3, and A.4, respectively. Because no quad-axle vehicles were recorded in the WIM data at this site, a table for quad-axle load distributions is not presented here. In Table A.2, the value corresponding to vehicle class C6 and load range 3–4 kips is 8.33, indicating that 8.33% single axles of Class 6 vehicles have axle loads between 3–4 kips.

### 3.3 A Complete Set of Truck Traffic and Axle Load Spectra at the I-70 WIM Station

Truck Traffic information was obtained from all of the ATR and WIM station that recorded sufficient data and processed to provide the required traffic input for the MEPDG. The compiled truck traffic data for MEPDG from all the ATR and WIM sites, including the truck traffic distributions and axle load spectra, will be provided in Excel files for INDOT. As an example, the complete truck traffic input for the MEPDG at the I-70 WIM

TABLE 3.3
**Average axle weight, axle spacing, and number of axle types by vehicle classes**

| | Vehicle Classes | | | | | | | | | |
|---|---|---|---|---|---|---|---|---|---|---|
| **Weight (kips)** | **C4** | **C5** | **C6** | **C7** | **C8** | **C9** | **C10** | **C11** | **C12** | **C13** |
| W1 | 11.86 | 4.90 | 12.50 | 14.61 | 9.16 | 11.96 | 12.16 | 11.46 | 12.17 | 18.32 |
| W2 | 12.92 | 4.29 | 8.40 | 11.17 | 10.81 | 12.29 | 11.40 | 16.63 | 10.18 | 17.59 |
| W3 | 10.63 | — | 7.82 | 13.10 | 8.29 | 11.75 | 11.29 | 16.02 | 9.81 | 19.99 |
| W4 | — | — | — | 13.77 | 7.8 | 11.68 | 7.58 | 13.28 | 12.46 | 17.69 |
| W5 | — | — | — | 10.46 | — | 11.39 | 9.73 | 13.20 | 12.39 | 17.66 |
| W6 | — | — | — | 10.83 | — | — | 9.41 | — | 11.36 | 18.48 |
| W7 | — | — | — | — | — | — | 6.25 | — | — | 17.89 |
| W8 | — | — | — | — | — | — | 8.77 | — | — | 17.20 |
| W9 | — | — | — | — | — | — | — | — | — | 17.17 |
| W10 | — | — | — | — | — | — | — | — | — | 16.97 |
| W11 | — | — | — | — | — | — | — | — | — | 16.49 |
| W12 | — | — | — | — | — | — | — | — | — | 15.87 |
| *Spacing (feet)* | | | | | | | | | | |
| S1-2 | 22.68 | 12.57 | 16.83 | 11.45 | 14.53 | 16.69 | 16.45 | 12.95 | 15.48 | 3.31 |
| S2-3 | 4.45 | — | 4.34 | 9.35 | 19.49 | 4.58 | 4.59 | 21.09 | 4.51 | 3.25 |
| S3-4 | — | — | — | 4.29 | 11.08 | 32.99 | 23.48 | 9.35 | 19.80 | 3.50 |
| S4-5 | — | — | — | 4.33 | — | 4.70 | 8.47 | 20.97 | 9.11 | 3.28 |
| S5-6 | — | — | — | 4.07 | — | — | 4.31 | — | 21.12 | 3.32 |
| S6-7 | — | — | — | — | — | — | 4.80 | — | — | 3.34 |
| S7-8 | — | — | — | — | — | — | 4.41 | — | — | 3.27 |
| S8-9 | — | — | — | — | — | — | — | — | — | 3.20 |
| S9-10 | — | — | — | — | — | — | — | — | — | 3.18 |
| S10-11 | — | — | — | — | — | — | — | — | — | 3.12 |
| S11-12 | — | — | — | — | — | — | — | — | — | 3.04 |
| *Axle Type* | | | | | | | | | | |
| Single | 1.81 | 2.00 | 1.00 | 1.22 | 2.14 | 1.19 | 1.47 | 4.75 | 3.79 | 0.26 |
| Tandem | 0.37 | — | 2.00 | 1.66 | 1.69 | 3.80 | 2.82 | 0.09 | 1.99 | 1.25 |
| Tridem | — | — | — | 1.27 | 0.01 | 0.01 | 1.74 | 0.16 | 0.21 | 9.41 |
| Quad | — | — | — | — | — | — | — | — | — | — |

site is presented in Appendix B to show the format and information on the truck traffic. The truck traffic presented was obtained using the WIM recorded data in 2018.

## 4. URBAN AREA BUS TRAFFIC

Although bus traffic is recorded at the ATR and WIM stations as Class 4 vehicles, the bus services within urban areas are mostly not included in the ATR and WIM database because the majority of the ATR and WIM stations are located on the roadways outside urban areas. The information on bus traffic inside cities would be useful for pavement design in urban areas. Effort was therefore made to obtain necessary bus traffic data in the Indiana urban areas to provide additional information for highway engineers with respect to city streets as well as highway sections passing through urban areas.

The Indiana Public Transit System consists of the following peer groups: Group One: large fixed route systems, Group Two: small fixed route systems, Group Three: urban demand response systems, Group Four: rural demand response systems, and the Northern Indiana Commuter Transportation District (INDOT, 2019). Transit systems included in Group One are large fixed route systems that operate an average of more than 1 million total vehicle miles per year, with more than 50% of the total vehicle miles operated in fixed route service. Group Two systems are small fixed route systems that operate less than 1 million total vehicle miles per year, with more than 50% of the total vehicle miles operated in fixed route service. The transit systems in Group Three operate in urbanized areas with populations greater than 50,000. Fifty percent or more of their total vehicle miles are operated in demand response or deviated fixed route service. Group Four systems include transit systems in urban areas with populations less than 50,000 and rural countywide and multi-county systems with varying population sizes. These systems operate 50% or more of their total vehicle miles in demand response or deviated fixed route service. The Northern Indiana Commuter Transportation District (NICTD) provides commuter rail service between South Bend, Indiana, and Chicago, Illinois. The cities and counties served by the peer groups are listed in Table 4.1.

Since Group Four systems operate mainly in demand response and the NICTD system is a commuter rail service, they are excluded from the urban bus traffic analysis. There was no existing database of bus traffic in Indiana urban areas. The Indiana public transit annual report (INDOT, 2019) and the bus schedule and route information of Indiana cities were utilized as the main sources of the urban bus traffic data. The bus

TABLE 4.1
**Service areas of the Indiana public transit systems**

| Peer Group | Service Area |
|---|---|
| Group One: large fixed route systems | Bloomington; Evansville; Fort Wayne; Indianapolis; Lafayette; Muncie; South Bend |
| Group Two: small fixed route systems | Anderson; Central Indiana; Columbus; Elkhart-Goshen; East Chicago; Gary; Michigan City; New Albany, Clarksville & Jeffersonville; Richmond; Terre Haute |
| Group Three: urban demand response systems | Kokomo; LaPorte; Northwestern Indiana; Valparaiso |
| Group Four: rural demand response systems | Bedford; Boone County; Cass County; Clinton County; Crawford, Harrison, Scott & Washington Counties; Dearborn, Decatur, Jefferson, Jennings, Ohio, Ripley & Switzerland Counties; DeKalb County; Fayette County; Franklin County; Fulton County; Hamilton County; Hancock County; Hendricks & Morgan Counties; Huntingburg; Huntington County; Jasper, Pulaski, Starke & Newton Counties; Jay, Randolph, Blackford & Henry Counties; Johnson, Shelby & Brown Counties; Knox County; Kosciusko County; LaGrange County; Madison County; Marion; Marshall County; Miami County; Mitchell; Monroe, Lawrence, Owen & Putnam Counties; New Castle; Noble County; Orange County; Rush County; Seymour; Southern Indiana (Daviess, Dubois, Gibson, Greene, Martin, Perry, Pike, Spencer, Sullivan & Warrick Counties); Steuben County; Union County; Vigo County; Wabash County; Washington; Waveland; Wells County; White County; Whitley County |
| Northern Indiana commuter transportation district | Rail Corridor between South Bend, IN and Chicago, IL |

TABLE 4.2
**Bus traffic in Lafayette/West Lafayette**

| | Number of Daily Services | | | |
|---|---|---|---|---|
| **Bus Route No.** | **Monday–Friday** | **Saturday** | **Sunday** | **AADTT** |
| 1A | 64 | 50 | 20 | 56 |
| 1B | 72 | 50 | 35 | 63 |
| 2A | 56 | 22 | 0 | 43 |
| 2B | 56 | 22 | 0 | 43 |
| 3 | 59 | 26 | 20 | 49 |
| 4A | 63 | 55 | 20 | 56 |
| 4B | 64 | 48 | 20 | 55 |
| 5 | 80 | 0 | 0 | 57 |
| 6A | 56 | 46 | 20 | 49 |
| 6B | 50 | 44 | 0 | 42 |
| 7 | 63 | 46 | 20 | 54 |
| 9 | 44 | 0 | 0 | 31 |
| 10 | 54 | 22 | 0 | 42 |
| 21A | 89 | 16 | 0 | 66 |
| 23 | 96 | 24 | 0 | 72 |
| 24 | 57 | 0 | 0 | 41 |
| 35 | 128 | 10 | 0 | 93 |
| 13 | 112 | 0 | 0 | 80 |

schedule and route information of each city is available on the bus service's web site. Table 4.2 presents the average annual daily bus traffic in Lafayette (including West Lafayette) obtained from the bus schedule and route information as an example of the city bus volume calculations on the fixed bus routes.

In addition to the bus traffic volumes, the bus axle load spectra are also needed for pavement design with MEPDG. The bus axle load values were obtained from the Indiana public transit annual report (INDOT, 2019) and from the information provided by bus manufacturers. The generated bus axle load data include vehicle capacity, engine type, curb weight, full-seat weight, full-bus weight, and gross vehicle weight rating (GVWR). The curb weight of a bus is the bus weight without any passengers on the bus. The full-seat weight represents the bus weight when all seats are occupied without standing passengers. The full-bus weight refers to the bus weight when the bus is full of seated and standing passengers. The gross vehicle weight rating expresses the bus maximum operating weight. The gross vehicle weight rating (GVWR) is the maximum operating weight of a vehicle as specified by the manufacturer, including the vehicle's chassis, body, engine, engine fluids, fuel, accessories, driver, and passengers. Some of the bus weights involve the number of passengers and their estimated body weights. The mean body weights of different age groups, races, and genders in the National Health Statistics Reports (Fryar et al., 2018) were used as passenger weights for estimating the full-seat weights and the full-bus weights. The typical types of buses serving in the three public transit peer groups are shown in Figure 4.1. These buses have different vehicle weights, axle arrangements, capacities, and other characteristics. The bus weight related data for the buses in the urban areas were obtained in terms of peer groups and types of buses. The data in public transit system Group One are presented in Table 4.3 and those for Group Two and Group Three are in Table 4.4.

MEPDG requires the axle loads in pavement design, thus the bus weights must be appropriately allocated to the bus axles. In order to allocate a bus weight to the bus axles, the weight distributions on the axles should be determined. It was found that one of the WIM stations was located on a city bus route. The WIM station was located on I-65, 8.2 miles north of Indiana and Kentucky state line. On this bus service route, the type of public transit bus has two single axles. Comparing the scheduled time that the service bus past the WIM site and the WIM recorded vehicle dada, the


(a) Group One (large fixed route systems) bus


(b) Group Two (small fixed route systems) bus


(c) Group Three (urban demand response systems) bus

**Figure 4.1** Typical public transit buses.

bus axle weights were identified. The distribution of vehicle weights was determined for the bus with two single axles as illustrated in Figure 4.2. As can be seen from the figure, the front axle bears 43% of the bus weight, and the remaining 57% of the bus weight falls on the rear axle.

In addition to buses with two axles, buses with three axles were also in service in some cities. However, there were no WIM stations on the bus transit routes for those buses with three axles. Since the buses with three axles did not pass any WIM sites, their axle loads were not directly measured and recorded. In order to estimate the load distribution over the three axles, all buses with three axles were extracted from the WIM database and the load distributions were calculated. The mean load distributions for the buses with three axles were calculated as 62%, 26%, and 12% for the front axle, the middle axle, and the rear axle, respectively. These calculated load distributions are utilized to represent the axle load distribution of the three-axle buses in the public transit system. Figure 4.3 displays the three-axle bus configuration and axle load allocations.

The generated public transit bus traffic information in the Indiana urban areas is stored in ArcMap, which is an ArcGIS based platform (Esri, 2020). ArcGIS is a geographic information system (GIS) for working with maps and geographic information maintained by the Environmental Systems Research Institute (Esri). ArcMap, a component of ArcGIS, represents geographic information as a collection of layers and other elements on a map. Figure 4.4 shows the ArcMap interface of the public transit bus traffic information.

In the ArcMap program, the statewide public transit GIS bus traffic map (Figure 4.5) contains all public transit bus routes in Indiana. In the map, the bus routes of the urban areas are stored in the green clusters and each green cluster represents the bus information on a set of bus routes in a given area. The ArcMap software also provides a bus traffic distribution map as shown in Figure 4.6. This map displays the bus traffic levels in Indiana in different colors. It can be seen in Figure 4.6 that the bus traffic volumes in Indianapolis, Lafayette, and Bloomington areas are relatively higher than other urban areas.

To find detailed bus traffic information, including street sections, bus volumes, and axle loads, the location can be selected on the GIS map shown in Figure 4.5 by clicking the corresponding cluster. For example, the Indianapolis bus routes can be displayed as shown in Figure 4.7.

A particular route can be selected to display the information of that route. As an example, bus route 13 in Indianapolis is selected on the program interface (Figure 4.8) and the route 13 is displayed on a new map in blue color (Figure 4.9). The bus traffic information can be retrieved and displayed as shown in Figure 4.10.

TABLE 4.3
**Bus weights in peer group one**

| Peer Group | City | Vehicle Capacity | Engine Type | Number of Vehicles | Curb Weight (lbs) | Full-Seat Weight (lbs) | Full-Bus Weight (lbs) | Gross Vehicle Weight Rating (GVWR) (lbs) |
|---|---|---|---|---|---|---|---|---|
| Group One: Large Fixed Route Systems | Lafayette | 11 | Diesel | 1 | 7,500 | 9,685 | 10,414 | 12,000 |
| | | 13 | CNG | 5 | 10,000 | 12,549 | 13,460 | 15,000 |
| | | 35 | Diesel | 5 | 25,100 | 31,656 | 38,029 | 40,000 |
| | | 40 | CNG/Diesel | 39 | 28,500 | 35,966 | 43,250 | 45,000 |
| | | 42 | CNG | 15 | 30,000 | 37,830 | 45,479 | 47,000 |
| | | 45 | Diesel | 3 | 27,000 | 35,377 | 43,571 | 45,000 |
| | | 54 | CNG | 1 | 38,000 | 48,016 | 57,849 | 59,000 |
| | | 60 | Diesel | 8 | 39,000 | 50,108 | 61,034 | 63,000 |
| | Indianapolis | 38 | Diesel | 123 | 25,700 | 32,802 | 39,722 | 41,000 |
| | | 39 | Electric/Diesel | 55 | 31,200 | 38,484 | 45,586 | 47,000 |
| | | 54 | Diesel | 11 | 35,000 | 45,016 | 54,849 | 56,000 |
| | Bloomington | 13 | CNG | 1 | 10,000 | 12,549 | 13,460 | 15,000 |
| | | 16 | CNG | 1 | 13,000 | 16,096 | 17,553 | 19,000 |
| | | 29 | Electric/Hybrid/Diesel | 3 | 29,000 | 34,463 | 37,012 | 39,000 |
| | | 31 | Diesel | 2 | 24,500 | 30,327 | 35,972 | 37,000 |
| | | 32 | Electric/Hybrid/Diesel | 23 | 29,300 | 35,309 | 41,137 | 43,000 |
| | | 40 | Diesel | 9 | 26,000 | 33,466 | 40,750 | 42,000 |
| | Evansville | 12 | Diesel | 3 | 8,000 | 10,367 | 11,278 | 13,000 |
| | | 15 | Diesel | 1 | 11,000 | 13,914 | 15,188 | 17,000 |
| | | 17 | Diesel | 7 | 11,900 | 15,178 | 16,635 | 18,000 |
| | | 18 | Diesel | 6 | 12,000 | 15,460 | 17,099 | 19,000 |
| | | 21 | Diesel | 2 | 14,000 | 18,006 | 19,827 | 21,000 |
| | | 22 | CNG | 1 | 15,500 | 19,688 | 21,691 | 23,000 |
| | | 26 | Electric/Diesel | 20 | 21,000 | 25,917 | 28,284 | 30,000 |
| | | 29 | Diesel | 2 | 21,500 | 26,963 | 29,512 | 31,000 |
| | | 31 | Diesel | 6 | 24,500 | 30,327 | 35,972 | 37,000 |
| | Fort Wayne | 14 | Diesel | 6 | 10,000 | 12,732 | 13,824 | 15,000 |
| | | 26 | Diesel | 3 | 17,500 | 22,417 | 24,784 | 26,000 |
| | | 32 | Hybrid/Diesel | 25 | 27,000 | 33,009 | 38,837 | 40,000 |
| | | 37 | Diesel | 3 | 25,000 | 31,920 | 38,658 | 40,000 |
| | | 38 | Hybrid | 5 | 28,500 | 35,602 | 42,522 | 44,000 |
| | Muncie | 13 | CNG/Diesel | 15 | 10,000 | 12,549 | 13,460 | 15,000 |
| | | 27 | Diesel | 3 | 18,000 | 23,099 | 25,466 | 27,000 |
| | | 32 | Electric/Diesel | 20 | 29,300 | 35,309 | 41,137 | 43,000 |
| | | 33 | Electric/Diesel | 10 | 29,400 | 35,591 | 41,601 | 43,000 |
| | South Bend | 35 | Diesel | 1 | 25,100 | 31,656 | 38,029 | 40,000 |
| | | 11 | Diesel | 16 | 7,500 | 9,685 | 10,414 | 12,000 |
| | | 12 | Diesel | 1 | 8,000 | 10,367 | 11,278 | 13,000 |
| | | 29 | CNG/Diesel | 48 | 24,000 | 29,463 | 32,012 | 34,000 |

TABLE 4.4
**Bus weights in peer group two and group three**

| Peer Group | City | Vehicle Capacity | Engine Type | Number of Vehicles | Curb Weight (lbs) | Full-Seat Weight (lbs) | Full-Bus Weight (lbs) | Gross Vehicle Weight Rating (GVWR) (lbs) |
|---|---|---|---|---|---|---|---|---|
| Group Two: Small Fixed Route Systems | Anderson | 11 | Diesel | 4 | 7,500 | 9,685 | 10,414 | 12,000 |
| | | 17 | Diesel | 7 | 11,900 | 15,178 | 16,635 | 18,000 |
| | | 18 | Diesel | 7 | 12,000 | 15,460 | 17,099 | 19,000 |
| | Columbus | 12 | CNG | 4 | 8,800 | 11,167 | 12,078 | 14,000 |
| | | 15 | CNG | 1 | 12,500 | 15,414 | 16,688 | 18,000 |
| | | 22 | Diesel | 5 | 14,100 | 18,288 | 20,291 | 22,000 |
| | | 44 | Diesel | 4 | 26,500 | 34,695 | 42,707 | 44,000 |
| | Elkhart-Goshen | 22 | Diesel | 1 | 14,100 | 18,288 | 20,291 | 22,000 |
| | | 25 | Diesel | 10 | 17,000 | 21,735 | 23,920 | 25,000 |
| | | 26 | Diesel | 2 | 17,500 | 22,417 | 24,784 | 26,000 |
| | Gary | 25 | Diesel | 17 | 17,000 | 21,735 | 23,920 | 25,000 |
| | | 31 | Diesel | 3 | 24,500 | 30,327 | 35,972 | 37,000 |
| | Michigan City | 14 | Diesel | 1 | 10,000 | 12,732 | 13,824 | 15,000 |
| | | 16 | Diesel | 2 | 11,900 | 14,996 | 16,453 | 18,000 |
| | | 30 | Diesel | 9 | 24,000 | 29,645 | 35,108 | 37,000 |
| | Richmond | 11 | CNG | 2 | 8,250 | 10,435 | 11,164 | 13,000 |
| | | 16 | CNG | 11 | 13,100 | 16,196 | 17,653 | 19,000 |
| | | 17 | CNG | 1 | 13,150 | 16,428 | 17,885 | 19,000 |
| | New Albany, Clarksville, & Jeffersonville | 28 | Diesel | 33 | 21,000 | 26,281 | 28,830 | 30,000 |
| | | 35 | Electric/Diesel | 11 | 31,000 | 37,556 | 43,929 | 45,000 |
| | | 36 | Electric/Diesel | 9 | 31,300 | 38,038 | 44,593 | 46,000 |
| | | 38 | Electric/Diesel | 38 | 31,500 | 38,602 | 45,522 | 47,000 |
| | | 40 | Electric/Diesel | 185 | 32,000 | 39,466 | 46,750 | 48,000 |
| | Terre Haute | 14 | CNG | 1 | 11,000 | 13,732 | 14,824 | 16,000 |
| | | 16 | Diesel | 1 | 11,900 | 14,996 | 16,453 | 18,000 |
| | | 22 | CNG/Diesel | 6 | 15,600 | 19,788 | 21,791 | 23,000 |
| | | 26 | Diesel | 6 | 17,500 | 22,417 | 24,784 | 26,000 |
| Group Three: Urban Demand Response Systems | Kokomo | 12 | CNG/Diesel | 17 | 8,800 | 11,167 | 12,078 | 14,000 |
| | | 14 | CNG | 6 | 11,000 | 13,732 | 14,824 | 16,000 |
| | | 31 | Diesel | 4 | 24,500 | 30,327 | 35,972 | 37,000 |
| | | 45 | Diesel | 3 | 27,000 | 35,377 | 43,571 | 45,000 |
| | Valparaiso | 16 | CNG | 5 | 13,100 | 16,196 | 17,653 | 19,000 |
| | | 53 | Diesel | 5 | 34,600 | 44,433 | 54,085 | 56,000 |


**Figure 4.2** Axle load distribution on two axles.

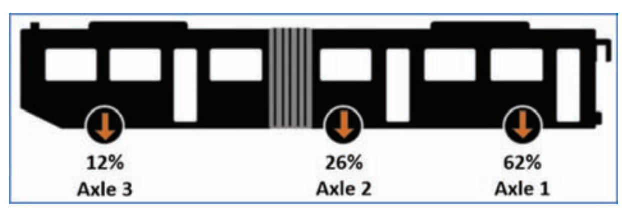


**Figure 4.3** Axle load distribution on three axles.

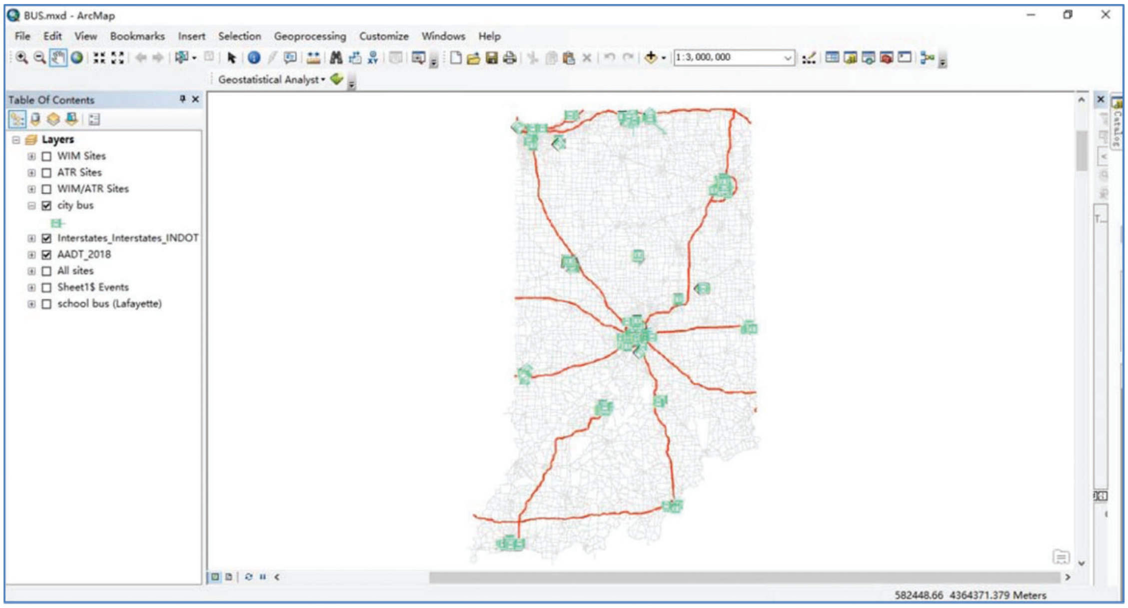


**Figure 4.4** ArcMap interface of the public transit bus traffic information.

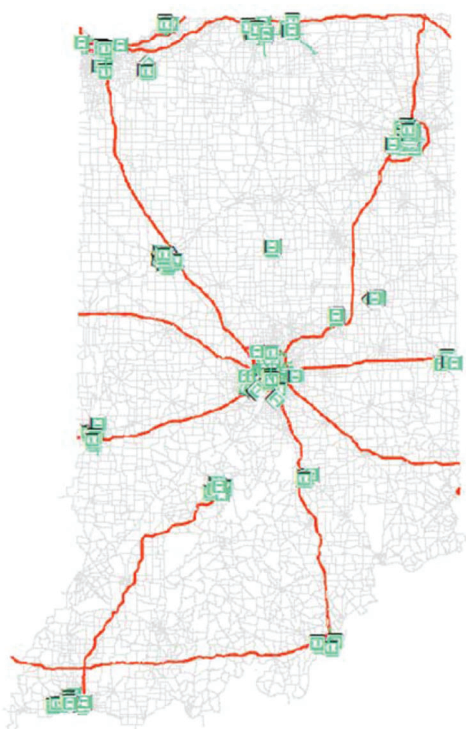

**Figure 4.5** GIS public transit bus map in Indiana.

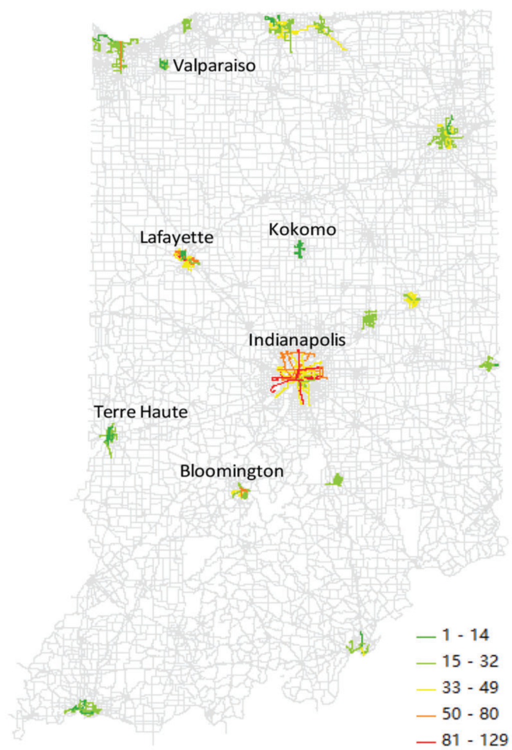


**Figure 4.6** Public transit bus traffic volume distribution.

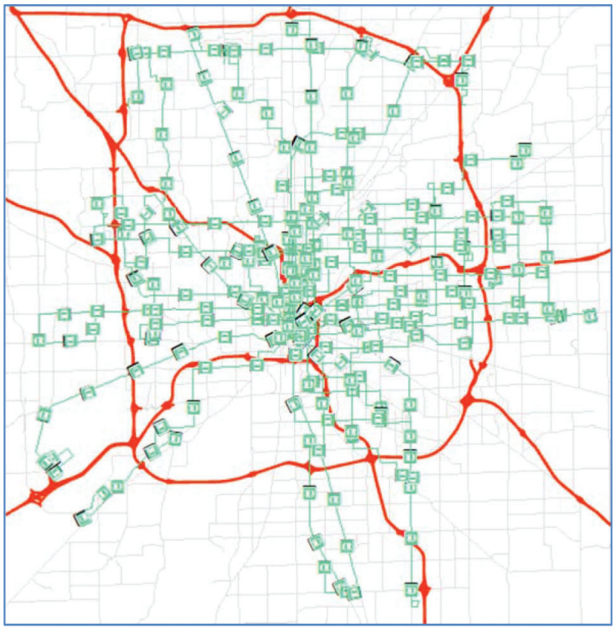

**Figure 4.7** Indianapolis public transit bus routes.

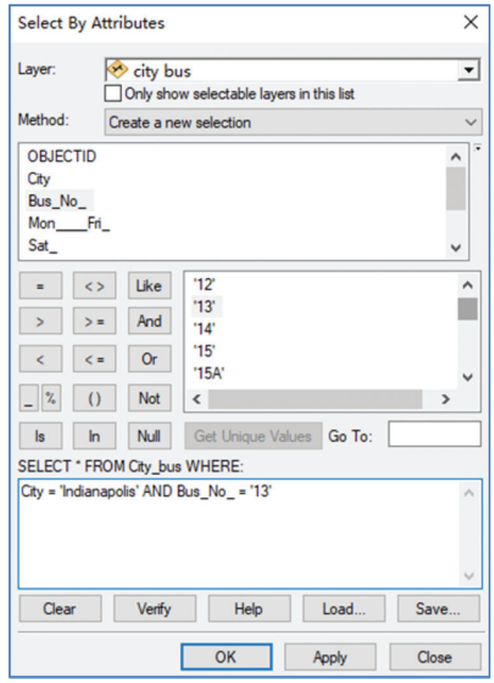


**Figure 4.8** Bus route selection.

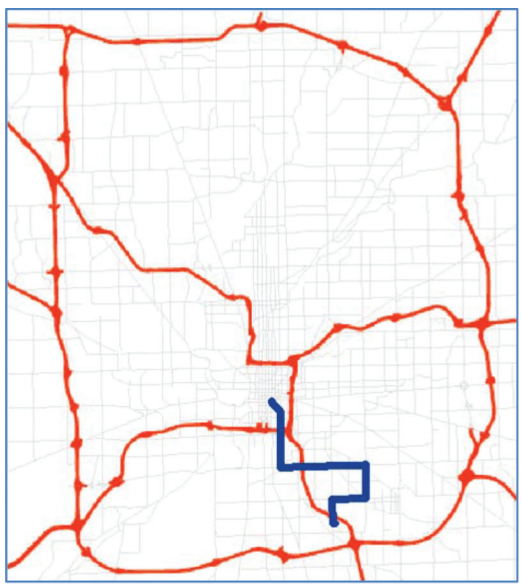

**Figure 4.9** Bus route 13 displayed on map.

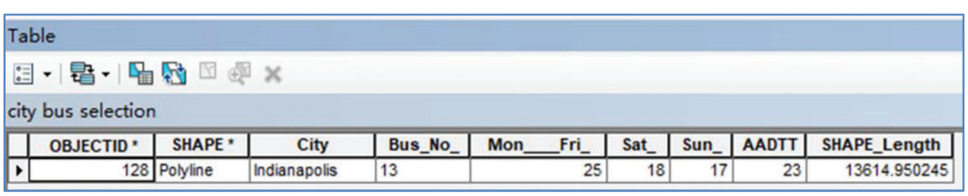

Table

city bus selection

| OBJECTID * | SHAPE * | City | Bus_No_ | Mon____Fri_ | Sat_ | Sun_ | AADTT | SHAPE_Length |
|---|---|---|---|---|---|---|---|---|
| 128 | Polyline | Indianapolis | 13 | 25 | 18 | 17 | 23 | 13614.950245 |

**Figure 4.10** Bus traffic information.

## 5. TRUCK WEIGHT ROAD GROUPS

The primary objective of this study is to update the traffic design input module, and thus to improve the current INDOT pavement design procedures. The current Truck Weight Road Groups (TWRG) are specified in 2013 Indiana Design Manual (page 44 in Chapter 304) (INDOT, 2013) as presented in Table 5.1. The AADTT values in the table include the truck traffic on all lanes and in both directions. It had been observed that the truck traffic volumes on many two-lane roads were much lower than 2,000 AADTT. On the other hand, the truck traffic volumes in some interstate segments were much higher than 20,000 AADTT. Therefore, it was necessary to examine groups A and D and determine if the groups should be further divided into more subgroups to accurately reflect the updated truck traffic and axle load spectra with respect to very low truck traffic on two-lane roads as well as very high truck traffic on interstate routes.

### 5.1 Truck Class Distributions

The truck traffic data from 90 ATR stations and 51 WIM stations in 2016, 2017, and 2018 were utilized to reveal the truck traffic distributions in terms of the truck weight road groups. The large amount of the truck traffic volumes in the 3 years from the 141 ATR and WIM stations were processed and sorted to examine their patterns and features. The processed data indicate that about 85% of the AADTT values on two-lane road are lower than 3,000. On the other hand, the truck traffic volumes on some interstate sections are much higher than 20,000 trucks per day. The statewide distribution of vehicle classes in the 3 years is shown in Figure 5.1. As can be seen in the figure, the highest number of trucks on Indiana highways are Class 9 vehicles followed by Class 5 vehicles.

The truck traffic data were then sorted according to the TWRG groups shown in Table 5.1 so that the truck class distributions in the TWRG groups can be examined separately. The truck class distributions for Groups A, B, C, and D are plotted in Figures 5.2, 5.3, 5.4, and 5.5, respectively. The most significant difference among the five groups is that in Group A (AADTT ≤ 3,000) the Class 5 volumes are much higher than Class 9 volumes as can be seen in Figure 5.2. That is, most of the trucks on low volume roads are Class 5 vehicles. Although the truck class distributions are all different in Groups B, C, and D, the general patterns of their vehicle class distributions are similar as illustrated in Figures 5.3, 5.4, and 5.5.

TABLE 5.1
**INDOT truck weight road groups**

| Group | Truck Traffic |
|---|---|
| A | AADTT ≤ 3,000 |
| B | 3,000 < AADTT ≤ 6,000 |
| C | 6,000 < AADTT ≤ 20,000 |
| D | AADTT > 20,000 |

### 5.2 Truck Weight Road Group A

To further investigate truck volumes in Group A, the truck traffic data from the INDOT GIS maps in the same 3 years (2016, 2017, and 2018) were also utilized in addition to the ATR and WIM recorded truck traffic data. The GIS data contain of 21,506 data points with AADTT ≤ 3,000. The frequency distribution of the 21,506 data points is presented in Figure 5.6. The frequency distribution reveals that most of the truck volumes in Group A are concentrated in the lower end of the range. The mean value of AADTT in Group A is 58. The four quartiles of 25%, 50%, 75%, and 100% are 16, 27, 73, and 3,000, respectively. Apparently, the truck traffic distribution in Group A is significantly skewed toward the very low end of the truck traffic.

The locations of ATR and WIM sites with lower than 3,000 AADTT are displayed in Figure 5.7. There are 43 ATR sites and 14 WIM sites with lower than 3,000 AADTT in the map. The truck traffic distributions in the ATR sites and in the WIM sites are shown in Figure 5.8. This figure indicates that at the ATR sites

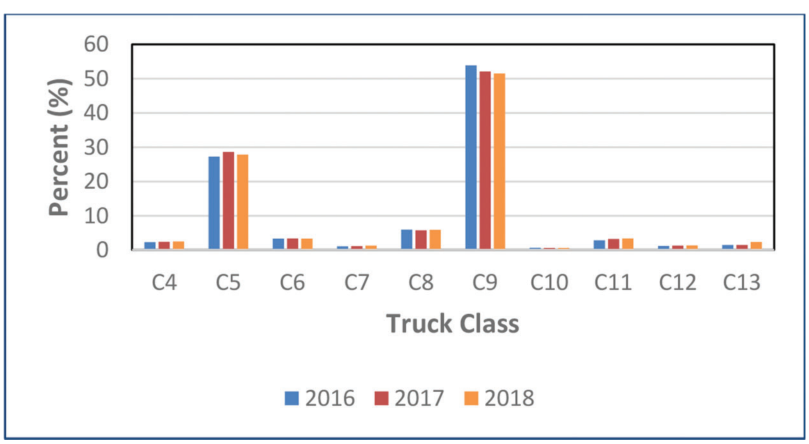


**Figure 5.1** Statewide truck class distribution.

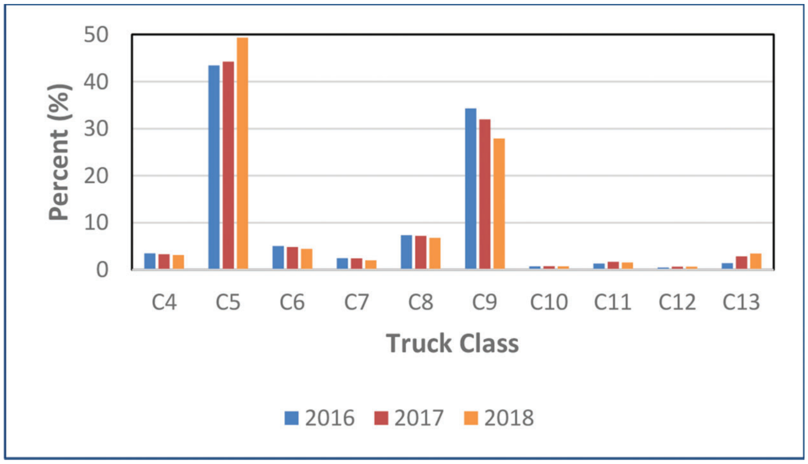


**Figure 5.2** Statewide Group A truck class distribution (AADTT ≤ 3,000).

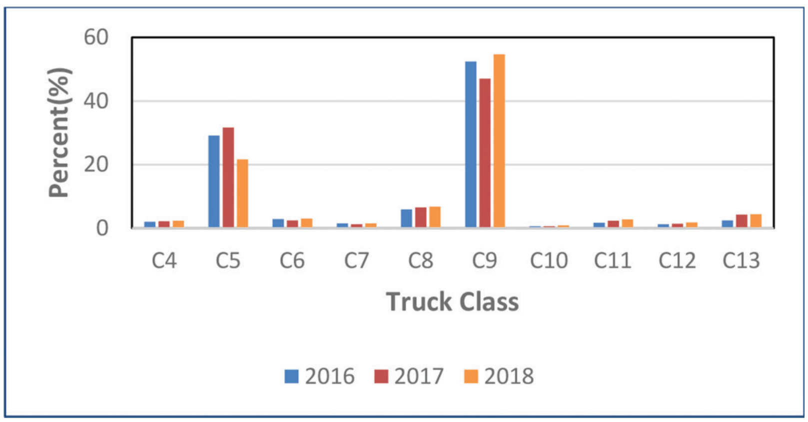


**Figure 5.3** Statewide Group B truck class distribution (3,001 < AADTT ≤ 6,000).

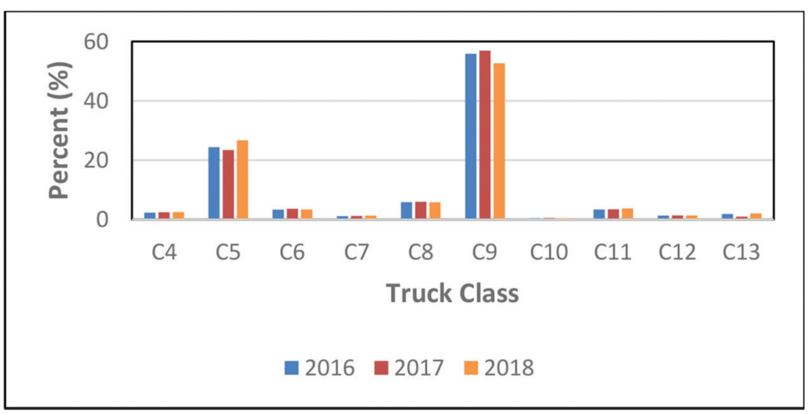


**Figure 5.4** Statewide Group C truck class distribution (6,001 < AADTT ≤ 20,000).

the highest frequencies of the truck volumes are in the truck traffic volume range less than 500. However, at the WIM sites the higest frequencies are within the AADTT range from 1,000 to 2,000.

Based on the above analysis and the practical experience of the Study Advisory Committee members, the subgroups of Group A as listed in Table 5.2 are proposed for future use in MEPDG pavement design. The truck class distributions with respect to the proposed subgroups are drawn in Figure 5.9. As can be seen in the figure, Class 5 vehicles are the dominating type of trucks in all subgroups. As the truck volume increases, the proportion of Class 9 vehicles increases and that of Class 5 vehicles decreases. The patterns of the truck class distributions are generally similar for all four subgroups.

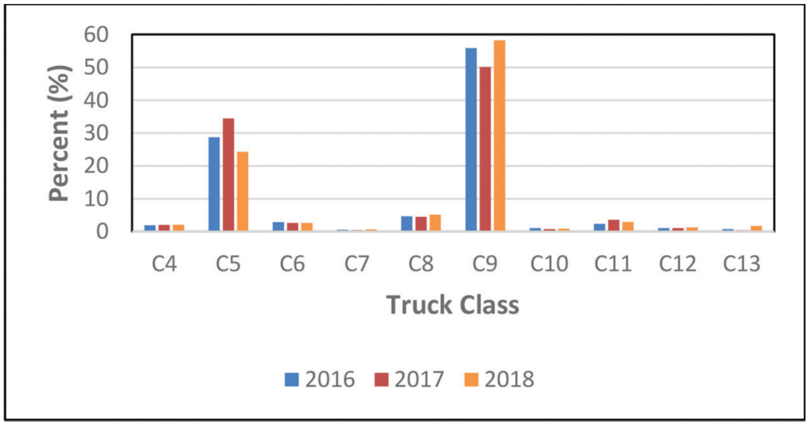


**Figure 5.5** Statewide Group D truck class distribution (AADTT > 20,000).

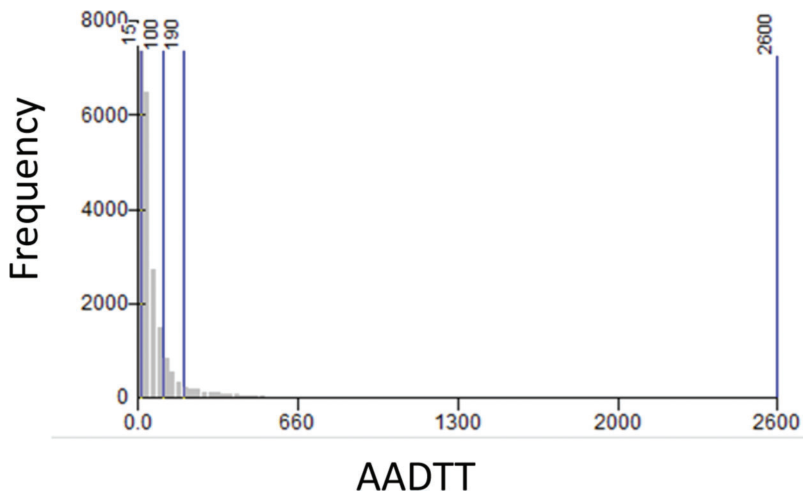


**Figure 5.6** Group A truck volume distribution (AADTT ≤ 3,000).

## 5.3 Truck Weight Road Group D

Group D is the truck weight road group with the highest truck volumes (AADTT > 20,000). The truck traffic volumes more than 20,000 occurred only on interstate highways as depicted in Figure 5.10, in which the locations of the Group D sites are marked in terms of WIM, ATR, and GIS data points. There were 136 road sections on interstate highways recorded AADTT values greater than 20,000. The truck traffic data in 2016, 2017, and 2018 indicate that the AADTT values at most of the sites in Group D were in the range between 20,000 and 40,000. An exception is the WIM site 402 on I-80 where the AADTT exceeded 70,000.

The statistical characteristics of the truck traffic data were calculated in order to explore the appropriate divisions of Group D truck traffic into subgroups. The calculated values of mean ($\mu$), standard deviation ($\sigma$), $\mu$-0.5$\sigma$, and $\mu$+0.5$\sigma$ are shown in Table 5.3.

If the truck traffic volumes in Group D were divided into the three subgroups in terms of mean and standard deviation: $0 < \text{AADTT} \leq \mu-0.5\sigma$, $\mu-0.5\sigma < \text{AADTT} \leq$

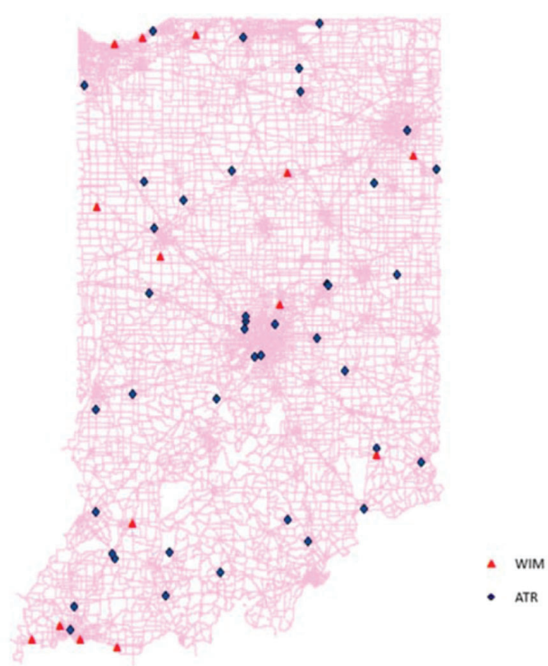


**Figure 5.7** Locations of ATR and WIM stations in Group A (AADTT ≤ 3,000).

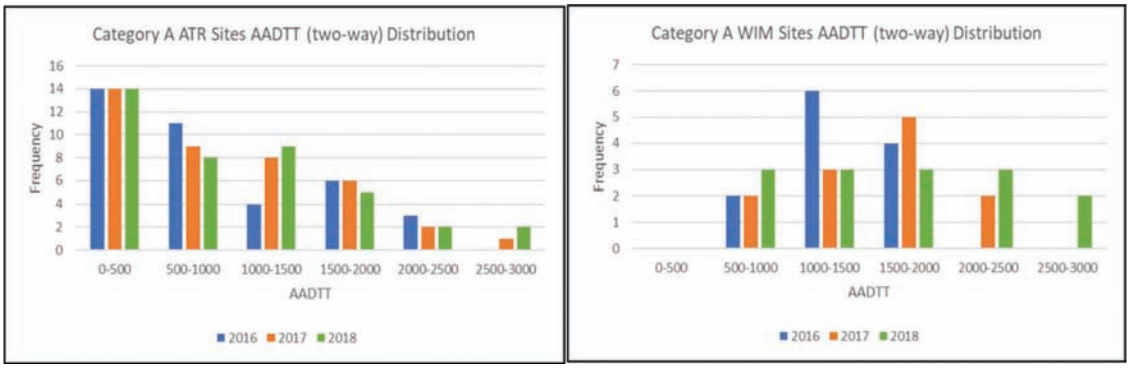


**Figure 5.8** Truck traffic distributions at ATR sites and WIM sites in Group A.

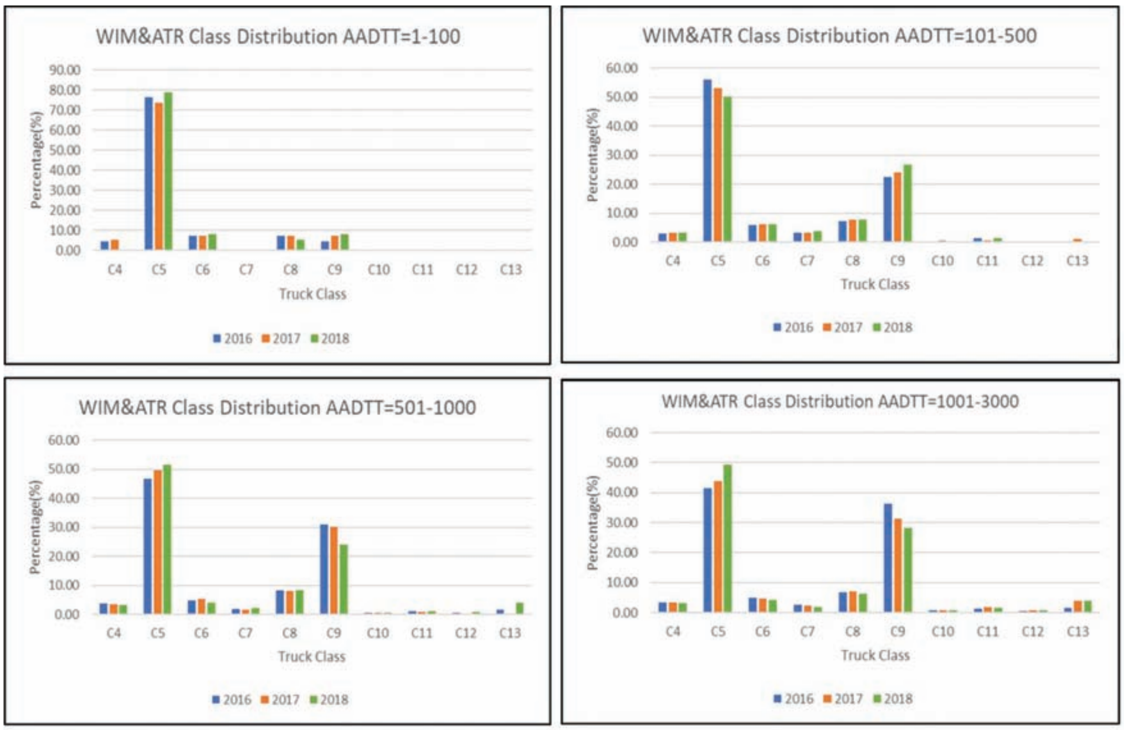


**Figure 5.9** Truck class distributions with combined ATR and WIM data in Group A.

TABLE 5.2
**Truck weight road subgroups of Group A**

| Group A (AADTT ≤ 3,000) | |
|---|---|
| **Subgroup** | **Truck Traffic** |
| A1 | 0 < AADTT ≤ 100 |
| A2 | 100 < AADTT ≤ 500 |
| A3 | 500 < AADTT ≤ 1,000 |
| A4 | 1,000 < AADTT ≤ 3,000 |

$\mu + 0.5\sigma$, and AADTT $> \mu + 0.5\sigma$, the ranges of the three subgroups would be as follows:

- Subgroup 1: 0 < AADTT ≤ 25,810
- Subgroup 2: 25,810 < AADTT ≤ 39,697
- Subgroup 3: AADTT > 39,697

TABLE 5.3
**Truck traffic statistics in Group D**

| $\mu$ | $\sigma$ | $\mu$-0.5$\sigma$ | $\mu$+0.5$\sigma$ |
|---|---|---|---|
| 32,753.5 | 13,887 | 25,810 | 39,697 |

The truck traffic volumes were also arranged in terms of quartiles to further inspect the ranges of the subgroups in a different way. The recorded truck traffic data in Group D are displayed as a scatter plot in Figure 5.11 to assess their spread along the four quartiles. The corresponding AADTT values of the quartiles are 25,027 for 25% quartile, 27,542 for 50% quartile, and 33,121 for 75% quartile. It should be noted that the 50% quartile is also the median of the data set. That is, in the Group D data set, half of the AADTT values are greater than 27,148 and half of those are less than 27,148.

Similar to the method using mean and standard deviation, Group D can be divided into the following three subgroups according to quartiles:

1. 20,000 < AADTT ≤ 25% quartile
2. 25% quartile < AADTT ≤ 75% quartile
3. AADTT > 75% quartile

The specific values of the three subgroups in terms of quartiles are as follows:

- Subgroup 1: 20,000 < AADTT ≤ 25,027
- Subgroup 2: 25,027 < AADTT ≤ 33,121
- Subgroup 3: AADTT > 33,121

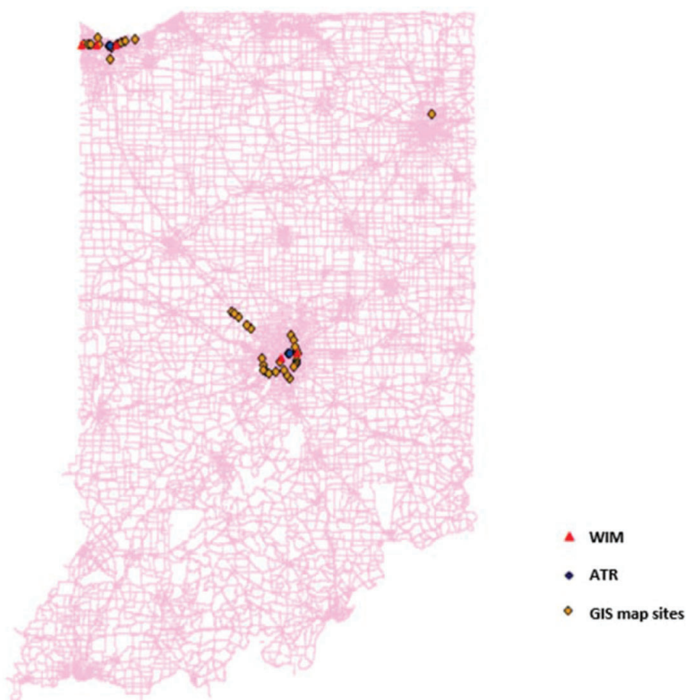


**Figure 5.10** Locations of in Group D (AADTT > 20,000).

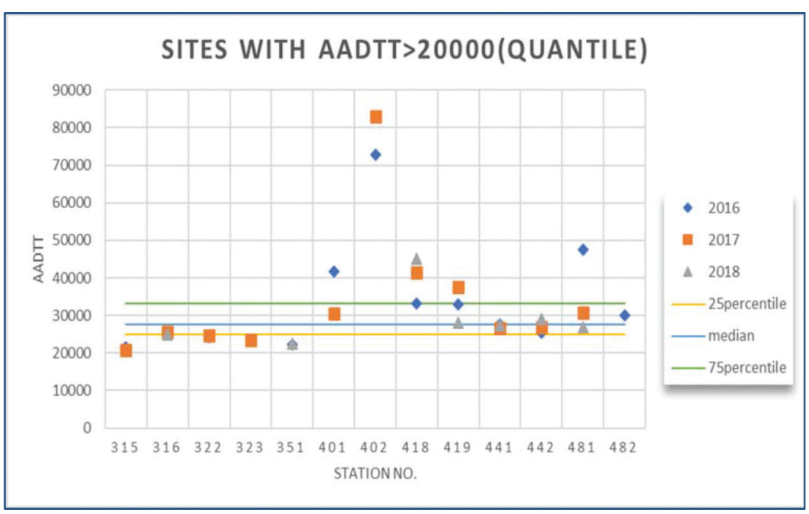


**Figure 5.11** Scatter plot of Group D truck volumes.

The subgroups obtained through mean and standard deviation as well as quartiles are presented in Table 5.4. The values of the subgroups from the two methods are actually quite close except for the up values in Subgroup 2 with 39,697 from the mean and standard deviation method and 33,121 from the quartile method. In fact, the ATR and WIM recorded truck traffic data actually showed the AADTT values at most of the sites in Group D were in the range between 20,000 and 40,000. Therefore, the value of 39,697 from the mean and standard deviation method should be a reasonable choice. For the purpose of practical and easy to use, the values are rounded to the nearest thousand for the proposed truck road subgroups of Group D in Table 5.5.

The truck class distributions of the proposed subgroups D1, D2, and D3 are illustrated in Figures 5.12, 5.13, and 5.14, respectively. All three figures demonstrate that Class 9 vehicles are the dominating type of trucks in all three subgroups. The patterns of the truck class distributions of the subgroups are generally similar. Group D truck traffic sections are all on interstate highways. The truck weight road groups, including subgroups D1, D2, and D3, are exhibited in a three-dimensional graph in Figure 5.15. The graph clearly indicates that Group D road groups are primarily located in three concentrated areas.

TABLE 5.4
**Possible subgroups of Group D**

| | AADTT Range | |
|---|---|---|
| **Subgroup** | **Mean and Standard Deviation** | **Quartile** |
| 1 | 20,000–25,810 | 20,000–25,027 |
| 2 | 25,810–39,697 | 25,027–33,121 |
| 3 | > 39,697 | > 33,121 |

TABLE 5.5
**Truck weight road subgroups of Group D**

| | Group D (AADTT ≥ 20,000) |
|---|---|
| **Subgroup** | **Truck Traffic** |
| D1 | 20,000 < AADTT ≤ 25,000 |
| D2 | 25,000 < AADTT ≤ 40,000 |
| D3 | AADTT > 40,000 |

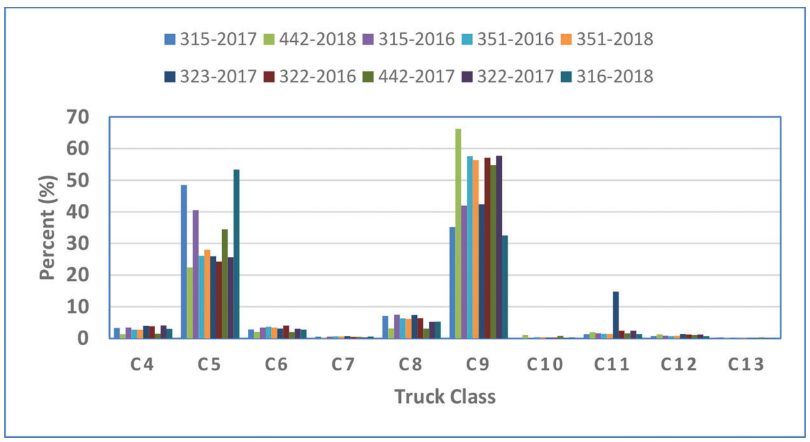


**Figure 5.12** Truck class distribution of Subgroup D1 (20,000 < AADTT ≤ 25,000).

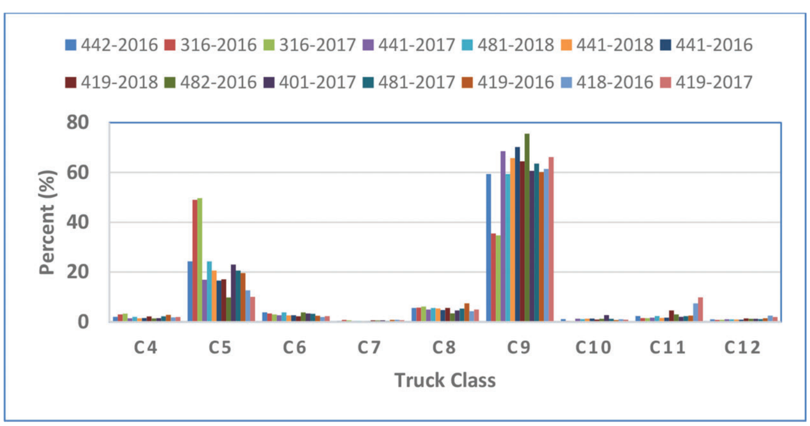


**Figure 5.13** Truck class distribution of Subgroup D2 (25,000 < AADTT ≤ 40,000).

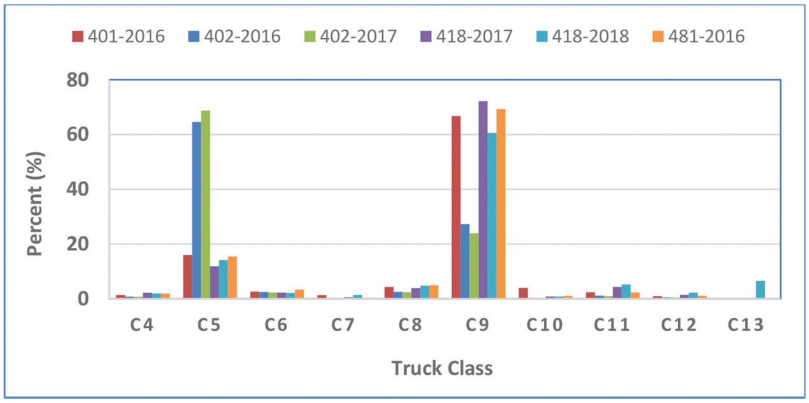


**Figure 5.14** Truck class distribution of Subgroup D3 (AADTT > 40,000).


**Figure 5.15** Three-dimensional display of truck weight road groups on Indiana interstate.

## 6. EQUIVALENT SINGLE AXLE LOAD VALUES

The Equivalent Single Axle Load (ESAL) values have been utilized in the American Association of State Highway and Transportation Officials pavement design method (AASHTO, 1993) to establish a damage relationship for comparing the effects of axles carrying different loads. In order to assess the impact of different types of vehicles on a pavement structure on a common basis, all vehicle axle loads are converted to a number of 18,000-lbs (80 kN) Equivalent Single Axle Loads (ESALs). WIM data were used 20 years ago to determine ESAL values for INDOT pavement design (Gulen et al., 2000). Although ESAL values are no longer used in pavement design with MEPDG, they are still useful in such areas as pavement asset management, pavement pay item calculation, safety analysis, and financial analysis. Therefore, it was desired to update ESAL values with the most recent available traffic data. In this study, new ESAL values were determined through two methods, the AASHTO equation method (AASHTO, 1993) and the axle group divisor method (Indiana Administrative Code, 2020), as described in the following sections.

### 6.1 AASHTO Equations

ESAL values are affected by not only the weights of individual axles, but also the configurations and arrangements of axles, such as single axles, tandem axles, and tridem axles. In order to use the traffic data for ESAL calculation, the WIM data were processed to group axle weights in terms of axle configurations. Because the vehicle loads impact rigid and flexible pavement differently, the ESAL equations for the two types of pavements are different. The WIM stations with axle load data on rigid (Portland cement concrete pavement or PCCP) and flexible (hot mix asphalt or HMA) pavements are listed in Table 6.1.

The AASHTO ESAL equation for rigid pavement is as follows (Pavement Interactive, n.d.a):

$$\frac{W_x}{W_{18}} = \left(\frac{L_{18}+L_{2s}}{L_x+L_{2x}}\right)^{4.62} \left(\frac{10^{G/\beta_x}}{10^{G/\beta_{18}}}\right)(L_{2x})^{3.28} \quad \text{(Eq. 6.1)}$$

Where:

$W_{18}$ = predicted number of 18,000 lb single axle load applications

$W_x$ = predicted number of $x \times 1{,}000$ lb single axle load applications. e.g., $W_{30}$ = number of 30,000 lb single axle applications

$L_x$ = axle load being evaluated (kips). e.g., $L_{30}$ = 30

$L_{18}$ = 18 (standard axle load in kips)

$L_{2x}$ = code for axle configuration: 1 for single axle; 2 for tandem axle; 3 for triple axle

$L_{2s}$ = code for standard axle = 1 (single axle)

$G = \log\left(\frac{4.5-p_t}{4.5-1.5}\right)$, a function of the ratio of loss in serviceability at time, t, to the potential loss taken at a point where $p_t$ = 1.5

$p_t$ = "terminal" serviceability index (point at which the pavement is considered to be at the end of its useful life)

$\beta = 1.0 + \left(\frac{3.63(L_x+L_{2x})^{5.20}}{(D+1)^{8.46}L_{22x}^{3.52}}\right)$, function which determines the relationship between serviceability and axle load applications. Where D = slab depth in inches.

The AASHTO ESAL equation for flexible pavement is as follows (Pavement Interactive, n.d.b):

$$\frac{W_x}{W_{18}} = \left(\frac{L_{18}+L_{2s}}{L_x+L_{2x}}\right)^{4.79} \left(\frac{10^{G/\beta_x}}{10^{G/\beta_{18}}}\right)(L_{2x})^{4.33} \quad \text{(Eq. 6.2)}$$

Where:

$W_{18}$ = number of 18,000 lb single axle load applications

$W_x$ = predicted number of $x \times 1{,}000$ lb single axle load applications. e.g., $W_{30}$ = number of 30,000 lb single axle applications

$L_x$ = axle load being evaluated (kips). e.g., $L_{30}$ =30

$L_{18}$ = 18 (standard axle load in kips)

$L_{2x}$ = code for axle configuration: 1 for single axle; 2 for tandem axle; 3 for triple axle

$L_{2s}$ = code for standard axle = 1 (single axle)

$G = \log\left(\frac{4.2-p_t}{4.2-1.5}\right)$, a function of the ratio of loss in serviceability at time, t, to the potential loss taken at a point where $p_t$ = 1.5

$p_t$ = "terminal" serviceability index (point at which the pavement is considered to be at the end of its useful life)

$ß = 0.4 + \left(\frac{0.081(L_x+L_{2x})^{3.23}}{(SN+1)^{5.19}L_{2x}^{3.23}}\right)$, function which determines the relationship between serviceability and axle load applications. Where SN = structure number

In addition to the WIM traffic data, the slab thickness (D) and terminal serviceability index ($p_t$) are needed to calculate the ESAL values for rigid pavement. The PCCP slab thickness of 10 inches and terminal serviceability index of 2.5 were assumed in ESAL calculation. For flexible pavement, the structural number (SN) of 5 and the terminal serviceability index ($p_t$) of 2.5 were utilized in the ESAL calculation of HMA pavements.

## 6.2 Axle Group Divisors

The Indiana Administrative Code specifies the following axle group divisor method for calculating ESAL values (Indiana Administrative Code, 2020):

1. The ESAL value for each axle group shall be calculated as follows:

   a. The ESAL value for each axle shall be calculated as the actual axle weight, divided by the axle group divisor (as defined in (4), below), all raised to the fourth power ((weight/divisor)$^4$).
   b. The numerator for each axle group is the sum of the axle weights of all individual axles within that axle group, or the combined gross axle weight (GAW).
   c. The divisor for each axle group depends on the number of axles in the group.
   d. Divisors shall be as follows:

      i. If the axle group consists of a single axle, the divisor is eighteen thousand (18,000) pounds.
      ii. If the axle group consists of a tandem axle (that is, two (2) individual axles), the divisor is thirty-three thousand two hundred (33,200) pounds.
      iii. If the axle group consists of a tridem axle (that is, three (3) individual axles), the divisor is forty-six thousand (46,000) pounds.

TABLE 6.1
**WIM stations on rigid and flexible pavements**

| Pavement Type | WIM Station No. |
|---|---|
| Rigid (PCCP) | 120, 200, 230, 351, 352, 401, 402, 420, 441, 442, 481, 482, 560, 630, 990, 999 |
| Flexible (HMA) | 100, 102, 106, 109, 210, 220, 270, 310, 315, 316, 321, 325, 326, 331, 332, 340, 360, 370, 406, 430, 436, 450, 460, 470, 490, 507, 520, 530, 540, 600, 610, 620, 640, 650, 660 |

iv. If the axle group consists of a quad axle (that is, four (4) individual axles), the divisor is fifty-seven thousand (57,000) pounds.
v. If the axle group consists of a quintuple axle (that is, five (5) individual axles), the divisor is sixty-five thousand (65,000) pounds.

e. The resultant fraction quantity is raised to the fourth power.

2. ESAL value for the sum of all axles of the vehicle shall be calculated as follows: (ESAL = Axle1 ESAL + Axle2 ESAL + Axle3 ESAL +…+ AxleN ESAL).

For example, if a Class 9 vehicle has the following axle load data:

- GAW = 71.2 kips
- Axle 1: single axle, axle load = 9.2 kips
- Axle 2: tandem axle, axle loads = 14.2 kips and 13.9 kips
- Axle 3: tandem axle, axle loads = 17.4 kips and 16.6 kips

The ESAL of the Class 9 truck can be calculated with the axle group divisors:

ESAL = ESAL(9.2 kips, single) + ESAL(14.2 + 13.9 kips, tandem) + ESAL(17.4 + 16.6 kips, tandem) = $(9.2/18)^4 + [(14.2 + 13.9)/33.2]^4 + [(17.4 + 16.6)/33.2)^4 = 1.681353$

### 6.3 ESAL Values

The 3-year WIM data of 2016, 2017, and 2018 were used for the data processing and analysis to calculate ESAL values. ESAL values were calculated for all of the WIM stations listed in Table 6.1 using both the AASHTO method and axle group divisor method. To describe the ESAL calculations, a WIM station on I-70 (WIM Site 106) was utilized to present the ESAL results. The location of the WIM station is shown in Figure 6.1. This section of the interstate highway has four lanes with HMA pavement. The ESAL values were calculated in groups of gross vehicle weight (GVW) consistent with the current INDOT practice. The maximum GVW of 126 kips, which is the current GVW limit for INDOT ESAL groups, was applied in the ESAL calculation. The ESAL values obtained with the AASHTO method and the axle load divisor method are shown in Table 6.2 and Table 6.3, respectively.

As can be seen in Tables 6.2 and 6.3, the ESAL values are presented in terms of GVW groups and vehicle classes. The vehicle class C0 represents the unclassified vehicles and C1, C2, and C3 are the first three types of the FHWA vehicle classification or the lightweight vehicles, including motorcycles, passenger cars, and four-tire single unit vehicles as depicted in Figure 6.2. It should be pointed out that the number of unclassified vehicles (C0) could be substantial in many WIM sites. Although they were not classified into particular types of vehicles due to various reasons, their axle loads were captured and recorded in the WIM database. In addition, the axle loads of unclassified vehicles tend to be considerably large. Therefore, it is essential to include unclassified vehicles in ESAL calculations.

The ESAL values on individual lanes at this WIM site were also obtained through the two calculation methods as listed in Table 6.2. This table includes the ESALs on all four lanes and the average of the four ESALs. The critical ESAL value in the last column of the table is defined as the highest lane ESAL value among the ESALs of the four lanes. It is important to identify the critical lane and its corresponding critical ESAL because the critical lane controls the pavement design, performance, and management. As shown in Table 6.2, the critical lane at this WIM site is Lane 3 (the eastbound driving lane) with a critical ESAL of 15,986,424 from the AASHTO method or a critical ESAL of 14,386,275 from the axle group divisor method.

With the traffic data at WIM 106, the average annual ESALs per truck for all types of trucks (C4 through C13) and for all types of trucks combined were also calculated with AASHTO and axle group divisor methods as presented in Table 6.3.

The ESAL values contained in Tables 6.2, 6.3, A.5, and A.6 are included in the final database along with truck volume and axle load spectra for this WIM site. Similar ESAL values for all WIM sites were obtained and will be provided for INDOT to use.

With all WIM sites combined, the obtained statewide average annual ESAL values for state roads, US routes, and interstate highways are included in Table 6.4. The values in the table contains ESAL values in terms of average of all ESALs as well as average of critical ESALs.


**Figure 6.1** WIM Station 106 on I-70 (Google, n.d.a).

TABLE 6.2
**Annual ESAL values on roadway lanes (WIM Site 106)**

| Method | Lane 1 | Lane 2 | Lane 3 | Lane 4 | Average | Critical |
|---|---|---|---|---|---|---|
| AASHTO | 2,595,924 | 1,419,681 | 15,986,424 | 675,872 | 5,169,475 | 15,986,424 |
| Axle Group Divisor | 2,599,606 | 1,258,462 | 14,386,275 | 635,848 | 4,720,048 | 14,386,275 |

TABLE 6.3
**Average annual ESALs per truck (WIM Site 106)**

| Method | C4 | C5 | C6 | C7 | C8 | C9 | C10 | C11 | C12 | C13 | All Types |
|---|---|---|---|---|---|---|---|---|---|---|---|
| AASHTO | 0.67 | 0.14 | 0.67 | 2.58 | 0.40 | 1.49 | 1.35 | 3.08 | 1.28 | 1.77 | 1.32 |
| Axle Group Divisor | 0.69 | 0.15 | 0.69 | 2.70 | 0.43 | 1.53 | 1.44 | 3.29 | 1.34 | 1.89 | 1.36 |

TABLE 6.4
**Average annual ESALs on different highways (all WIM sites)**

| | State Roads | US Routes | Interstate | All Roads Combined |
|---|---|---|---|---|
| All ESALs (AASHTO) | 5,145,581 | 2,097,309 | 34,249,589 | 21,817,344 |
| All ESALs (Axle Group Divisor) | 4,425,600 | 1,850,587 | 24,497,963 | 15,794,815 |
| Critical ESALs (AASHTO) | 4,102,108 | 1,461,136 | 20,894,434 | 13,480,725 |
| Critical ESALs (Axle Group Divisor) | 3,491,718 | 1,257,990 | 14,654,550 | 9,595,831 |

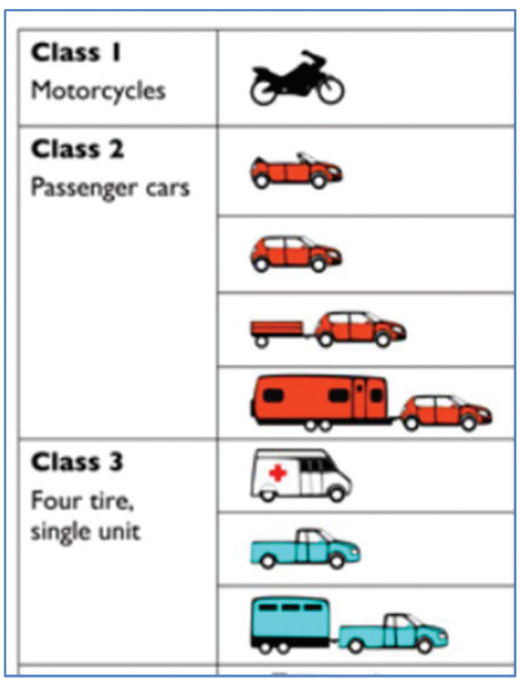

**Figure 6.2** Lightweight vehicles (C1, C2, C3).

## 6.4 Analysis and Observations

### *6.4.1 Comparison of the Two ESAL Calculation Methods*

As described above, two methods were utilized to calculate the ESAL values at WIM Site 106. To compare the two methods, the ESAL values from the two methods are listed in Table 6.5 along with the calculated differences. The ESAL differences (%) between the two methods are plotted in Figure 6.3.

If the first two points (GVW $<$ 6 kips) are excluded as outliers, it is shown in Table 6.5 and Figure 6.3 that, compared with the AASHTO method, the axle group divisor method yielded greater ESALs up to about 80 kips of GVW and smaller ESALs beyond 80 kips. The maximum of the differences is about 20%.

### *6.4.2 Effect of Unclassified Vehicles*

The WIM data at Site 106 as well as at many other WIM sites contain a sizable number of unclassified vehicles. It was observed that most of the unclassified vehicles tend to have axle loads similar to heavy trucks. Furthermore, ESAL calculations use axle loads but do not require vehicle classifications. Therefore, unclassified vehicles should be included in the ESAL calculations to reflect the actual vehicle load impact on pavement structures. The ESAL values and the ESAL differences between with and without unclassified vehicles are included in Table 6.6 for both AASHTO and axle group divisor methods. The ESAL differences are illustrated in Figure 6.4 for the two ESAL calculation methods. It is apparent that the ESAL differences are generally larger when GVW is greater than 90 kips. It is also apparent that most of the differences are significant, from 30% to near 100%. The graph in Figure 6.4 shows that percent differences in the AASHTO

TABLE 6.5
**Comparison of ESALs from two methods**

| GVW (kips) | AASHTO ESAL (A) | Axle Group Divisor ESAL (B) | Difference (B-A) | % Difference (B-A)/A |
|---|---|---|---|---|
| 3 | 31 | 20 | -11 | -35.1% |
| 6 | 3,108 | 3,043 | -65 | -2.1% |
| 9 | 3,801 | 4,338 | 537 | 14.1% |
| 12 | 2,876 | 3,368 | 492 | 17.1% |
| 15 | 3,339 | 3,775 | 436 | 13.1% |
| 18 | 5,981 | 6,546 | 565 | 9.5% |
| 21 | 12,824 | 13,606 | 782 | 6.1% |
| 24 | 19,271 | 20,064 | 794 | 4.1% |
| 27 | 23,756 | 24,562 | 807 | 3.4% |
| 30 | 31,474 | 32,666 | 1,192 | 3.8% |
| 33 | 41,675 | 43,630 | 1,955 | 4.7% |
| 36 | 56,665 | 60,028 | 3,363 | 5.9% |
| 39 | 65,705 | 70,399 | 4,694 | 7.1% |
| 42 | 80,915 | 87,579 | 6,664 | 8.2% |
| 45 | 101,453 | 109,884 | 8,431 | 8.3% |
| 48 | 125,889 | 135,785 | 9,896 | 7.9% |
| 51 | 139,144 | 150,533 | 11,389 | 8.2% |
| 54 | 156,611 | 169,099 | 12,489 | 8.0% |
| 57 | 179,363 | 192,524 | 13,162 | 7.3% |
| 60 | 209,774 | 223,580 | 13,806 | 6.6% |
| 63 | 251,389 | 265,599 | 14,210 | 5.7% |
| 66 | 302,622 | 316,712 | 14,090 | 4.7% |
| 69 | 378,500 | 392,335 | 13,835 | 3.7% |
| 72 | 469,329 | 482,229 | 12,900 | 2.7% |
| 75 | 604,400 | 615,399 | 10,999 | 1.8% |
| 78 | 761,022 | 769,659 | 8,637 | 1.1% |
| 81 | 891,603 | 897,404 | 5,801 | 0.7% |
| 84 | 882,049 | 881,451 | -598 | -0.1% |
| 87 | 785,073 | 777,672 | -7,401 | -0.9% |
| 90 | 736,137 | 717,072 | -19,065 | -2.6% |
| 93 | 633,135 | 609,340 | -23,795 | -3.8% |
| 96 | 620,597 | 580,651 | -39,945 | -6.4% |
| 99 | 646,601 | 594,248 | -52,353 | -8.1% |
| 102 | 710,163 | 642,883 | -67,280 | -9.5% |
| 105 | 831,802 | 739,189 | -92,614 | -11.1% |
| 108 | 982,091 | 856,504 | -125,587 | -12.8% |
| 111 | 1,066,800 | 925,419 | -141,381 | -13.3% |
| 114 | 1,159,984 | 989,977 | -170,007 | -14.7% |
| 117 | 1,346,141 | 1,128,282 | -217,859 | -16.2% |
| 120 | 1,644,927 | 1,350,679 | -294,248 | -17.9% |
| 123 | 1,736,871 | 1,411,937 | -324,934 | -18.7% |
| 126 | 1,973,012 | 1,580,520 | -392,492 | -19.9% |

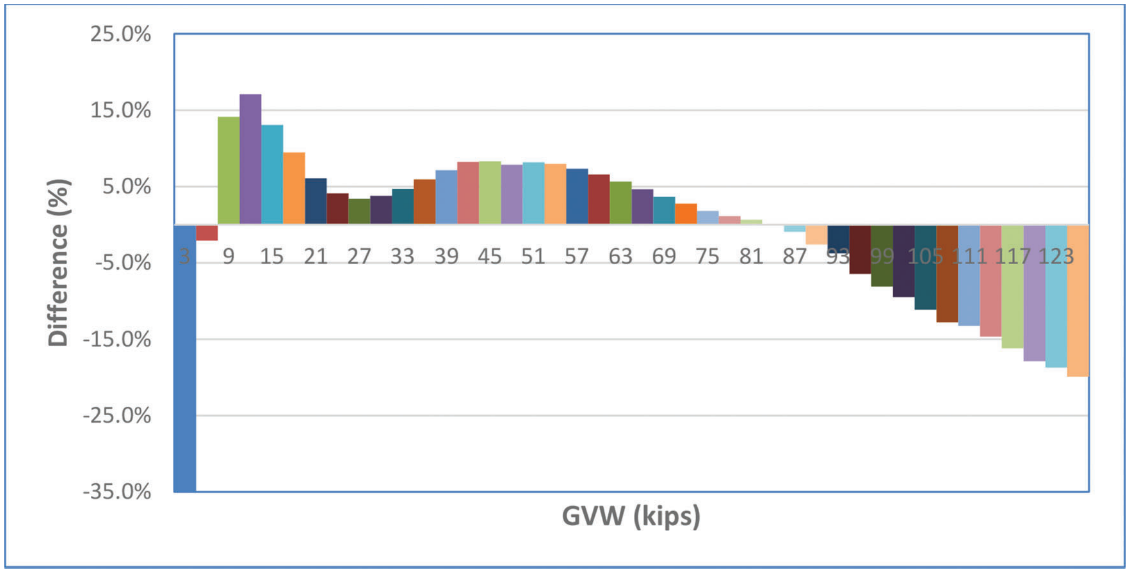


**Figure 6.3** ESAL differences between AASHTO and axle group divisor methods.

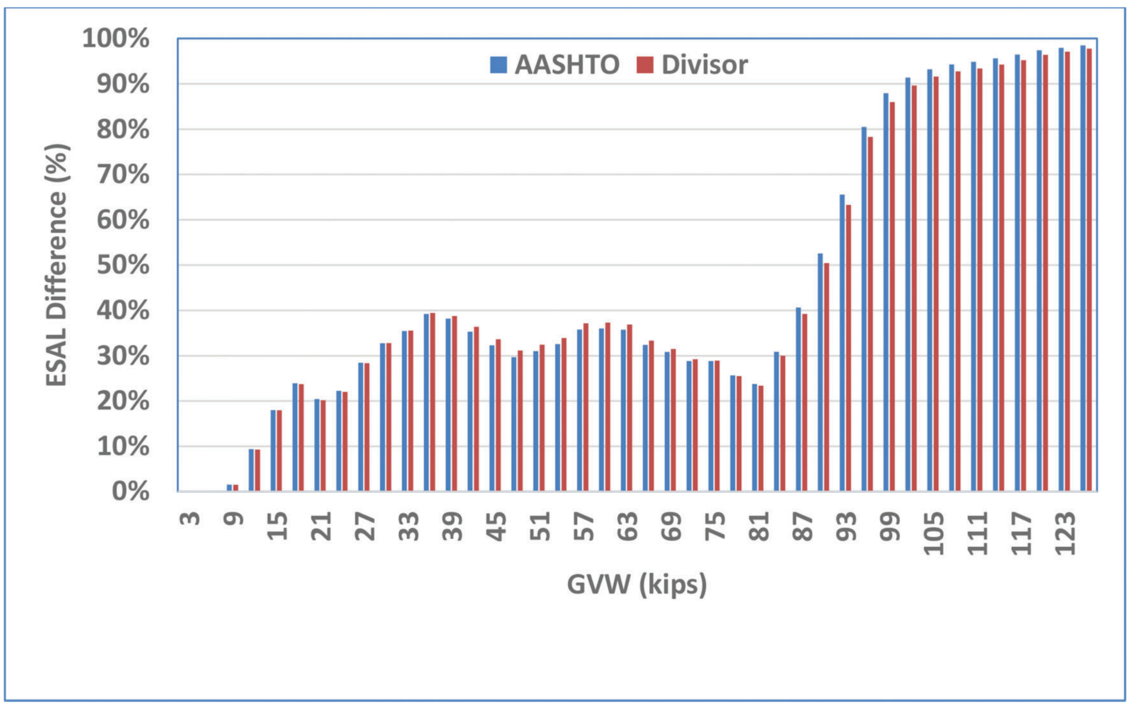


**Figure 6.4** Differences between ESAL values with and without unclassified vehicles.

method and in the axle group divisor are fairly close. It is evident that unclassified vehicles must be included in ESAL calculation. Otherwise, the ESAL values would be considerably underestimated.

*6.4.3 Effect of Lightweight Vehicles*

Lightweight vehicles (C1, C2, C3) were included in the ESAL calculations as the WIM data also contain axle load values of lightweight vehicles. To evaluate the effect of lightweight vehicles on ESALs, the ratios of ESAL from lightweight vehicles to ESAL from trucks are calculated and show in Table 6.7. The values indicate that, except for a few of low GVW values, the majority of the ratios are as low as 0 or close to 0. Therefore, it appears that the lightweight vehicles contribute to ESAL values insignificantly.

It should be emphasized that the analysis in this section was based on the traffic data from WIM Site 106. It is site specific and might not draw general conclusions. However, it provides a set of procedural steps for analyzing effects of different factors.

TABLE 6.6
**ESALs with and without unclassified vehicles**

| | AASHTO | | | Axle Group Divisor | | |
|---|---|---|---|---|---|---|
| | ESAL with C0 | ESAL w/o C0 | % Diff | ESAL with C0 | ESAL w/o C0 | % Diff |
| GVW (kips) | (A) | (B) | (A-B)/A | (A) | (B) | (A-B)/A |
| 3 | 31 | 31 | 0% | 20 | 20 | 0% |
| 6 | 3,108 | 3,104 | 0% | 3,043 | 3,040 | 0% |
| 9 | 3,801 | 3,741 | 2% | 4,338 | 4,272 | 2% |
| 12 | 2,876 | 2,606 | 9% | 3,368 | 3,055 | 9% |
| 15 | 3,339 | 2,738 | 18% | 3,775 | 3,097 | 18% |
| 18 | 5,981 | 4,550 | 24% | 6,546 | 4,993 | 24% |
| 21 | 12,824 | 10,202 | 20% | 13,606 | 10,861 | 20% |
| 24 | 19,271 | 14,982 | 22% | 20,064 | 15,649 | 22% |
| 27 | 23,756 | 16,994 | 28% | 24,562 | 17,600 | 28% |
| 30 | 31,474 | 21,161 | 33% | 32,666 | 21,952 | 33% |
| 33 | 41,675 | 26,905 | 35% | 43,630 | 28,125 | 36% |
| 36 | 56,665 | 34,432 | 39% | 60,028 | 36,353 | 39% |
| 39 | 65,705 | 40,604 | 38% | 70,399 | 43,110 | 39% |
| 42 | 80,915 | 52,340 | 35% | 87,579 | 55,708 | 36% |
| 45 | 101,453 | 68,687 | 32% | 109,884 | 72,918 | 34% |
| 48 | 125,889 | 88,499 | 30% | 135,785 | 93,461 | 31% |
| 51 | 139,144 | 95,951 | 31% | 150,533 | 101,717 | 32% |
| 54 | 156,611 | 105,596 | 33% | 169,099 | 111,763 | 34% |
| 57 | 179,363 | 115,189 | 36% | 192,524 | 121,005 | 37% |
| 60 | 209,774 | 134,226 | 36% | 223,580 | 140,123 | 37% |
| 63 | 251,389 | 161,479 | 36% | 265,599 | 167,608 | 37% |
| 66 | 302,622 | 204,544 | 32% | 316,712 | 211,122 | 33% |
| 69 | 378,500 | 261,864 | 31% | 392,335 | 268,758 | 31% |
| 72 | 469,329 | 334,082 | 29% | 482,229 | 341,368 | 29% |
| 75 | 604,400 | 430,157 | 29% | 615,399 | 437,525 | 29% |
| 78 | 761,022 | 565,664 | 26% | 769,659 | 573,261 | 26% |
| 81 | 891,603 | 679,638 | 24% | 897,404 | 687,371 | 23% |
| 84 | 882,049 | 609,944 | 31% | 881,451 | 616,987 | 30% |
| 87 | 785,073 | 466,068 | 41% | 777,672 | 472,559 | 39% |
| 90 | 736,137 | 349,153 | 53% | 717,072 | 355,371 | 50% |
| 93 | 633,135 | 217,996 | 66% | 609,340 | 223,706 | 63% |
| 96 | 620,597 | 120,996 | 81% | 580,651 | 126,163 | 78% |
| 99 | 646,601 | 78,173 | 88% | 594,248 | 83,364 | 86% |
| 102 | 710,163 | 61,302 | 91% | 642,883 | 66,595 | 90% |
| 105 | 831,802 | 56,537 | 93% | 739,189 | 62,109 | 92% |
| 108 | 982,091 | 56,106 | 94% | 856,504 | 62,226 | 93% |
| 111 | 1,066,800 | 54,694 | 95% | 925,419 | 61,168 | 93% |
| 114 | 1,159,984 | 50,565 | 96% | 989,977 | 56,930 | 94% |
| 117 | 1,346,141 | 47,518 | 96% | 1,128,282 | 53,798 | 95% |
| 120 | 1,644,927 | 42,630 | 97% | 1,350,679 | 48,517 | 96% |
| 123 | 1,736,871 | 35,673 | 98% | 1,411,937 | 40,880 | 97% |
| 126 | 1,973,012 | 30,379 | 98% | 1,580,520 | 35,005 | 98% |

TABLE 6.7
**Effect of lightweight vehicles on ESALs**

| | AASHTO | | | Axle Group Divisor | | |
|---|---|---|---|---|---|---|
| | Truck | Lightweight | Ratio | Truck | Lightweight | Ratio |
| GVW (kips) | (A) | (B) | B/A | (A) | (B) | B/A |
| 3 | 0 | 31 | — | 0 | 20 | — |
| 6 | 40 | 3,067 | 76.34 | 43 | 3,000 | 69.35 |
| 9 | 1,124 | 2,677 | 2.38 | 1,303 | 3,035 | 2.33 |
| 12 | 2,117 | 759 | 0.36 | 2,482 | 886 | 0.36 |
| 15 | 2,810 | 529 | 0.19 | 3,180 | 595 | 0.19 |
| 18 | 5,436 | 545 | 0.10 | 5,959 | 587 | 0.10 |
| 21 | 12,237 | 587 | 0.05 | 12,991 | 615 | 0.05 |
| 24 | 18,646 | 624 | 0.03 | 19,422 | 642 | 0.03 |
| 27 | 23,169 | 587 | 0.03 | 23,961 | 601 | 0.03 |
| 30 | 30,740 | 734 | 0.02 | 31,906 | 759 | 0.02 |
| 33 | 40,822 | 853 | 0.02 | 42,738 | 892 | 0.02 |
| 36 | 55,437 | 1,228 | 0.02 | 58,710 | 1,317 | 0.02 |
| 39 | 64,646 | 1,059 | 0.02 | 69,250 | 1,149 | 0.02 |
| 42 | 79,403 | 1,512 | 0.02 | 85,891 | 1,688 | 0.02 |
| 45 | 99,722 | 1,731 | 0.02 | 107,916 | 1,968 | 0.02 |
| 48 | 124,302 | 1,586 | 0.01 | 133,976 | 1,810 | 0.01 |
| 51 | 137,421 | 1,723 | 0.01 | 148,571 | 1,963 | 0.01 |
| 54 | 154,210 | 2,401 | 0.02 | 166,378 | 2,722 | 0.02 |
| 57 | 178,955 | 407 | 0.00 | 192,067 | 458 | 0.00 |
| 60 | 209,660 | 114 | 0.00 | 223,452 | 128 | 0.00 |
| 63 | 251,251 | 138 | 0.00 | 265,443 | 156 | 0.00 |
| 66 | 302,473 | 150 | 0.00 | 316,542 | 170 | 0.00 |
| 69 | 378,480 | 20 | 0.00 | 392,312 | 23 | 0.00 |
| 72 | 469,220 | 109 | 0.00 | 482,103 | 126 | 0.00 |
| 75 | 604,316 | 84 | 0.00 | 615,303 | 95 | 0.00 |
| 78 | 760,931 | 92 | 0.00 | 769,555 | 104 | 0.00 |
| 81 | 891,563 | 40 | 0.00 | 897,358 | 46 | 0.00 |
| 84 | 881,993 | 56 | 0.00 | 881,386 | 64 | 0.00 |
| 87 | 784,962 | 111 | 0.00 | 777,544 | 128 | 0.00 |
| 90 | 736,069 | 67 | 0.00 | 716,995 | 77 | 0.00 |
| 93 | 633,135 | 0 | 0.00 | 609,340 | 0 | 0.00 |
| 96 | 620,597 | 0 | 0.00 | 580,651 | 0 | 0.00 |
| 99 | 646,601 | 0 | 0.00 | 594,248 | 0 | 0.00 |
| 102 | 710,163 | 0 | 0.00 | 642,883 | 0 | 0.00 |
| 105 | 831,802 | 0 | 0.00 | 739,189 | 0 | 0.00 |
| 108 | 982,091 | 0 | 0.00 | 856,504 | 0 | 0.00 |
| 111 | 1,066,800 | 0 | 0.00 | 925,419 | 0 | 0.00 |
| 114 | 1,159,984 | 0 | 0.00 | 989,977 | 0 | 0.00 |
| 117 | 1,346,141 | 0 | 0.00 | 1,128,282 | 0 | 0.00 |
| 120 | 1,644,927 | 0 | 0.00 | 1,350,679 | 0 | 0.00 |
| 123 | 1,736,871 | 0 | 0.00 | 1,411,937 | 0 | 0.00 |
| 126 | 1,973,012 | 0 | 0.00 | 1,580,520 | 0 | 0.00 |

## 7. VEHICLE PLATOON ANALYSIS

Automated vehicle platooning has emerged as a new potential way to increase road capacity and improve travel efficiency. However, in this study, the analysis dealt with only the naturally formed vehicle platoons. As can be often observed, vehicles often move in groups or platoons with relative short headways between them (Figure 7.1). Vehicle platoons affect not only traffic flows and highway operations, but also the mechanism of axle loads impacting pavement. Platoon analysis in this study focused on the longitudinal vehicle platoons because they are directly related to loading conditions of highway pavement. In the longitudinal platoon analysis, traffic flows on individual lanes were examined and analyzed with respect to the distances or time headways between leading and following vehicles.

### 7.1 Platoon Critical Intervals

The critical interval must be first established for conducting vehicle platooning analysis (Aziza et al., 2014). A critical interval (CI) is the time headway between two consective moving vehicles that is used to define if the two vehicles belong to a vehicle platoon. A small CI would result in very few vehicle platoons. On the other hand, a large CI would involve more vehicles in the traffic flow into vehicle platoons. Therefore, it is important to choose a reasonalbe CI value in platoon analysis.

In statistics, ordinary least squares (ols) is a type of linear least squares method for estimating the unknown parameters in a linear regression model (Neter et al., 1996). As a critical interval increases, the percent of vehicles on the roadway increares. A critical interval should be at a point where a increased time headway would not cause a large percent increase of platooned vehicles. In order to establish such a pattern, the ols regression model was utilized to analyze cumulative traffic flow data from all WIM sites. A series of time headways (in seconds) were applied to examine the proportions of vehicles in platoons. At each step, a headway increase of 0.05 seconds was used and the percent of vehicles belonging to platoons was recorded. Thus, a diagram of the grouped vehicle percentages versus the corresponding headway threholds can be plotted as displayed with the blue line in Figure 7.2.

The data points in the blue line in Figure 7.2 were then separeated into two sets: one including the left side portion and the other including the right side portion. Ols regressions were conducted with the left set of the data points and with the right set of the data points. The data separations and consequent ols regressions were repeated several times. The regression line with the highest $r^2$ value was select from the left side and another was similarly selected from the right side. The headway value corresponding to the intersection of the two selected regression lines was then determined as the critercal interval. As indicated in Figure 7.2, the crtical interval in this example is about 2.7 seconds. The graph on the right side of Figure 7.2 shows that, with a critical interval of 2.7 seconds, the increase of platooned vehicles is relatively low.

Through this method, the critical interval (rounded to the nearest 0.5 seconds) is 2.5 seconds for Lines 1, 2, 3, and 5 are 2.5 seconds, and 1.5 seconds for Line 5. A lower crtical interval for Line 5 could be attributed to the fact that traffic flow on Line 5 was comprised of more lightweight and faster moving vehicles than other lanes. Using the critical intervals as platoon thresholds, it was found that on average about 50%–58% of all vehicles and about 35%–49% of trucks are grouped into platoons and the platoon sizes range from 3 to 17 vehicles.

### 7.2 Platoon Characteristics

The behavior of a vehicle platoon is largely determined by the leader of the platoon. The most commonly observed vehicles in Indiana are led by lightweight vehicles (Classes 1, 2, and 3). Some of the typical platoons in terms of leading vehicles are illustrated in Figure 7.3.

With the established critical intervals, the vehicle volume and platoon distributions by leading vehicle types were obtained using a month of data from one WIM station as shown in Figure 7.4. The figure indicates that vehicle volumes and platoons are directly related for all types of leading vehicles. As most of the vehicles in the traffic flow were lightweight vehicles, the largest portion of the platoons were led by lightweight vehicles. It is interesting to note in Figure 7.4 that Class 13 vehicle volume was higher than other types of trucks at this location. In fact, it was observed Class 13 volumes were fairly high during the winter months on interstate highways.

The relationships between leading vehicle weights and platoon sizes were explored to reveal the effect of leading vehicles. Figure 7.5 shows these relationships for platoons led by lightweight vehicles (top left chart), Class 5 vehicles (top right), Class 9 vehicles (bottom left), and Class 13 vehicles (bottom right). The four graphs in Figure 7.5 demonstrate the following effects:

1. Platoons led by lightweight vehicles (Classes 1, 2, and 3 vehicles) spread widely in platoon sizes, ranging from 2 to 17 vehicles.
2. The maximum platoon sizes of platoons led by trucks are smaller than those of platoons led by lightweight vehicles.
3. For a given platoon size, platoons led by trucks cover a wide range of GVW values.

Similarly, the relationships between leading vehicle weights and platoon travel speeds were also examined. It was expected that platoon speeds would decrease as the GVW of leading vehicles increase. However, it was not always the case as displayed in Figure 7.6 for platoons led by lightweight vehicles and Class 13 trucks. For these two types of platoons, the platoon speeds were in an upward trend as the vehicle weights increase.

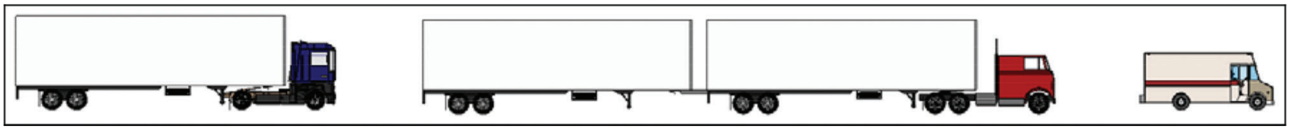

**Figure 7.1** An example of vehicle platoon.

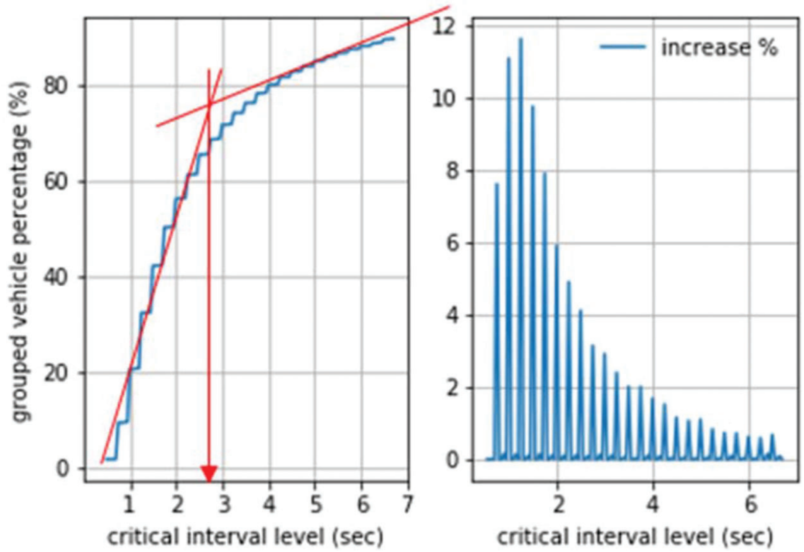


**Figure 7.2** Relationship between headway and percent of vehicles in platoons.

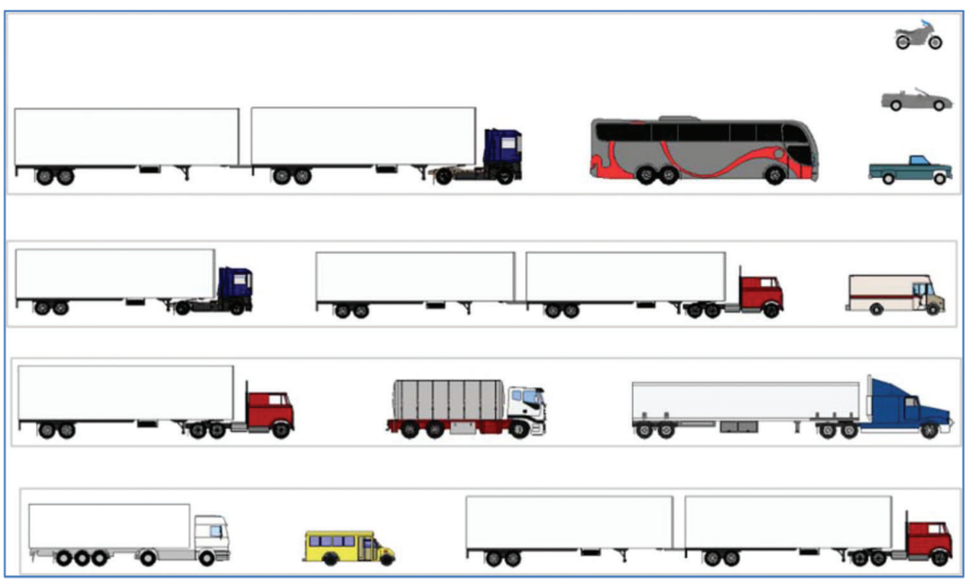

**Figure 7.3** Platoons led by lightweight, Class 5, Class 9, and Class 13 Vehicles.

The distributions of axle load with respect to the for cases of platoons are shown in Figures 7.7 and 7.8, where Cases 1, 2, 3, and 4 represent the platoons led by lightweight, Class 5, Class 9, and Class 13 vehicles, respectively. Figure 7.7 shows the distribution of individual axle loads, while Figure 7.8 is the distribution of average axle load per platoon with respect to the four cases of platoons. The observations in the figures include the following:

1. In Figure 7.7, platoons of Cases 1, 2, and 3 appear in high proportions within axle load less than 4 kips, indicating all three types of platoons are mix of trucks and lightweight vehicles.
2. Figure 7.8 shows very low proportion of Case 3 platoons are in the average platoon axle load less than 4 kips range. This means that most of the vehicles in platoons led by Class 9 trucks are trucks rather than lightweight vehicles.
3. Figure 7.7 and Figure 7.8 demonstrate that both the individual axle load and the average platoon axle load of Case

4 platoons spread beyond 14 kips, which implies that most platoons led by Class 13 trucks are truck only platoons.

The WIM traffic data showed that vehicle platoons in rural areas, especially in rural areas adjacent to urban areas, consist of more trucks. In order to examine the platoon patterns in rural areas, the traffic data from WIM Site 507 on I-65 near Seymour and WIM Site 430 on I-94 near Michigan City were utilized for the analysis. The traffic volumes on the two sections are high at the two sections of interstate highways. To show the platoon patterns in different time periods (morning and afternoon) and on different lanes, the proportions of Class 9 trucks that were grouped into platoons were calculated. Class 9 trucks were used because their volumes were the highest among all types of trucks. The critical intervals from 2.0 seconds to 4.5 seconds were applied to reflect the effects of vehicle headways on platoons. The proportions of Class 9 vehicles grouped into platoons based on traffic volumes as well as truck volumes are plotted in Figures 7.9, 7.10, 7.11, and 7.12 for the two WIM sites. The plots indicate that higher proportions of trucks travel in platoons in the afternoon than in the morning on both driving lane (Lane 1) and passing lane (Lane 2). The plots also exhibit that trucks on passing lane are more likely to move in platoons than on driving lane.

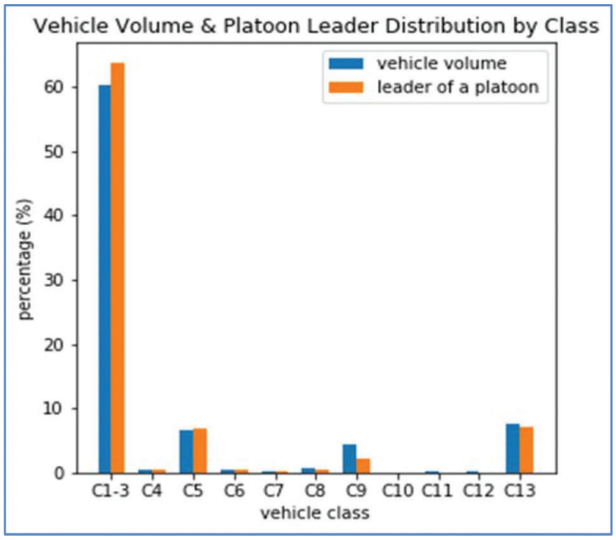


**Figure 7.4** Platoon distributions by type of leading vehicles.

### 7.3 Statistical Tests of Highway Vehicle Platoons

In order to analyze the variations of platoons, weekly platoons were obtained for each month in 2018 at WIM Site 315 on I-70 in Indianapolis. Three weekly platoon distributions in January, April, and August among the 12 months are presented in Figures 7.13, 7.14, and 7.15 to display the number of platoons every 15 minutes

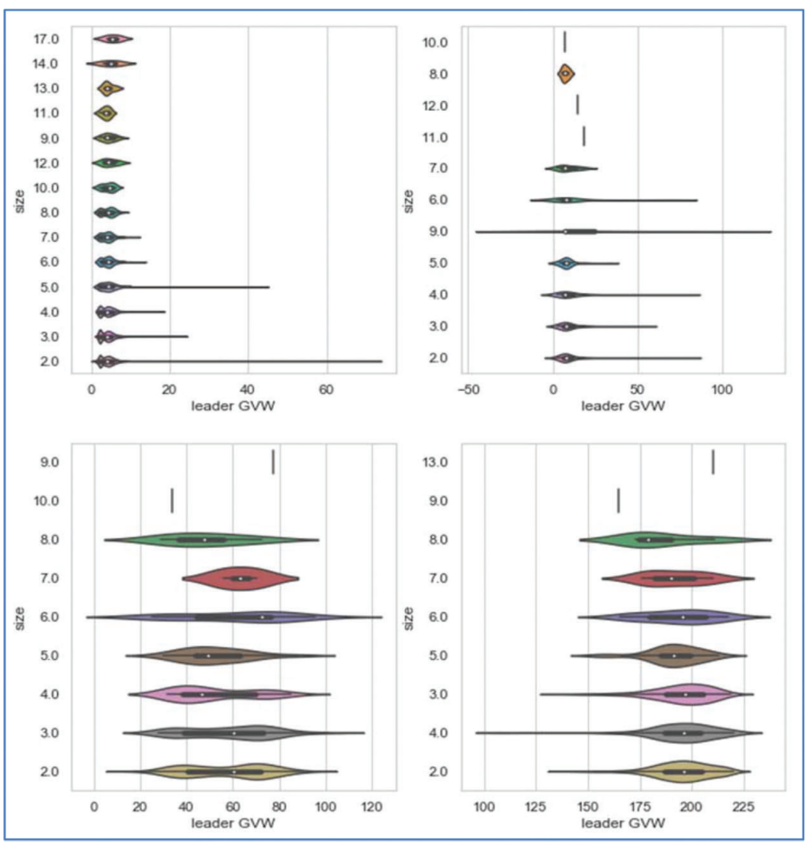


**Figure 7.5** Relationship between leading vehicle load (kips) and platoon size.

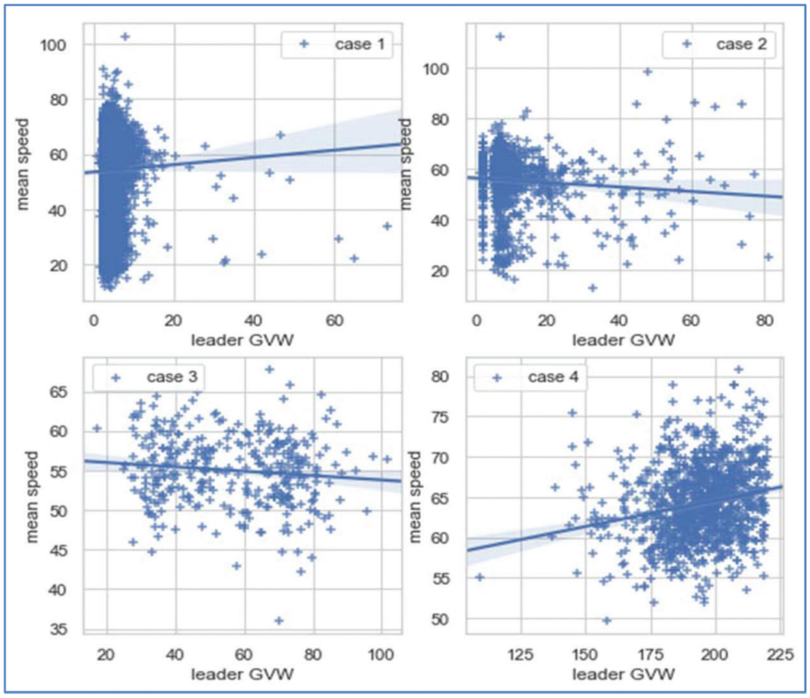


**Figure 7.6** Relationship between leading vehicle load (kips) and platoon speed (mph).

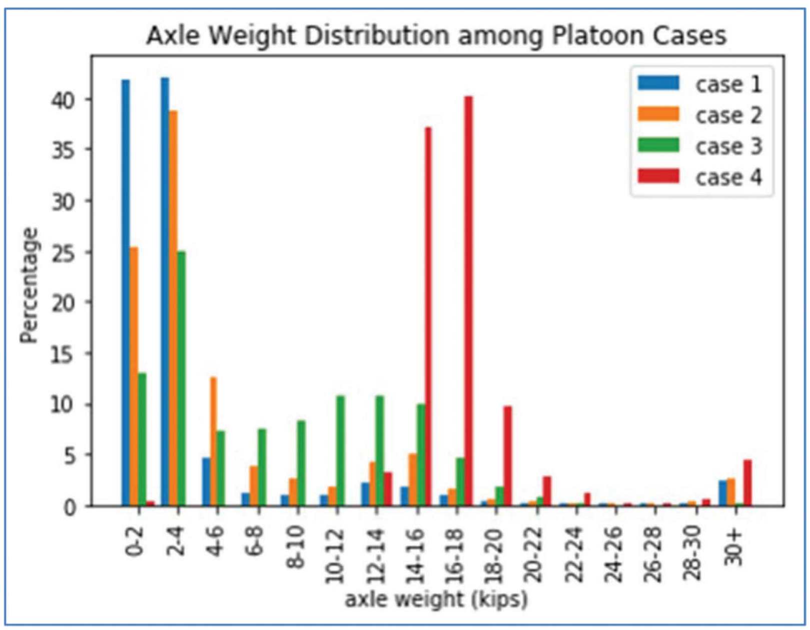


**Figure 7.7** Distribution of axle loads of platoons

within a week. As can be seen in these figures, the number of platoons fluctuate continuously. Because the calculated platoon values cover different hours, days, and months, it was necessary to analyze the effects of time of day, weekdays, weekends, and seasons with appropriate statistical experimental design.

A factorial design expressed by the following equation was constructed to test the effects of several factors, including roadway lanes, time periods of day, days of week, and months or seasons:

$$\begin{aligned} y_{ijklm} = \mu + \tau_i + \beta_j + \gamma_k + \delta_l + (\tau\beta)_{ij} + (\beta\gamma)_{jk} + (\gamma\delta)_{kl} \\ + (\tau\gamma)_{ik} + (\tau\delta)_{il} + (\beta\delta)_{jl} + (\tau\beta\gamma)_{ijk} \\ + (\tau\beta\delta)_{ijl} + (\tau\gamma\delta)_{ikl} + (\beta\gamma\delta)_{jkl} + \varepsilon_{ijlkm} \end{aligned} \qquad \text{(Eq. 7.1)}$$

Where:
$\mu$ = grand mean

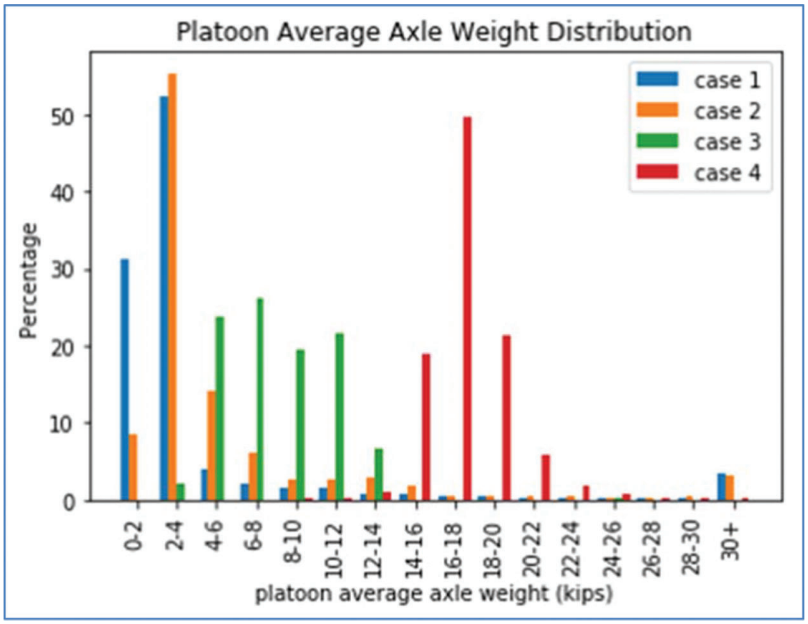


**Figure 7.8** Distribution of average axle loads of platoons.

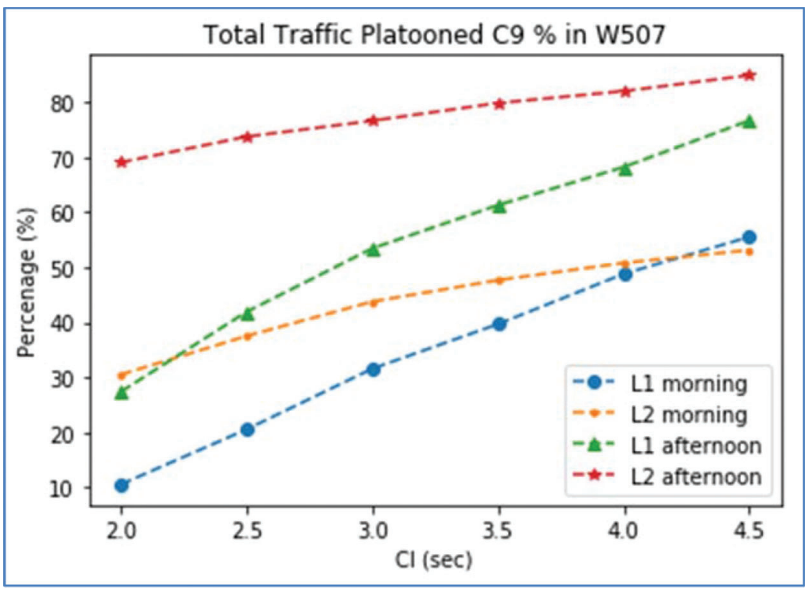


**Figure 7.9** Proportions of Class 9 vehicles in platoons on I-65 (based on traffic volume).

$\tau_i$ = i$^{th}$ level effect of factor A
$\beta_j$ = j$^{th}$ level effect of factor B
$\gamma_k$ = k$^{th}$ level effect of factor C
$\delta_l$ = l$^{th}$ level effect of factor D
$\varepsilon_{ijlkm}$ = residuals with normal distribution $N(0, \sigma^2)$

Applying the factorial design, test Model 1 with the effects of lane, time period of day, month, and day of week was established as listed in Table 7.1. The statistical test results are presented in Table 7.2. Similarly, test Model 2 was formed to test the effects of lane, time period of day, season, and weekday and weekend as shown in Table 7.3. The statistical test results from Model 2 are presented in Table 7.4.

The distribution of the model resuduals is depicted in Figure 7.16. The nomality of the model resuduals was tested with the normal Q-Q plot in Figure 7.17. The two figures indicate that the model residuals are normally distributed. In addition, no apparent outliers or influential points can be found in the plots. The residuals seem to satisfy the model assumptions of normality, random, and independence.

Based on the statistical outputs in Table 7.2 and 7.4, with a significant level $\alpha = 0.1\%$, it can be concluded that the effects of all the selected factors of the two models are statistically significant. It means that these factors, including of lane, time, month, season, day of week, and weekday/weekend, will significantly affect

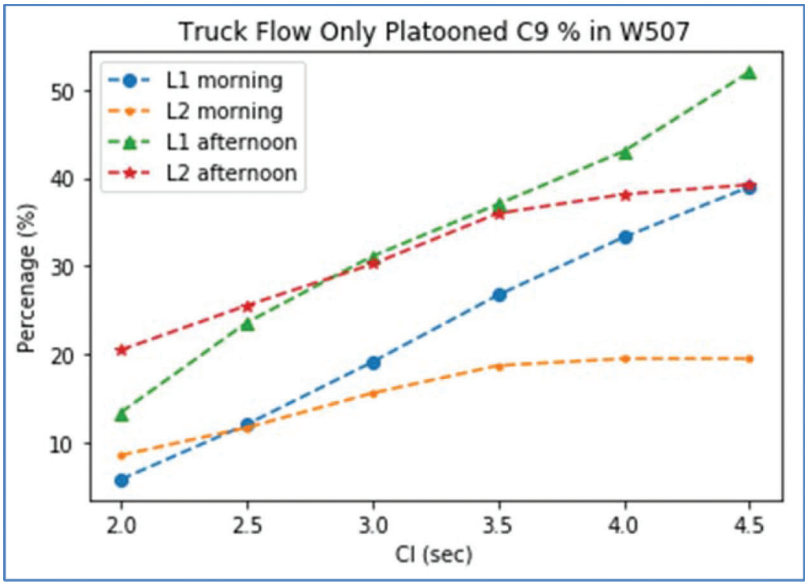


**Figure 7.10** Proportions of class 9 vehicles in platoons on I-65 (based on truck volume).

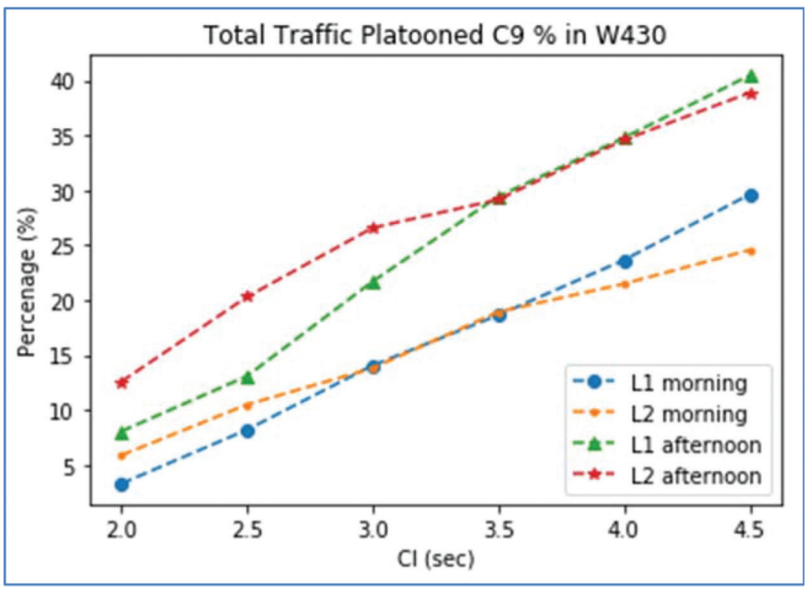


**Figure 7.11** Proportions of Class 9 vehicles in platoons on I-94 (based on traffic volume).

the number of platoons. In addition, most of the interaction effects of these factors are also statistically significant. The few of factor interactions that are not statistically significant include the following: Lane*Month*Week, Lane*Time*Month*Week, Lane*Season*Work, and Lane*Time*Season*Work.

Through the statistical tests, it can be concluded that number of vehicle platoons are affected by the main factors of roadway lanes, time periods of day, days of week, months, and seasons. The vehicle platoons are also affected by many forms of combinations of the main factors.

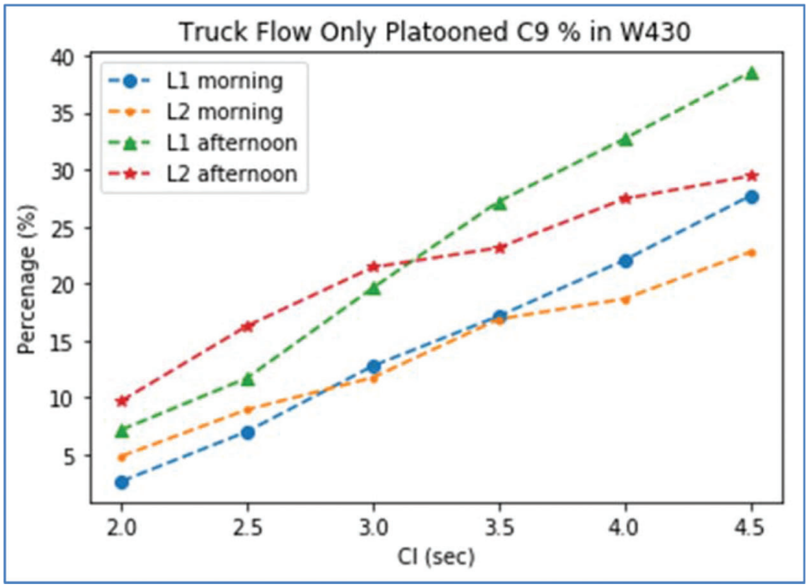


**Figure 7.12** Proportions of Class 9 vehicles in platoons on I-94 (based on truck volume).

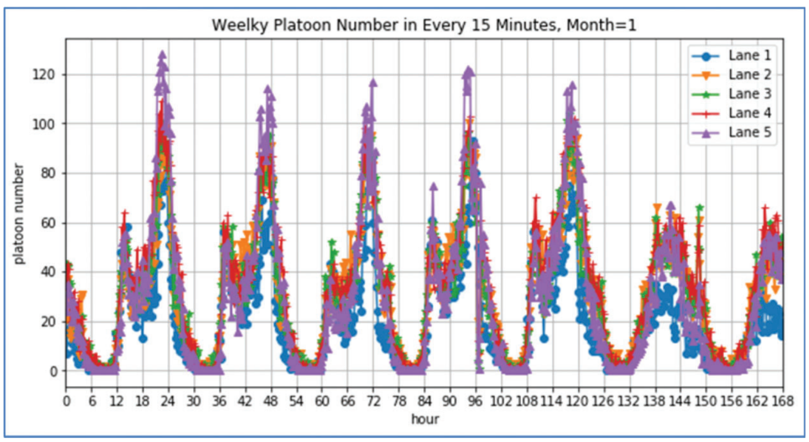


**Figure 7.13** Weekly platoon distributions in January.

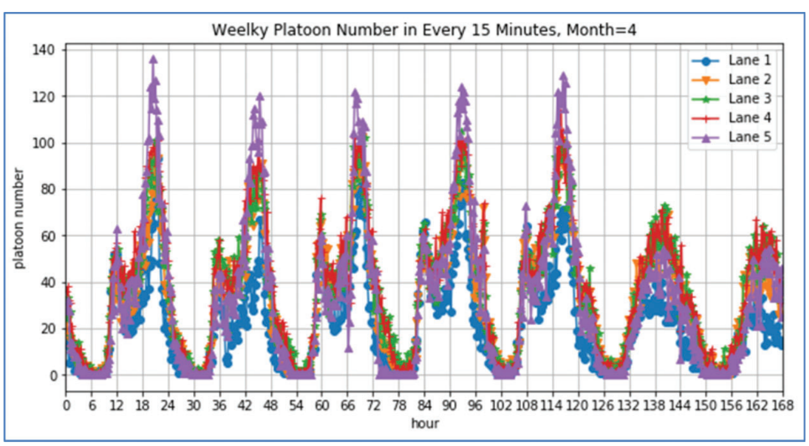


**Figure 7.14** Weekly platoon distributions in April.

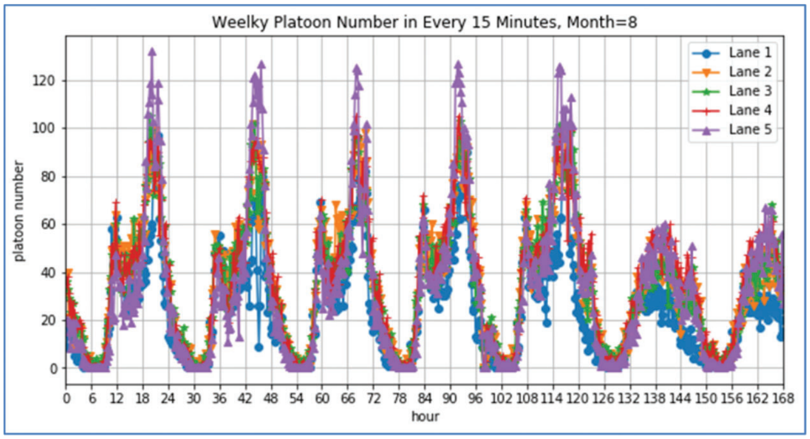


**Figure 7.15** Weekly platoon distributions in August.

TABLE 7.1
**Factorial design Model 1**

| Factor | Levels | Values |
|---|---|---|
| $\tau$: Lane | 5 | 1, 2, 3, 4, 5 |
| $\beta$: Time | 4<br>(0:00–6:00, 6:00–12:00, 12:00–18:00, 18:00–0:00) | 1, 2, 3, 4 |
| $\gamma$: Month | 12 | 1, 2, 3, 4, 5, 6, 7, 8, 9, 10, 11, 12 |
| $\delta$: Day of Week | 7 | 1, 2, 3, 4, 5, 6, 7 |

TABLE 7.2
**AVOVA table of Model 1**

| Source of Variation | Degree of Freedom | Type III Sum of Squares | Mean Square | F Value | Pr > F |
|---|---|---|---|---|---|
| Lane | 4 | 984,407.18 | 246,101.79 | 1,089.28 | < 0.0001 |
| Time | 3 | 12,923,864.74 | 4,307,954.91 | 19,067.6 | < 0.0001 |
| Lane*Time | 12 | 436,030.34 | 36,335.86 | 160.83 | < 0.0001 |
| Month | 11 | 740,102.02 | 67,282 | 297.8 | < 0.0001 |
| Lane*Month | 44 | 265,862.06 | 6,042.32 | 26.74 | < 0.0001 |
| Time*Month | 33 | 170,177.74 | 51,547.81 | 228.16 | < 0.0001 |
| Lane*Time*Month | 132 | 220,447.39 | 1,670.06 | 7.39 | < 0.0001 |
| Week | 6 | 920,171.22 | 153,361.87 | 678.8 | < 0.0001 |
| Lane*Week | 24 | 36,068.96 | 1,502.87 | 6.65 | < 0.0001 |
| Time*Week | 18 | 1,049,086.67 | 58,282.59 | 257.97 | < 0.0001 |
| Lane*Time*Week | 72 | 49,663.01 | 689.76 | 3.05 | < 0.0001 |
| Month*Week | 66 | 352,070.22 | 5,334.4 | 23.61 | < 0.0001 |
| Lane*Month*Week | 264 | 56,660.66 | 214.62 | 0.95 | 0.7102 |
| Time*Month*Week | 198 | 570,216.76 | 2,879.88 | 12.75 | < 0.0001 |
| Lane*Time*Month*Week | 792 | 110,093.72 | 139.01 | 0.62 | 1.0 |

TABLE 7.3
**Factorial design Model 2**

| Factor | Levels | Values |
|---|---|---|
| $\tau$: Lane | 5 | 1, 2, 3, 4, 5 |
| $\beta$: Time | 4<br>(0:00–6:00, 6:00–12:00, 12:00–18:00, 18:00–0:00) | 1, 2, 3, 4 |
| $\gamma$: Season | 4<br>(Spring: March–May, Summer: June–August, Fall: September–November, Winter: December–February) | 1, 2, 3, 4 |
| $\delta$: Weekday vs. Weekend | 2<br>(Monday–Friday, Saturday–Sunday) | 1, 2 |

TABLE 7.4
**AVOVA table of Model 2**

| Source of Variation | Degree of Freedom | Type III Sum of Squares | Mean Square | F Value | Pr > F |
|---|---|---|---|---|---|
| Lane | 4 | 900,099.9 | 225,024.975 | 803.46 | < 0.0001 |
| Time | 3 | 8,501,537.737 | 2,833,845.912 | 10,118.3 | < 0.0001 |
| Lane*Time | 12 | 334,243.321 | 27,853.61 | 99.45 | < 0.0001 |
| Season | 3 | 209,105.033 | 69,701.678 | 248.87 | < 0.0001 |
| Lane*Season | 12 | 56,014.091 | 4,667.841 | 16.67 | < 0.0001 |
| Time*Season | 9 | 754,546.683 | 83,838.52 | 299.35 | < 0.0001 |
| Lane*Time*Season | 36 | 62,103.921 | 1,725.109 | 6.16 | < 0.0001 |
| Work | 1 | 773,957.48 | 773,957.48 | 2,763.44 | < 0.0001 |
| Lane*Work | 4 | 27,042.286 | 6,760.572 | 24.14 | < 0.0001 |
| Time*Work | 3 | 1,003,439.816 | 334479.939 | 1,194.27 | < 0.0001 |
| Lane*Time*Work | 12 | 34,594.98 | 2,882.915 | 10.29 | < 0.0001 |
| Season*Work | 3 | 56,803.079 | 18,934.36 | 67.61 | < 0.0001 |
| Lane*Season*Work | 12 | 6,140.987 | 511.749 | 1.83 | 0.0384 |
| Time*Season*Work | 9 | 138,978.632 | 15,442.07 | 55.14 | < 0.0001 |
| Lane*Time*Season*Work | 36 | 9,134.307 | 253.731 | 0.91 | 0.6304 |

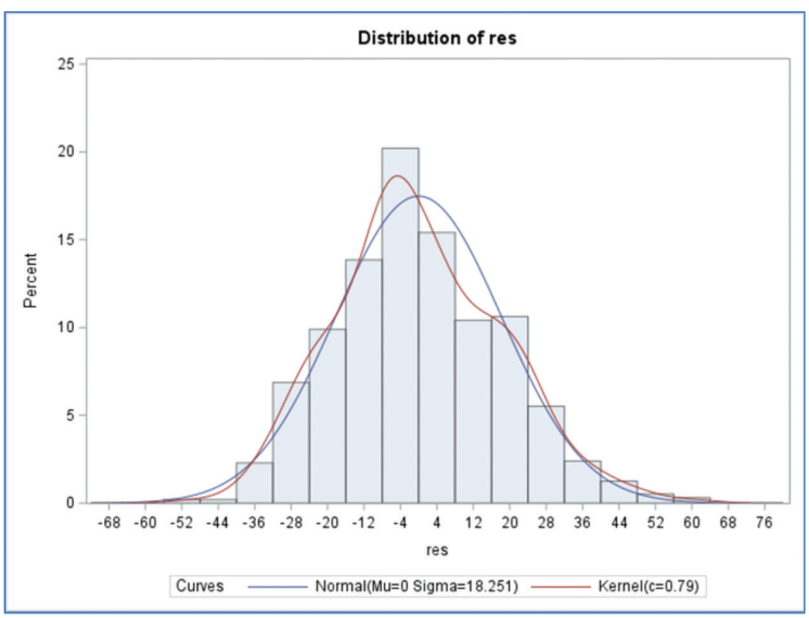


**Figure 7.16** Model residual distribution.

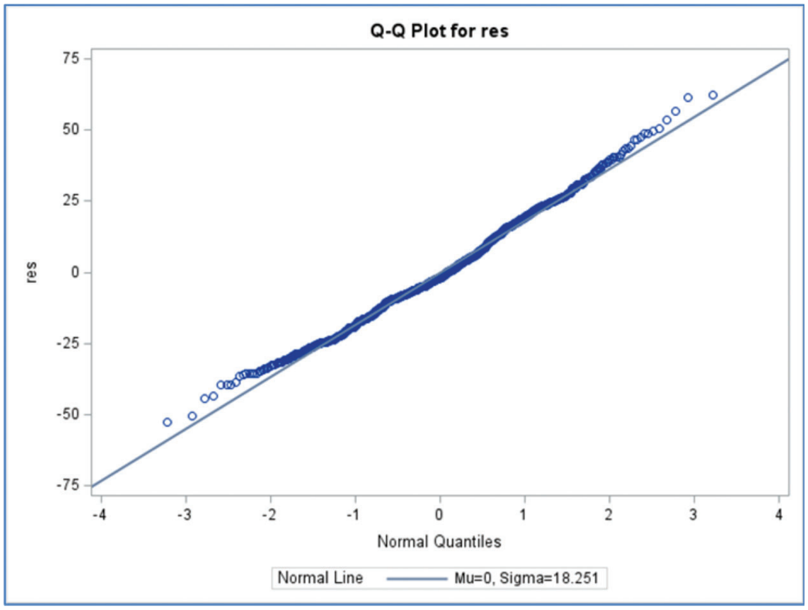


**Figure 7.17** Normal Q-Q plot of model residuals.

## 8. EFFECTS OF UNCLASSIFIED VEHICLES

In the WIM dataset the unclassified vehicles, denoted as Class 0 or C0, are those that the WIM device failed to identify their vehicle types based on the integrated criteria. The quantities of unclassified vehicles have great effect on pavement design. There are many possible reasons for a vehicle not to be classified, such as vehicle tailgating, lane changing, irregular vehicle size, and WIM equipment problems. An unreasonably large value of unclassified vehicles usually indicates that the WIM device is not working properly. These unclassified vehicles could be any types of vehicles, including passenger cars, buses, and trucks. Overestimate or underestimate of the truck percentages in the unclassified vehicles will undoubtedly affect the axle load inputs in pavement design. This issue is more critical when part of the unclassified vehicles in WIM data have empty or extreme large measurements on vehicle speed, axle load and vehicle weight, and axle configuration. In order to minimize the effects of unclassified vehicles, a neural network (NN) based deep learning approach (Paszke et al., 2019) was employed to identify the feature attributes of the unclassified vehicles and to assign them into appropriate vehicle groups.

### 8.1 Dataset Processing and Neural Network Input

A dataset with a total of 100,000 classified vehicles was retrieved from one of the WIM sites for attribute analysis with the neural network (NN) based deep learning method. There are more than a hundred attributes in the WIM dataset. It is essential to use only the most relevant attributes for effective data training. As an example, the distributions of the three key attributes of speed, vehicle length, and gross vehicle weight are displayed with boxplots in Figures 8.1, 8.2, and 8.3. Boxplots are a standardized way of displaying the distribution of data based on a five number summary, including minimum, first quartile (Q1), median (second quartile: Q2), third quartile (Q3), and maximum. It can be observed in the figures that:

1. The differences between speeds of lightweight vehicles (C1, C2, C3) and trucks do not exhibit a clear pattern. Thus, the attribute of speed might provide only limited information in the NN training and learning process.
2. Distributions of vehicle lengths vary among individual vehicle classes. However, the differences of vehicle lengths between some vehicle classes are not significant. Therefore, vehicle length data would provide some indications of particular types of vehicles.
3. There exist significant differences in GVW distribution between lightweight vehicles and trucks, which would add key measures to the training model.

Based on the principles of WIM vehicle classifications, attributes related to vehicle axles are essential to accurately further divide vehicles into multiple types. However, the attributes must be processed before the information can be efficiently applied in NN model training. In addition to *speed*, *length*, and *GVW*, the mean of the axle weights (*meanAxleWeight*) and the mean of axle spaces (*meanAxleSpace*) were included as numerical variables in the NN model training. The distributions of these two variables are displayed in Figure 8.4 and Figure 8.5. The boxplots of *meanAxle Weight* (Figure 8.4) reveal clear distinctions among truck classes in terms of four quartiles and thus provide additional features of vehicle characteristics. Axle spacing distributions shown in Figure 8.5 would offer further clues to distinguish different types of vehicles.

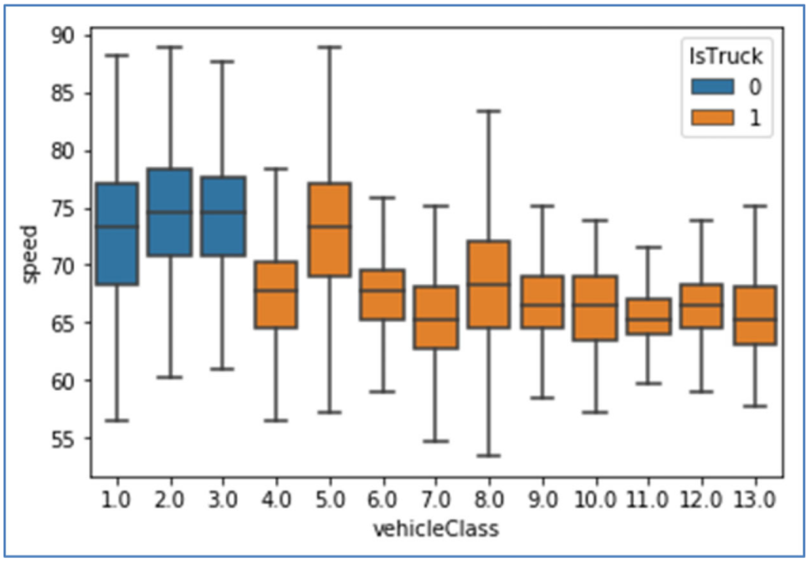


**Figure 8.1** Speed distributions.

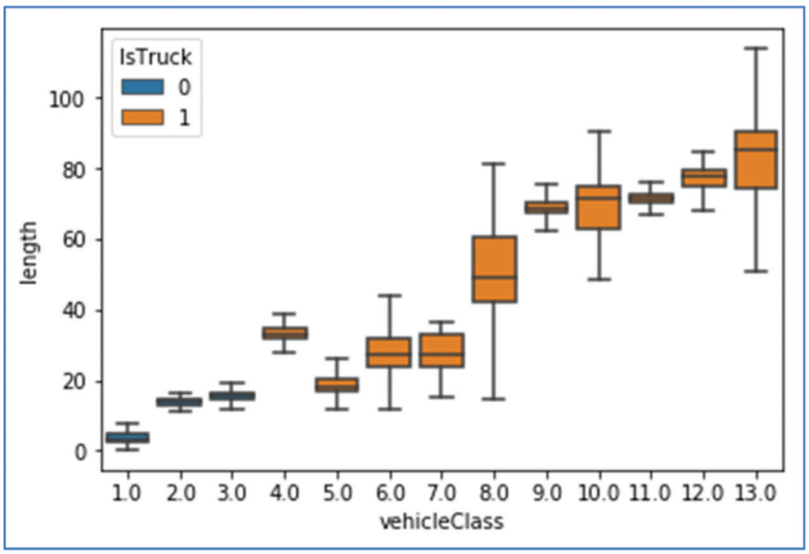


**Figure 8.2** Vehicle length distributions.

For instance, the largest axle spaces can be used to identify Class 4 vehicles (buses).

Through this primary process, three types of axle configurations (single, tandem, and tridem) were found to be major factors affecting vehicle classifications. Therefore, altogether eight features related to the WIM data were identified as influencing characteristic variables and were embedded as the categorical input of the NN model as presented in Table 8.1.

## 8.2 Model Training and Testing

### *8.2.1 Main Terminologies Related to the Neural Network Model*

Before further discussing the NN process, it is necessary to briefly introduce some terminologies used in the learning algorithms. "Error" is the term represents the difference between the actual output and the predicted output. The function that is used to compute this error is known as "Loss Function." Different loss functions will yield different errors for the same prediction, and thus have a considerable effect on the performance of the model. "Cross-entropy" is commonly used in machine learning as a loss function. "Cross-entropy loss" measures the performance of a classification model whose output is a probability value between 0 and 1. Cross-entropy loss increases as the predicted probability diverges from the actual label. A "confusion matrix" is a table that is often used to describe the performance of a classification model on a set of test data for which the true values are known.

The following example of a simple confusion matrix is presented to explain the main concept. If there are

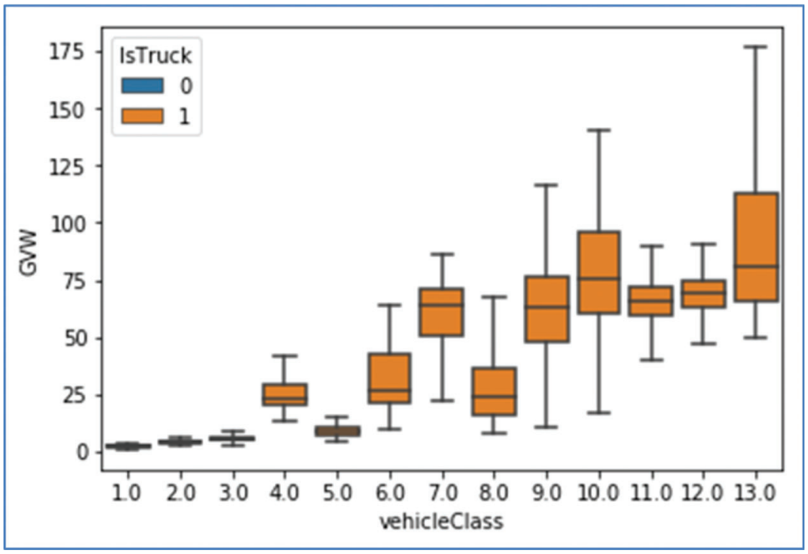


**Figure 8.3** Gross vehicle weight distributions.

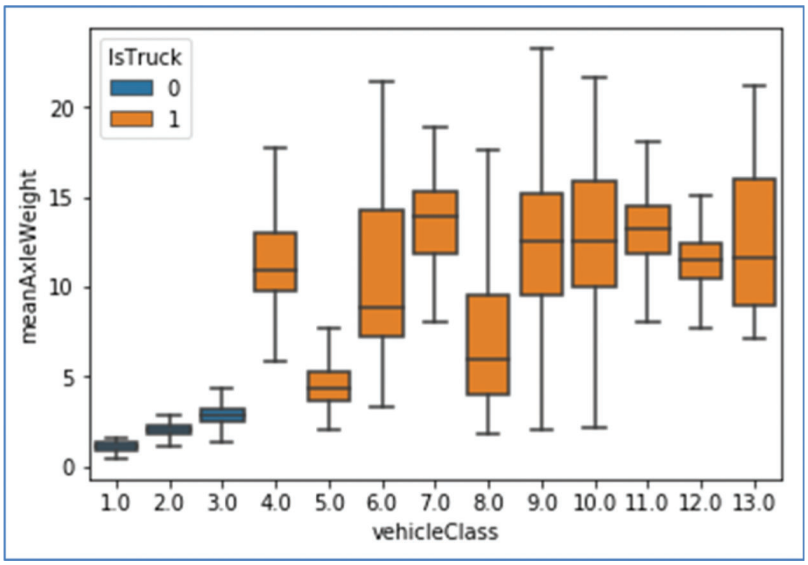


**Figure 8.4** Boxplots of *meanAxleWeight* distribution.

180 classified vehicles from WIM data. It is verified that 110 of the 180 vehicles are Class-9 vehicles and 70 of the 180 vehicles are other types of vehicles (or Non-Class-9 vehicles). The actual and predicted vehicle types are listed in Table 8.2 as a confusion matrix. In the confusion matrix, the basic terms can be defined as following:

- True positives (TP): These are cases in which the vehicles are actually Class-9 and predicted vehicles are also Class-9. In this example, TP = 110.
- True negatives (TN): When the vehicles are actually Non-Class-9 vehicles and the predicted vehicles are also Non-Class-9. In this example, TN = 40.
- False positives (FP): When the vehicles are actually Non-Class-9 vehicles and the predicted vehicles are Class-9 (Also known as a "Type I error"). In this example, FP = 20.
- False negatives (FN): When the vehicles are actually Class-9 vehicles and the predicted vehicles are Non-Class-9 (Also known as a "Type II error"). In this example, FN = 10.
- Accuracy: Overall frequency of correct classification. In this example, Accuracy = (TP + TN)/total = (110 + 40)/180 = 0.83.
- Precision: When the model predicts Class-9, the frequency that the prediction is correct. In this example, Precision = TP/(Predicted Class-9) = 110/130 = 0.85.

### *8.2.2 Design of the Neural Network Model*

The characteristic variables listed in Table 8.1 were applied as the input layer in the NN model. The 13 vehicle classes were designed as the neurons in the output layer. The topology of the NN model is illustrate in

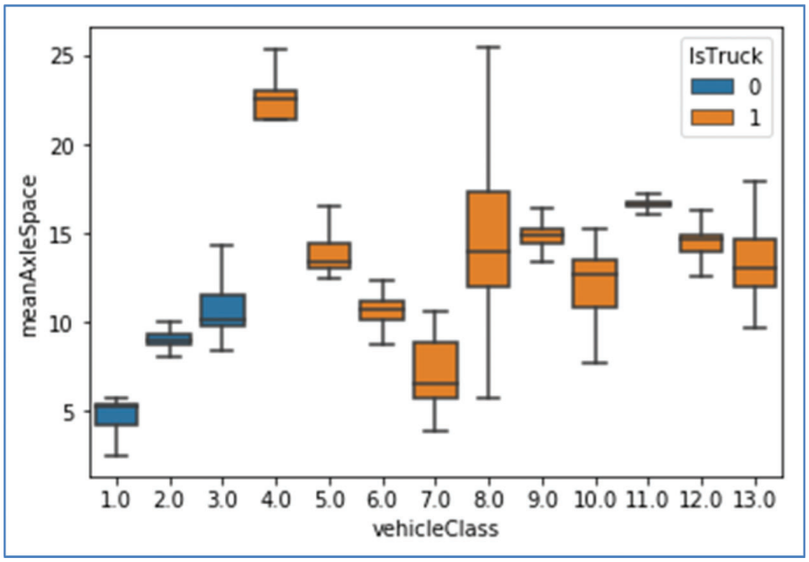


**Figure 8.5** Boxplots of *meanAxleSpace* distribution.

TABLE 8.1
**Characteristic variables of the NN model inputs**

| Feature No. | Variable | Description |
|---|---|---|
| 1 | *GVW* | Gross vehicle weight |
| 2 | *length* | Total vehicle length |
| 3 | *speed* | Vehicle driving speed |
| 4 | *meanAxleWeight* | Mean value of vehicle axle weight |
| 5 | *meanAxleSpace* | Mean value of spaces between adjacent vehicle axles |
| 6 | *Single* | Number of single axles of the vehicle |
| 7 | *Tandem* | Number of tandem axles of the vehicle |
| 8 | *Tridem* | Number of tridem axles of the vehicle |

TABLE 8.2
**Example of confusion matrix**

| | | Actual Vehicle Class | |
|---|---|---|---|
| **n = 180** | | **Class-9** | **Non-Class-9** |
| Predicted Vehicle Class | Class-9 | 110 | 20 |
| | Non-Class-9 | 10 | 40 |

Figure 8.6. As the topology shows, between the input and output layers there are three hidden layers with 200, 100, and 50 neurons, respectively. The code of the training model structure with functions and layer neurons is shown in Figure 8.7.

The dataset with the processed feature variables was divided into a labeled set (WIM-classified data or C1, C2, …, C13) and an unlabeled set (unclassified data or C0). The labeled set was served as the learning database to train and test the model. A total of 80,000 randomly selected labeled vehicles were divided into two groups, one as the training dataset and the other as the testing dataset.

The training dataset was first utilized to train the model. In the training process, the Cross Entropy Loss function was used to measure the performance of the training and optimizing process. In terms of the training process, an epoch refers to one cycle through the full training dataset. The training model was performed 300 epochs. The learning curve of the model is depicted in Figure 8.8. The learning curve indicates that the training loss reduced rapidly initially and gradually stabilized as the number of epochs increased. After 300 epochs, the loss reached 0.1571.

After the training process, the testing dataset was then applied to evaluate the accuracy of the NN model in identifying vehicle class. The confusion matrix in Figure 8.9 was produced. As the values in the diagonal cells represent the correct predictions in a confusion matrix, the high diagonal values in then confusion matrix in Figure 8.9 shows an evidence that the model yielded predictions with high accuracy. The computer output indicates that the overall accuracy score is 0.9525 and the average precision is 0.9500. It is worth pointing out that the low values corresponding to Class 13 vehicles in the confusion matrix are caused by lack of

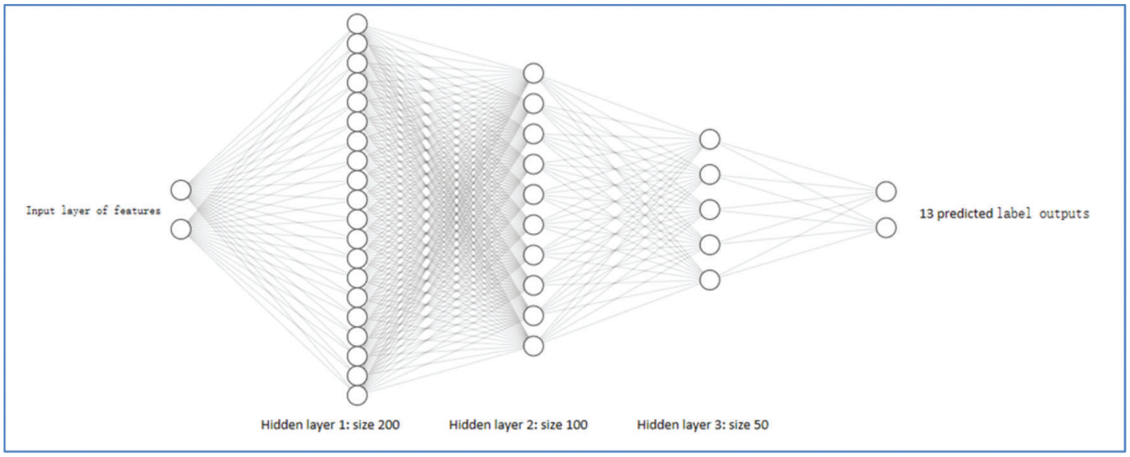


**Figure 8.6** Topology of the neural network model.

```
Model(
  (all_embeddings): ModuleList(
    (0): Embedding(8, 4)
    (1): Embedding(7, 4)
    (2): Embedding(3, 2)
  )
  (embedding_dropout): Dropout(p=0.4, inplace=False)
  (batch_norm_num): BatchNorm1d(5, eps=1e-05, momentum=0.1, affine=True, track_running_stats=True)
  (layers): Sequential(
    (0): Linear(in_features=15, out_features=200, bias=True)
    (1): ReLU(inplace=True)
    (2): BatchNorm1d(200, eps=1e-05, momentum=0.1, affine=True, track_running_stats=True)
    (3): Dropout(p=0.4, inplace=False)
    (4): Linear(in_features=200, out_features=100, bias=True)
    (5): ReLU(inplace=True)
    (6): BatchNorm1d(100, eps=1e-05, momentum=0.1, affine=True, track_running_stats=True)
    (7): Dropout(p=0.4, inplace=False)
    (8): Linear(in_features=100, out_features=50, bias=True)
    (9): ReLU(inplace=True)
    (10): BatchNorm1d(50, eps=1e-05, momentum=0.1, affine=True, track_running_stats=True)
    (11): Dropout(p=0.4, inplace=False)
    (12): Linear(in_features=50, out_features=13, bias=True)
  )
)
```

**Figure 8.7** The neural network model training sample code.

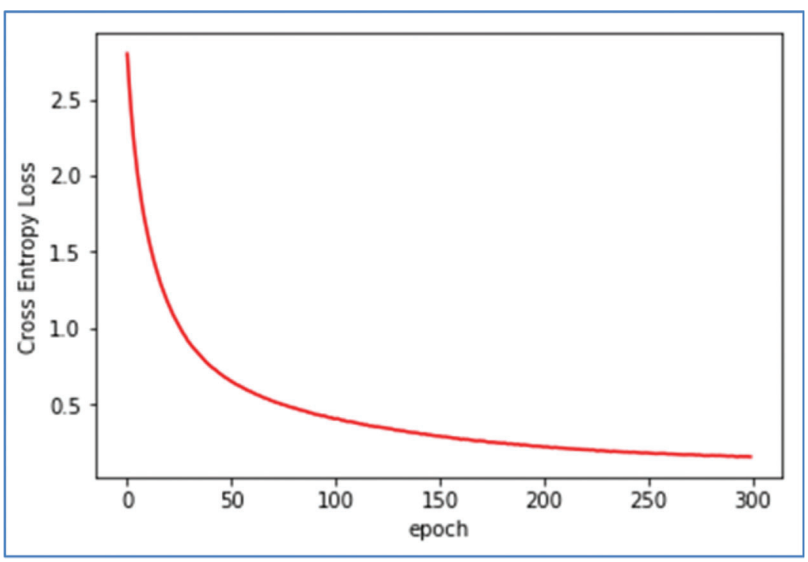


**Figure 8.8** The learning curve of the training process.

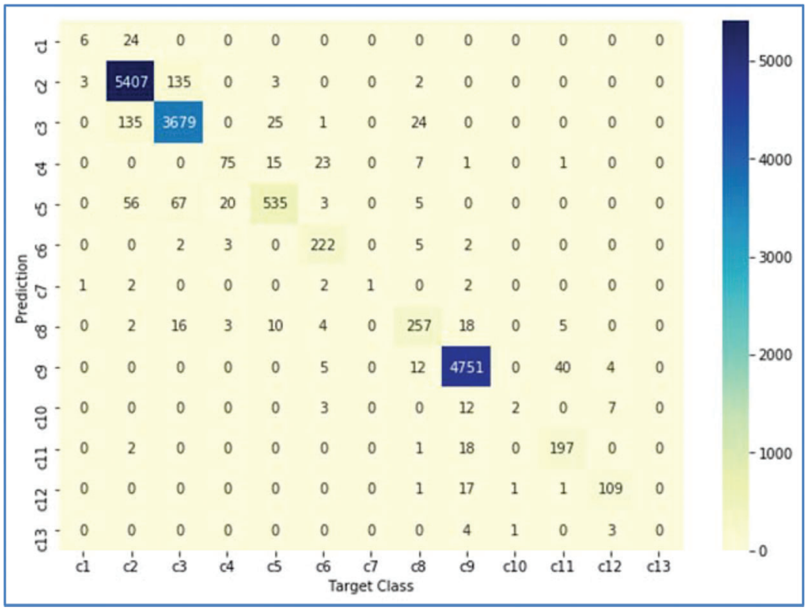


**Figure 8.9** The confusion matrix.

Class 13 vehicles in the dataset, but not because of poor accuracy.

## 8.3 Model Application

After the NN model was trained and validated using the labeled dataset, it was applied to evaluate the unlabeled dataset from the same WIM site. That is, the model was used to process the unlabeled dataset to assign the unclassified vehicles (C0) into other vehicle classes (C1, C2, …, C13) through the neural network learning algorithm based on the characteristic features. A total of 3,409 unclassified vehicles were processed through the NN model and they were allocated to the vehicle classes of C1, C2, …, C13. The allocations of the unclassified vehicles are shown in Figure 8.10. For comparison purpose, the original distribution of classified vehicles is presented in Figure 8.11. The distributions in the two figures are fairly similar in the general patterns. However, the details indicate that the proportions of vehicles in C6, C8, and C11 in Figure 8.10 are higher than their counterparts in Figure 8.11, which may mean that C6, C8, and C11 vehicles are more prone to misclassification. On the other hand, the proportions of C9 vehicles in the two figures may imply that C9 vehicles are less likely to be misclassified.

The proportions displayed in Figure 8.10 are highly important for AADTT values with respect to MEPDG. Without these proportions, the unclassified vehicles are either discarded or assigned to the truck groups arbitrarily. The proportions from the NN model can be used to allocate the unclassified vehicles into the 13 classes of vehicles in a rational manner so that pavement designs through MEPDG would produce more appropriately and realistically results.

Since unclassified vehicles vary considerably on different roadways, the NN model should be applied at each WIM site separately to reflect the particular characteristics of the site. The unclassified vehicle data in 2019 from 43 WIM stations were processed for the NN model. The data from each WIM station were utilized to go through the learning and testing steps and then the calculating and predicting steps. The proportions of unclassified vehicles to be allocated to the vehicle classes for all WIM sites were obtained as shown in Table 8.3. Also shown in Table 8.3 are the percent of unclassified vehicles, the WIM recorded AADTT, the updated AADTT after allocations, and the percent of AADTT increase. The results from the NN model indicate that the average accuracy of the model predictions is 0.943. The only WIM site with a low accuracy (0.8605) is WIM Site 482. At this site, 98.1% of the recorded vehicles were unclassified vehicles. The NN model could not effectively classify the vehicles because the number of unclassified vehicles is extremely higher than that of classified vehicles in the WIM data. It is most likely that the WIM device at WIM Site 482 malfunctioned and the traffic data were not valid.

Using the obtained proportions for allocations, the AADTT values are updated by adding the allocated unclassified vehicles in the original AADTT. As can be seen in the Table 8.3, the AADTT increases range from 1.0% to 86.5% with an average increase of 14.4%. To illustrate the effects of allocated unclassified vehicles, Figures 8.12, 8.13, and 8.14 are drawn for low, medium, and high C0 volumes, respectively. Apparently, the effects of unclassified vehicles on pavement design could be significant if they were not appropriately allocated. The allocations resulted from the NN model will improve the quality of truck volume input for MEPDG and will consequently improve pavement design.

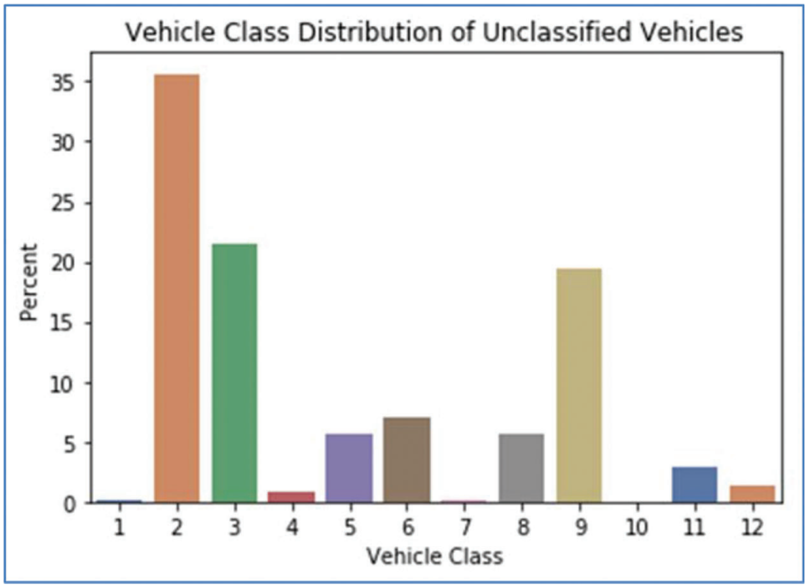


**Figure 8.10** Proportions of unclassified vehicle allocations.

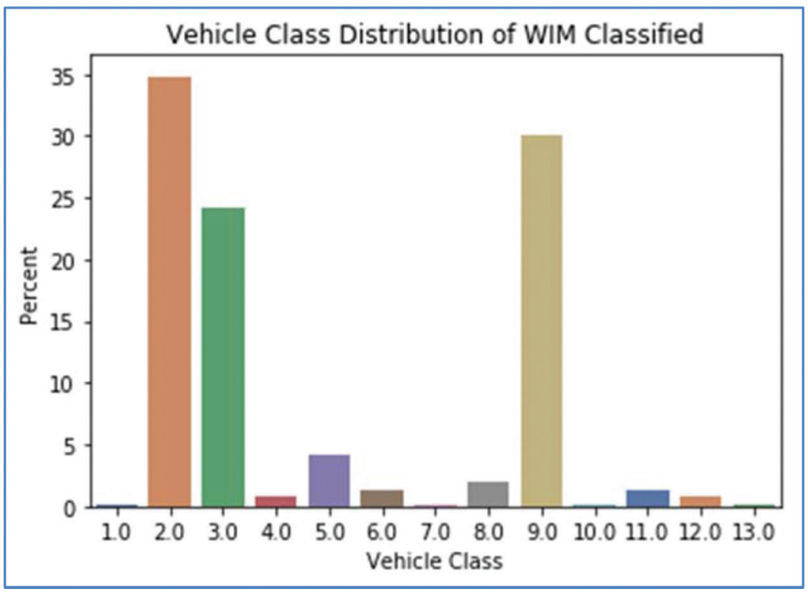


**Figure 8.11** Distribution of classified vehicles.

It should be noted that the NN model was established based on the characteristic features in the WIM recorded data with respect to unclassified vehicles. The allocations obtained from the NN model provide a much better way for including the unclassified vehicles in the truck volumes than disregarding or arbitrarily assign them to truck classes. However, the NN method could be further enhanced by including additional information, such as image and video sources.

### 8.4 Validation with Traffic Videos

The morning traffic stream was video recorded for a few hours on April 13, 2018 near the WIM Site 370 on I-70 for a previous study (Bunnell et al., 2018). The video data were provided by INDOT to analyze unclassified vehicles in this study. In order to match the WIM recorded data and the video images during the 200-minute time period, a total of 124 unclassified vehicles were retrieved from the WIM data. All of the 124 unclassified vehicles were detected and properly labeled by comparing with the video records. Three of the images of misclassified vehicles are shown in Figure 8.15. Image (a) shows a Class 3 vehicle that was recorded as an unclassified vehicle. Image (b) is a Class 9 vehicle that was marked as an unclassified vehicle. Image (c) displays two adjacent Class 2 vehicles that were assigned as one unclassified vehicle. During the

TABLE 8.3
**Proportions of unclassified vehicle allocations of WIM Sites (2019)**

| WIM | % Unclassified Vehicles (C0) Allocated to Vehicle Classes | | | | | | | | | | | | | | | | AADTT |
|---|---|---|---|---|---|---|---|---|---|---|---|---|---|---|---|---|---|
| | | | | | | | | | | | | | | | | Update | Increase |
| No. | C1 | C2 | C3 | C4 | C5 | C6 | C7 | C8 | C9 | C10 | C11 | C12 | C13 | C0 (%) | AADTT | AADTT | (%) |
| 102 | 0.1 | 29.1 | 44.4 | 0.7 | 5.5 | 4.3 | 1.4 | 2.6 | 10.6 | 0.1 | 0.0 | 0.0 | 1.2 | 19.4 | 1,662 | 2,033 | 22.3 |
| 109 | 0.0 | 37.6 | 35.5 | 0.3 | 10.8 | 1.1 | 0.2 | 2.8 | 10.5 | 0.0 | 0.2 | 1.0 | 0.0 | 1.6 | 7,762 | 7,942 | 2.3 |
| 315 | 0.0 | 50.4 | 33.0 | 0.2 | 7.2 | 2.6 | 0.6 | 0.7 | 4.0 | 0.0 | 0.0 | 0.0 | 1.2 | 15.5 | 6,347 | 8,205 | 29.3 |
| 316 | 0.0 | 54.6 | 37.2 | 0.2 | 6.7 | 0.0 | 0.0 | 0.1 | 1.2 | 0.0 | 0.0 | 0.0 | 0.0 | 11.9 | 5,460 | 6,268 | 14.8 |
| 436 | 0.0 | 43.1 | 26.7 | 0.1 | 7.4 | 1.3 | 0.0 | 6.9 | 13.1 | 1.2 | 0.2 | 0.0 | 0.0 | 0.9 | 5,433 | 5,489 | 1.0 |
| 507 | 0.2 | 40.5 | 29.6 | 0.8 | 4.0 | 1.1 | 0.2 | 5.5 | 15.3 | 0.2 | 0.7 | 1.9 | 0.0 | 8.6 | 11,374 | 12,371 | 8.8 |
| 100 | 0.0 | 47.7 | 14.6 | 0.2 | 8.0 | 3.1 | 0.1 | 9.2 | 15.5 | 0.2 | 0.4 | 1.1 | 0.1 | 2.2 | 1,209 | 1,236 | 2.2 |
| 120 | 0.7 | 25.3 | 34.0 | 0.6 | 2.4 | 2.3 | 0.1 | 5.5 | 28.0 | 0.1 | 0.3 | 0.7 | 0.0 | 23.8 | 4,901 | 6,564 | 33.9 |
| 200 | 0.1 | 38.7 | 39.6 | 0.7 | 10.2 | 0.5 | 0.0 | 1.2 | 8.9 | 0.1 | 0.0 | 0.1 | 0.1 | 8.9 | 7,168 | 7,669 | 7.0 |
| 210 | 1.6 | 34.2 | 38.4 | 0.3 | 5.5 | 4.8 | 0.1 | 0.8 | 14.2 | 0.0 | 0.1 | 0.0 | 0.0 | 45.7 | 1,442 | 2,689 | 86.5 |
| 220 | 0.1 | 46.2 | 31.2 | 1.3 | 6.4 | 3.4 | 0.4 | 1.9 | 8.9 | 0.0 | 0.3 | 0.0 | 0.0 | 4.2 | 1,730 | 1,828 | 5.7 |
| 240 | 0.2 | 24.6 | 35.3 | 0.9 | 1.4 | 6.6 | 0.0 | 3.5 | 25.2 | 1.1 | 0.2 | 1.0 | 0.1 | 7.0 | 6,248 | 6,647 | 6.4 |
| 310 | 0.0 | 60.6 | 27.0 | 0.0 | 8.7 | 0.3 | 0.0 | 1.6 | 1.7 | 0.0 | 0.0 | 0.0 | 0.0 | 0.7 | 2,152 | 2,181 | 1.3 |
| 331 | 0.1 | 40.8 | 35.9 | 0.4 | 13.0 | 2.1 | 0.2 | 1.8 | 5.5 | 0.0 | 0.1 | 0.2 | 0.0 | 13.7 | 11,571 | 13,416 | 15.9 |
| 332 | 0.0 | 48.2 | 38.7 | 0.6 | 2.4 | 7.0 | 0.1 | 1.0 | 2.0 | 0.0 | 0.1 | 0.0 | 0.0 | 22.8 | 2,962 | 3,554 | 20.0 |
| 351 | 0.0 | 64.1 | 28.1 | 0.1 | 4.0 | 0.4 | 0.0 | 0.5 | 2.8 | 0.0 | 0.0 | 0.0 | 0.0 | 16.4 | 8,220 | 9,233 | 12.3 |
| 352 | 0.0 | 38.9 | 36.8 | 0.1 | 7.0 | 0.9 | 0.1 | 2.0 | 13.6 | 0.0 | 0.4 | 0.2 | 0.0 | 8.7 | 9,081 | 10,750 | 18.4 |
| 360 | 0.1 | 29.7 | 21.3 | 0.7 | 7.0 | 14.4 | 0.1 | 3.9 | 19.5 | 0.1 | 0.8 | 2.5 | 0.0 | 3.3 | 16,319 | 16,979 | 4.0 |
| 370 | 0.1 | 41.9 | 28.2 | 0.0 | 4.6 | 3.1 | 0.1 | 1.9 | 17.3 | 0.0 | 1.5 | 1.5 | 0.0 | 9.9 | 7,538 | 8,148 | 8.1 |
| 401 | 0.0 | 71.0 | 8.0 | 0.4 | 3.7 | 1.3 | 0.0 | 4.2 | 10.2 | 0.1 | 0.8 | 0.2 | 0.0 | 3.2 | 24,780 | 25,416 | 2.6 |
| 402 | 0.0 | 44.9 | 37.5 | 0.6 | 6.1 | 2.7 | 0.0 | 1.0 | 6.8 | 0.1 | 0.3 | 0.1 | 0.0 | 11.6 | 56,826 | 61,322 | 7.9 |
| 420 | 0.0 | 54.4 | 37.1 | 0.7 | 2.6 | 0.3 | 0.0 | 0.3 | 4.1 | 0.0 | 0.1 | 0.2 | 0.0 | 7.3 | 18,078 | 18,666 | 3.3 |
| 430 | 0.0 | 0.0 | 23.8 | 5.7 | 10.7 | 4.7 | 0.0 | 7.2 | 45.4 | 0.4 | 0.7 | 1.2 | 0.2 | 13.8 | 12,506 | 14,171 | 13.3 |
| 441 | 0.0 | 57.4 | 15.2 | 0.6 | 4.5 | 1.7 | 0.0 | 2.9 | 15.5 | 0.8 | 0.4 | 0.5 | 0.6 | 13.1 | 12,725 | 14,666 | 15.3 |
| 442 | 0.2 | 36.4 | 35.6 | 0.9 | 4.9 | 2.8 | 0.0 | 1.4 | 16.5 | 0.2 | 0.7 | 0.5 | 0.1 | 22.9 | 13,634 | 17,594 | 29.0 |
| 450 | 0.2 | 38.9 | 39.2 | 0.5 | 14.3 | 3.5 | 0.3 | 1.3 | 1.9 | 0.0 | 0.0 | 0.0 | 0.0 | 4.7 | 809 | 896 | 10.8 |
| 470 | 0.0 | 60.5 | 20.4 | 0.1 | 5.8 | 2.5 | 0.0 | 1.9 | 8.8 | 0.0 | 0.0 | 0.0 | 0.0 | 0.8 | 5,468 | 5,520 | 1.0 |
| 481 | 0.0 | 38.6 | 48.5 | 0.6 | 2.9 | 1.1 | 0.0 | 1.4 | 6.5 | 0.0 | 0.2 | 0.1 | 0.0 | 0.3 | 18,098 | 20,275 | 12.0 |
| 482 | 0.0 | 0.0 | 0.0 | 0.0 | 0.0 | 0.0 | 0.0 | 0.0 | 0.0 | 0.0 | 0.0 | 0.0 | 0.0 | 98.1 | 461 | — | — |
| 490 | 0.0 | 68.3 | 18.0 | 0.1 | 4.5 | 1.0 | 0.0 | 0.5 | 5.8 | 0.1 | 0.0 | 0.0 | 1.7 | 3.3 | 1,345 | 1,403 | 4.3 |
| 520 | 0.0 | 44.1 | 24.0 | 0.0 | 17.1 | 0.9 | 0.1 | 3.6 | 10.1 | 0.1 | 0.0 | 0.0 | 0.0 | 1.4 | 849 | 866 | 2.0 |
| 530 | 0.0 | 55.6 | 32.6 | 0.7 | 1.7 | 2.0 | 0.0 | 1.1 | 6.0 | 0.0 | 0.1 | 0.3 | 0.0 | 10.8 | 6,952 | 7,377 | 6.1 |
| 540 | 0.0 | 38.2 | 40.3 | 0.6 | 7.0 | 1.6 | 0.0 | 1.7 | 10.1 | 0.1 | 0.1 | 0.3 | 0.0 | 28.9 | 5,131 | 7,067 | 37.7 |
| 560 | 0.0 | 46.8 | 27.0 | 0.5 | 9.0 | 1.4 | 0.3 | 2.9 | 11.4 | 0.0 | 0.3 | 0.5 | 0.0 | 7.6 | 12,642 | 13,694 | 8.3 |
| 600 | 0.0 | 60.2 | 20.4 | 0.0 | 8.2 | 1.2 | 0.1 | 4.6 | 5.2 | 0.2 | 0.0 | 0.0 | 0.0 | 1.9 | 474 | 482 | 1.7 |
| 610 | 0.0 | 44.2 | 33.8 | 0.4 | 4.2 | 3.0 | 0.1 | 2.5 | 11.1 | 0.0 | 0.2 | 0.5 | 0.0 | 21.0 | 5,512 | 6,432 | 16.7 |
| 620 | 0.0 | 45.7 | 20.4 | 0.7 | 4.2 | 0.5 | 0.0 | 8.1 | 18.2 | 0.2 | 1.0 | 1.0 | 0.0 | 1.7 | 2,733 | 2,777 | 1.6 |
| 630 | 0.0 | 55.3 | 37.1 | 0.2 | 6.0 | 0.4 | 0.0 | 0.4 | 0.6 | 0.0 | 0.0 | 0.0 | 0.0 | 27.6 | 769 | 944 | 22.8 |
| 640 | 0.0 | 41.7 | 26.1 | 0.1 | 20.8 | 3.7 | 0.2 | 1.2 | 2.3 | 0.0 | 0.0 | 0.0 | 3.9 | 22.3 | 941 | 1,598 | 69.8 |
| 650 | 0.0 | 52.9 | 36.7 | 0.3 | 4.2 | 0.2 | 0.0 | 2.3 | 3.5 | 0.0 | 0.0 | 0.0 | 0.0 | 3.4 | 2,758 | 2,850 | 3.3 |
| 660 | 10.6 | 50.9 | 29.3 | 0.4 | 3.4 | 1.1 | 0.5 | 1.0 | 2.9 | 0.0 | 0.0 | 0.0 | 0.0 | 26.0 | 824 | 1,068 | 29.6 |
| 999 | 0.1 | 46.7 | 16.6 | 1.3 | 4.5 | 1.5 | 0.0 | 2.7 | 23.6 | 0.0 | 0.7 | 2.3 | 0.0 | 2.3 | 8,217 | 8,375 | 1.9 |
| 999 | 0.0 | 46.1 | 42.8 | 0.2 | 6.7 | 0.9 | 0.0 | 0.8 | 1.7 | 0.4 | 0.0 | 0.0 | 0.5 | 3.9 | 3,982 | 4,110 | 3.2 |

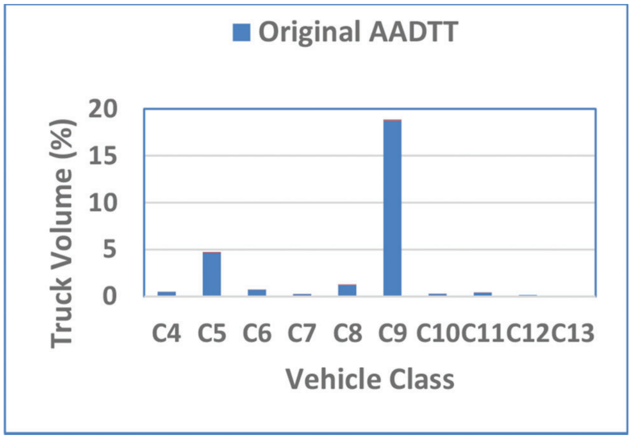


**Figure 8.12** Allocation of low unclassified vehicle volume (WIM Site 436).

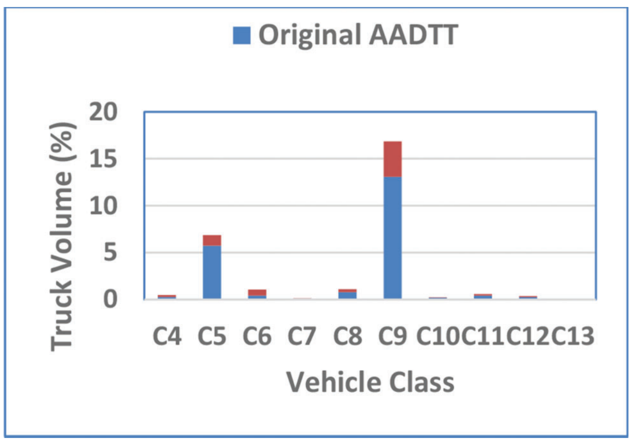


**Figure 8.13** Allocation of medium unclassified vehicle volume (WIM Site 442).

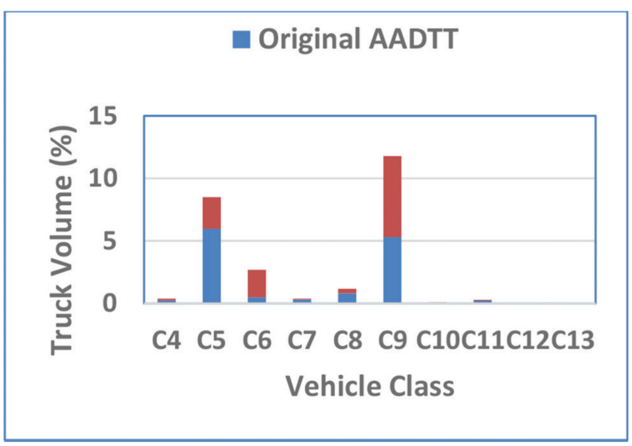


**Figure 8.14** Allocation of high unclassified vehicle volume (WIM Site 210).

labeling process, some cases of failing to classify vehicles were identified by comparing the WIM data and the video records as listed below:

1. WIM device failed to capture or measure the features (speeds, axle loads, and axle spaces) of vehicles while they were changing lanes and thus placed the vehicles as unclassified. WIM data often contain zero values of speeds, axle loads, and axle spaces.
2. One vehicle was classified as two vehicles (misclassified and/or unclassified) during lane changing movement, one vehicle per lane. Thus, there is one non-existing vehicle under this situation.
3. Two adjacent vehicles were recorded as one because they moved very closely as shown in Figure 8.15(c).
4. Passenger cars with trailers and some types of recreational vehicles (RV) were recorded as unclassified vehicles in the WIM data.

As presented in Table 8.1 in the previous section, the characteristic variables of the NN model include GVW, length, speed, meanAxleWeight, meanAxleSpace, Single, Tandem, and Tridem. However, among the 124 unclassified vehicles matched with the video records, only 75 of them have WIM data with non-zero values related to the eight characteristic variables. The WIM data of the other 49 unclassified vehicles have incomplete and inaccurate values or even all zero values of the characteristic variables.

The NN model was applied to process the 124 labeled unclassified vehicles that matched WIM data and the video files, including the 75 with non-zero data values and the 49 with incomplete or zero data values. The model predicts all of the 49 unclassified vehicles with incomplete or zero data values as Class 2 vehicles (passenger cars), while the video shows that 11 of them are trucks and 11 of them are actually the double counted (non-existing) ones during lane changing. The reason for this inaccurate prediction is that the WIM data contain incomplete or zero values. That is, the low quality of input data resulted in the low quality of the model output. A total of 38 out of the 75 unclassified vehicles with non-zero inputs were correctly classified by the NN model. Among the 37 vehicles that were misclassified by the NN model, 17 of them were misclassified as Class 8 and Class 9 trucks, while they are actually Class 2 and Class 3 vehicles with a trailer attached (see Figure 8.15(a)). The NN model failed to distinguish the trailer axles from the semi-truck axles. Another 11 of the 37 vehicles were misclassified as Class 8 and Class 9 trucks by the NN model, while the video shows they are in reality two adjacent lightweight vehicles (Class 2 or Class 3) moving closely. The comparison of the video labeled and the model predicted vehicle types is demonstrated in Figure 8.16. In the figure, “0” in the horizontal axis represents the group of double counted or non-existing vehicles.

As Figure 8.16 shows, the NN model produced fairly good predictions with the limited and incomplete WIM data and with the video of only a few hours at one location. Through manually examining the videos and matching the WIM data, some causes for misclassifying vehicles were identified. It is believed that the accuracy of assigning unclassified vehicles can be considerably improved if more video data are available at more WIM stations. Video and image data can be used to identify additional key features of moving

(a) Class 3 Vehicle (b) Class 9 Vehicle (c) Two Class 2 Vehicles

**Figure 8.15** Images of misclassified vehicles.

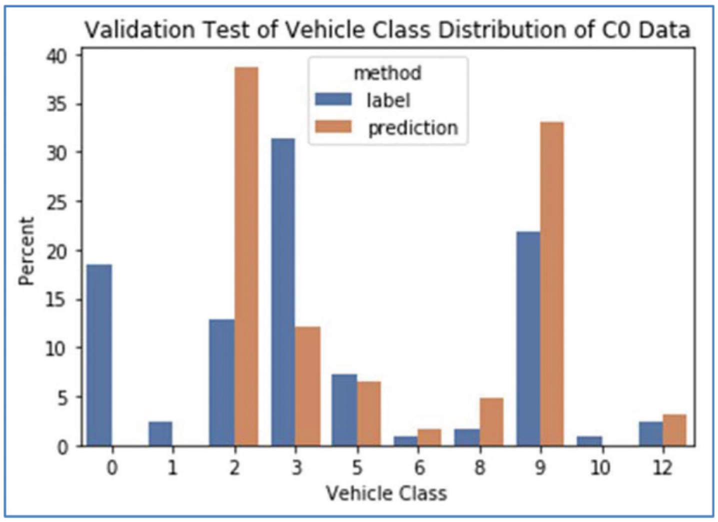


**Figure 8.16** Comparison between video labeled and model predicted classifications.

vehicles that WIM devices are not able to detect and record. The combination of video/image and WIM data will provide key information and sources for further improving vehicle classification efficiency and quality. It is proposed that the neural network algorithms and image processing techniques are employed to tackle the unclassified vehicles issues related to WIM data.

## 9. TRUCK TRAFFIC DATA REPOSITORY AND VISUALIZATION

### 9.1 Data Repository

The compiled truck traffic data in this study will be utilized for pavement design with MEPDG software. The required truck traffic related data for MEPDG include truck volume distributions and axle load spectra. As described in Chapter 3, the truck traffic and axle load information has been compiled and stored in Excel files for all ATR and WIM stations. In an attempt to make the truck data in an easily accessible manner for pavement design, the truck volume distributions and axle load spectra were converted into the Extensible Markup Language (XML) format for the MEPDG pavement design software.

The truck traffic data repository module was created with MicroStation V8i. MicroStation (Bentley, 2020) is a computer-aided design (CAD) software platform for two- and three- dimensional design and drafting, developed and sold by Bentley Systems and used in the architectural and engineering industries. It generates 2D/3D vector graphics objects and elements and includes building information modeling (BIM) features. For easy access and identification, in the repository the ATR and WIM stations were grouped in terms of the nearest cities that they located. Figure 9.1 is an illustration of an interface of the repository model. The interface shows the cities on the Indiana map, where the blue bars are actually the city names that can be exhibited if the map view is enlarged by zooming in.

A user can double click on a city name to display the ATR and WIM stations near and around the city. The information on each of the ATR and WIM stations includes the type of station (ATR or WIM), station

**Figure 9.1** Interface of the repository model.

number, route ID and mile marker, AADT and AADTT of 3 years (2016, 2017, and 2018). As an example, Figure 9.2 shows the essential information on a WIM station after double-clicking on the city name "Lafayette."

The interface shown in Figure 9.2 contains only general truck traffic information. The detailed truck traffic information can be exported to a computer or a hard drive following the following steps.

1. Generate templates: Click the "Element" → "Tags" → "Generate Templates" (see Figure 9.3).
2. Select parameters: Choose a tag set, such as West Lafayette, and then add tags into the report columns, and name the report file, such as *wls1*. Leave other settings unchanged. (see Figure 9.4)
3. Save templates: Click "File" → "Save as" → Use the report file name to save the template (wls1.tmp) at a selected location on a computer or hard drive. (see Figure 9.5)
4. Generate report: Click "Element" → "Tags" → "Generate Reports" (see Figure 9.6).
5. Save report: Choose a location, name the file, add it into the "Selected Files" and then click "Done" (see Figure 9.7).
6. View report: Go to the default location of tag files (the default path is Drive:\Bently\Microstation\WorkSpace

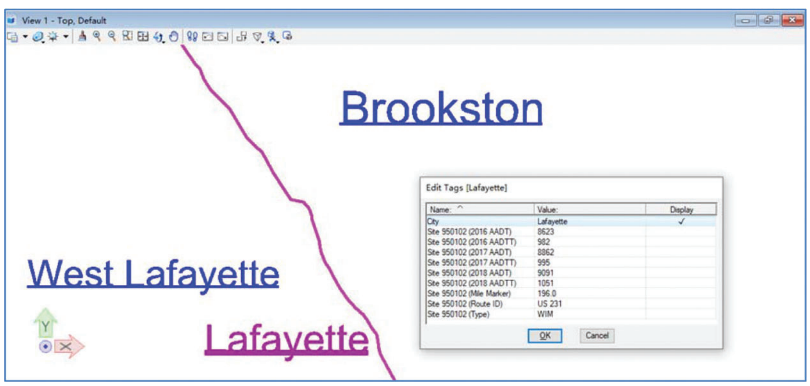


**Figure 9.2** Tag information of a WIM station.

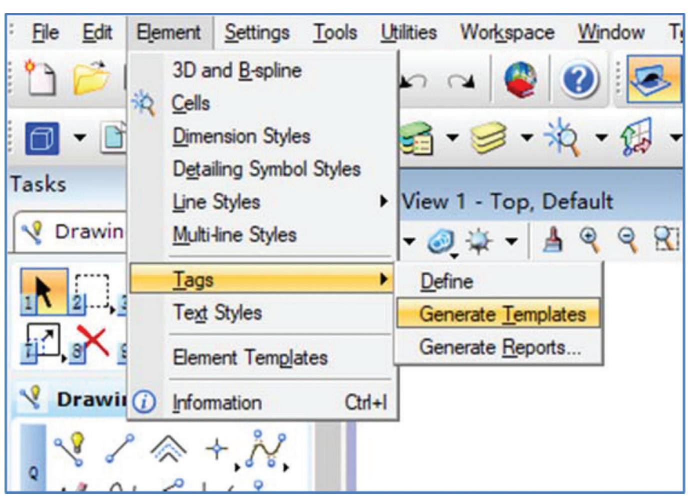


**Figure 9.3** Generating templates.

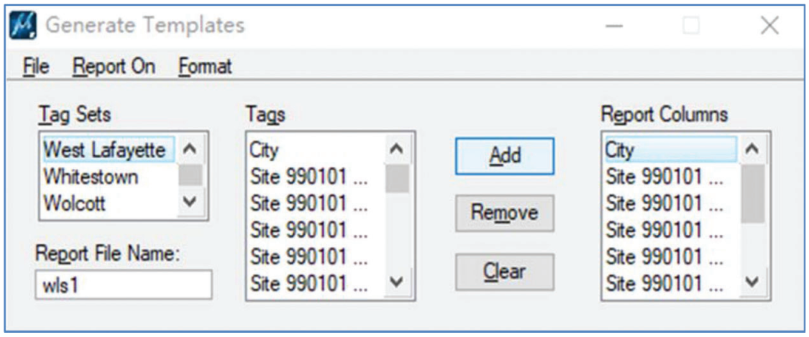


**Figure 9.4** Select parameters.

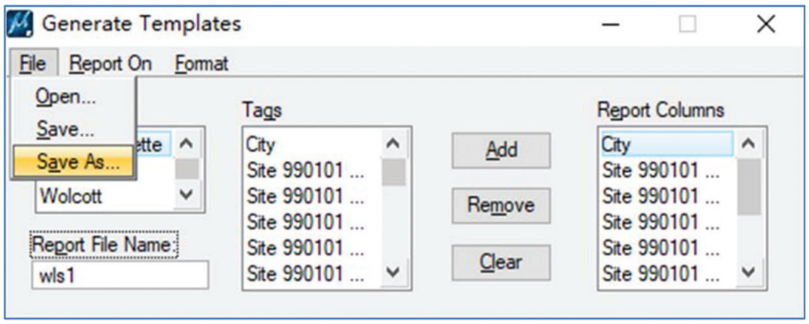


**Figure 9.5** Save templates.

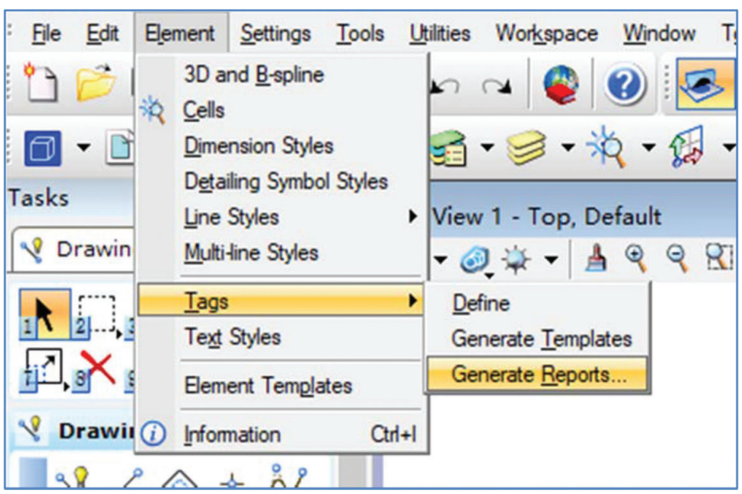


**Figure 9.6** Generate report.

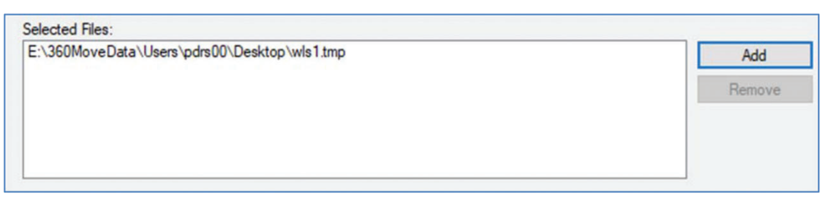


**Figure 9.7** Save report.

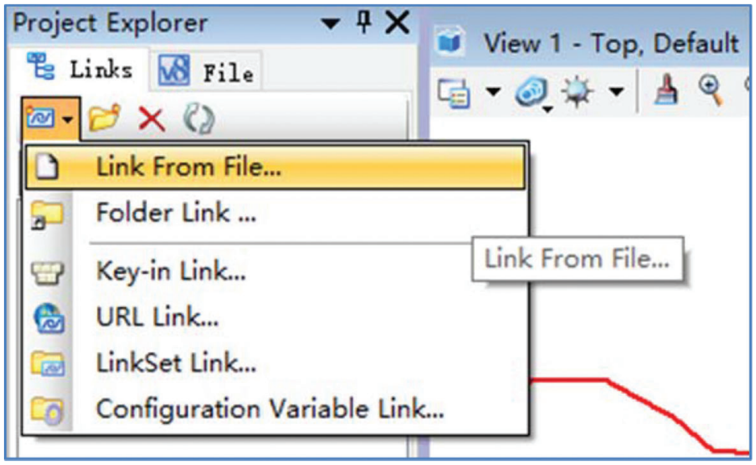


**Figure 9.8** Link GIS files.

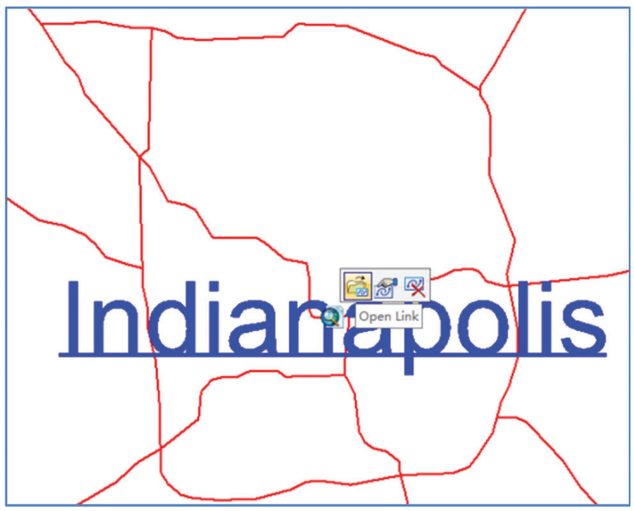


**Figure 9.9** Add link.

\Projects\Examples\General\out) and open the file. You may save the file format from rpt to csv.

## 9.2 Link Other Sources or Files to the Repository

INDOT produces annual GIS maps of statewide traffic volumes. The CAD based truck traffic repository model and the GIS maps are in different formats and on different platforms. It may be necessary or helpful to link the truck traffic repository to the GIS map. The steps to link are as follows:

1. In the MicroStation V8i project explorer, click the "Create Link" → "Link from File" and then select all GIS files that need to be associated (Figure 9.8).
2. Add link: Right-click on any GIS file in the project explorer and select "add link to element" and then put the link on a selected city tag, such as Indianapolis (Figure 9.9). The link can then be opened, edited, or removed. In addition to GIS maps, other types of files, including pdf, image, and data sheet files, can also be linked with the repository model if needed.

## 9.3 Data Storage and Visualization Model

In order to better demonstrate the road and traffic conditions of individual ATR and WIM stations, a BIM based data storage and visualization model was also created for traffic and truck volume and road condition at each ATR and WIM station. The data storage and visualization model is based on the Revit BIM software.

At each ATR or WIM station, the BIM model can show not only the traffic related data, such as AADT, AADTT, lane distribution, directional distribution, and truck volumes in terms of C1 to C13, but also 2D and 3D images of pavement structure, pavement lanes, and pavement thickness. Figure 9.10 illustrates a portion of the data storage and visualization model at one WIM station, which includes data storage and 2D and 3D displays of the roadway section.

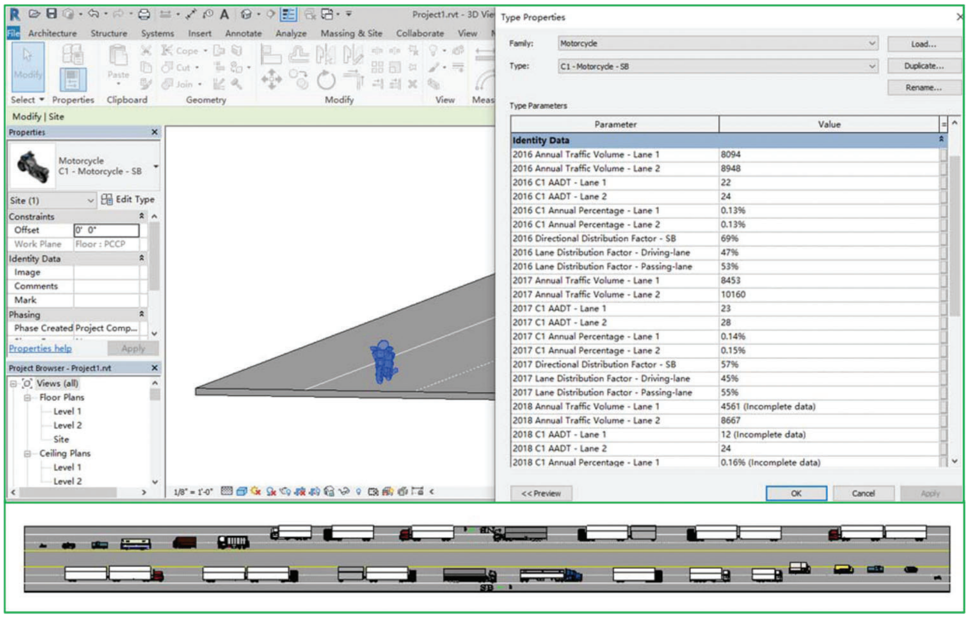


**Figure 9.10** Data storage and visualization.

## 10. TABLEAU INTERACTIVE VISUALIZATION DASHBOARD

### 10.1 Data Visualization

The traffic input module for MEPDG design has been updated and discussed in the previous chapters. The results from this study, including averaged annual daily (truck) traffic distributions, axle load spectra, and monthly and directional factors, are stored and presented in the forms of detailed tables, figures, and spatial files. The analyses on vehicle platooning and unclassified vehicles are provided with structured data results. In order to provide a tool for INODT engineers to have easy and effective access to the traffic data, additional efforts were made to create an interactive visualization dashboard. The dashboard is based on Tableau desktop software (Tableau, 2020). Tableau is a data visualization tool used to help in simplifying raw data into the easily understandable format. The visualizations created with Tableau are in the form of dashboards and worksheets.

The intention to develop the visualization dashboard was to enable user to access the truck traffic data, compare traffic performances of ATR and WIM sites, identify missing data problems, and examine the changing patterns and trends of truck volumes. The functions of the visualization dashboard implemented include:

1. Access needed information, identify traffic patterns, and compare the characteristics of truck traffic in different sites.
2. Create a basis for determining appropriate locations of possible new ATR or WIM stations to be added in the future to the system. This is because the visualized information, including yearly volume change tendencies, site density in area of selection, and the level of traffic volumes, should all be considered for the choice of desired new locations.
3. Identify potential road sections of traffic congestion, which are the locations with relatively high traffic volumes and less roadway lanes.
4. Signal possible malfunctions of ATR or WIM devices. The identifications of device malfunctions, such as missing data or uncharacteristic data values, could be captured and displayed by the visualization dashboard.
5. Catch significant changes in terms of traffic and truck traffic volumes.
6. Provide user friendly functionality and compatibility for future data expansion. The Excel worksheets of data sources can be displayed, modified, and updated to include new data.

### 10.2 Visualization Dashboard

#### *10.2.1 Data Features and Main Displays*

As presented in the previous chapters, this study has generated various types of tables, figures, and maps. To create a suitable data structures for the dashboard, data rearrangement was first processed before extracted into the Tableau platform. The AADTT data were divided into directional data at the ATR and WIM stations with recorded traffic data in two directions. A spatial file was used to transfer the spatial geometry into latitude and longitude coordinates so that different data sources could be collaborated in the roadway maps. The data features behind the Excel worksheet are listed in Table 10.1.

Figure 10.1 shows an overview of the interactive visualization dashboard, which is composed of the following five views displaying different aspects of traffic data.

TABLE 10.1
**Data features for the interactive visualization dashboard**

| Feature | Description |
|---|---|
| Latitude/Longitude | Coordinates of the data site |
| Site | Site name |
| Year | Year of data (2016–2019) |
| Counted Days | Number of the days in the year with recorded data |
| Direction | Vehicle travel direction |
| Direction Order | Direction(s) order in data |
| Lanes Counted | Number of recorded lanes of road |
| C4, C5, …, C13 | Annual average daily truck volume in truck classes |
| AADT | Average annual daily traffic |
| AADTT | Average annual daily truck traffic |
| C4%, C5%, …, C13% | % of C4, C5, …, C13 in AADTT |
| City | The closest city near the site |
| County | The name of county the site is located |
| District | The name of district the site is located |
| Mile Marker | Route mile marker of the site location |
| Distance | Distance in miles a rural site from city (zeros for urban sites) |
| Route No. | Roadway route no. |
| Site ID | ATR or WIM Station ID |
| Site Type | Type of device (WIM or ATR) |


**Figure 10.1** Visualization dashboard.

1. A grouped bar chart of truck traffic class distributions with selected district, county, route, traffic directions, and sites.
2. A line chart showing the traffic changing patterns in time series.
3. Boxplots displaying the ranges of traffic volumes (AADT) and truck traffic volumes (AADTT) among the selected sites in rural and urban areas.
4. A map showing the all locations of ATR and WIM stations with highlighted abnormal sites.

5. A Tableau butterfly chart alongside the map view displaying side by side directional truck class distributions of selected sites.

In the dashboard, the data filters and the selection actions are connected with all five views so that the views will filtered/zoomed simultaneously with user's selection on data of interest. Scatterplots with regression equations are also created in the meantime in a workbook that is not displayed on the dashboard. The worksheet contains additional information on truck traffic distributions and their changing trends. The main visualization worksheets are described in the following.

### *10.2.2 Map Visualization*

The first worksheet is the visualization of map as shown in Figure 10.2. In this visualization worksheet, the map of the state of Indiana is formed with the traffic data in Excel produced for MEPDG and the route geometries from a spatial data file. The primary roadway spatial file is connected with the tabular data by transferring the route geometry into points with latitude and longitude coordinates. Filters on route geometry and county names is applied so that only highways and counties with available WIM or ATR sites are displayed in the map along with the selection lists. The map has two layers. The first layer is the highway routes displayed in grey in the map as the reference information of site locations. The second layer consisting shape markers aligned with the map to represent the locations of the WIM and ATR sites. Two icons with different shapes are utilized to denote urban and rural areas. The tabular data sources in the dashboard include all data recorded during 2016 to 2019. The red-blue color bar indicate the days that the device recorded traffic data during a year, with deep red representing the number of days with no data recorded and deep blue representing the number of days with full data recorded.

The value of *truck traffic directional ratio* on the map is the ratio of eastbound-volume to westbound-volume or the ratio of northbound-volume to southbound-volume. A ratio value close to 1.0 indicates good balance between the truck traffic in two directions, while a ratio value of 0 or extremely large implies that the ATR or WIM device at the site records the truck volume in only one direction. The tooltip hovered provides detailed information on traffic volumes and distributions.

### *10.2.3 Butterfly Charts*

Butterfly charts are embeded in the map and are visible in the form of tooltips. Figure 10.3 presents an example of butterfly chart view for ATR Site 204. The information pertaning to the site indicates that it is a two-way six-lane ATR site on I-69 with other location information, such as district, county, and city. The butterfly charts show that the volumes of Class 9 and Class 13 vehicles are not balanced in the two directions in terms of of the bar lengths on the two sides of the central certical axis. The truck traffic directional ratio of 1.492 implies that the northbound truck traffic volume is considerably greater than the southbound truck traffic volume. The average values of AADT and AADTT are also displayed. In addition, it is indicated

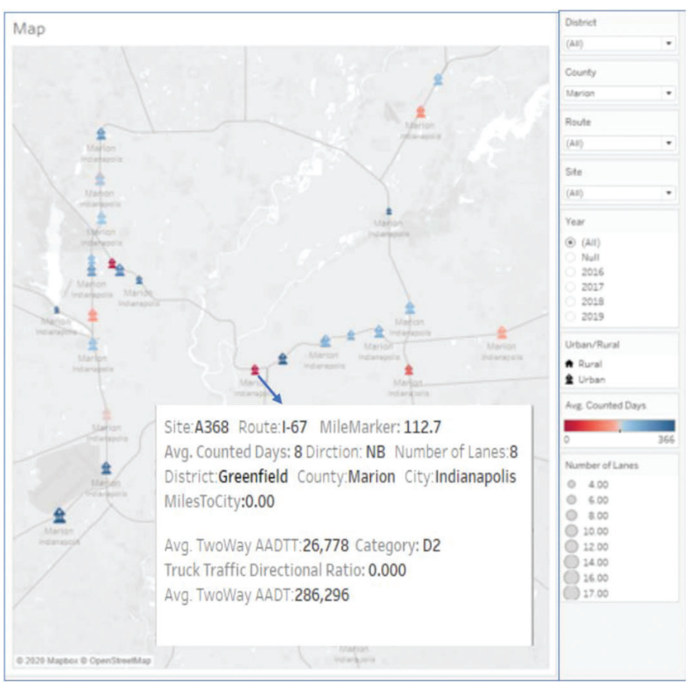


**Figure 10.2** Map visualization.

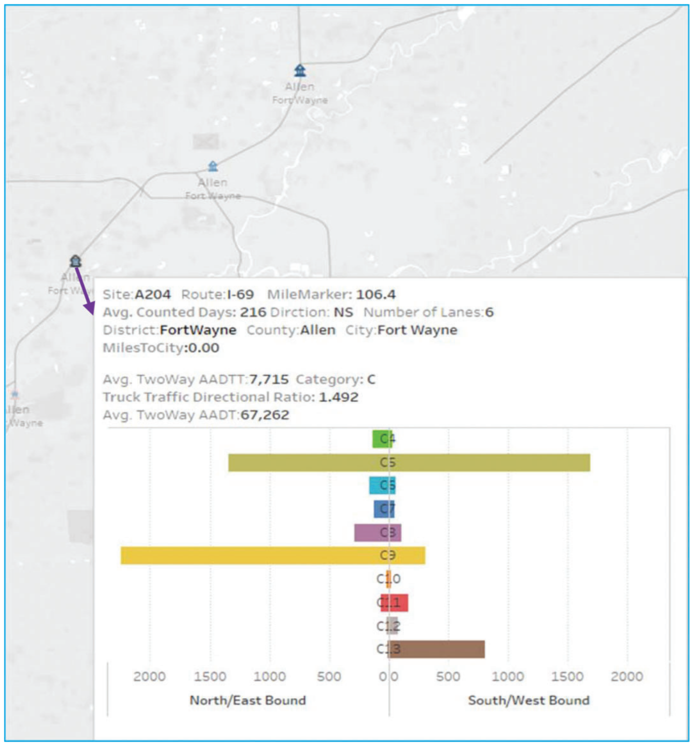


**Figure 10.3** Butterfly charts.


**Figure 10.4** Truck traffic bar charts.

that the truck weight road category is C on this roadway section.

### *10.2.4 Truck Traffic Bar Charts*

Bar charts are commonly utilized to visually show the realtive differences of quantitative data. Truck traffic volume distributions are displayed in bar charts as shown in Figure 10.4 in the dashboard. The bar charts demonstrate the 4-year truck volumes in terms of truck classes. The relative differences in truck traffic volumes can be clearly perceived and compared by the bar lengths. If a single site is selected, the visualization will show the AADTT vlaues of truck classes in the site.

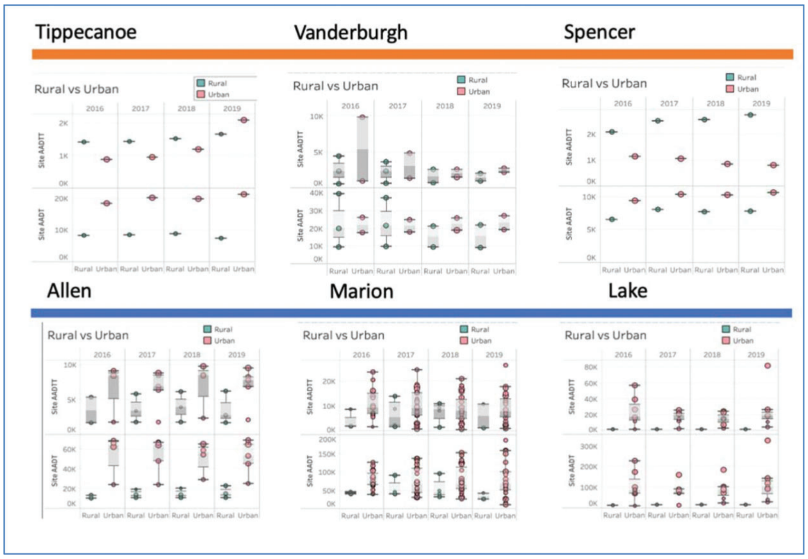


**Figure 10.5** Boxplots of different areas.

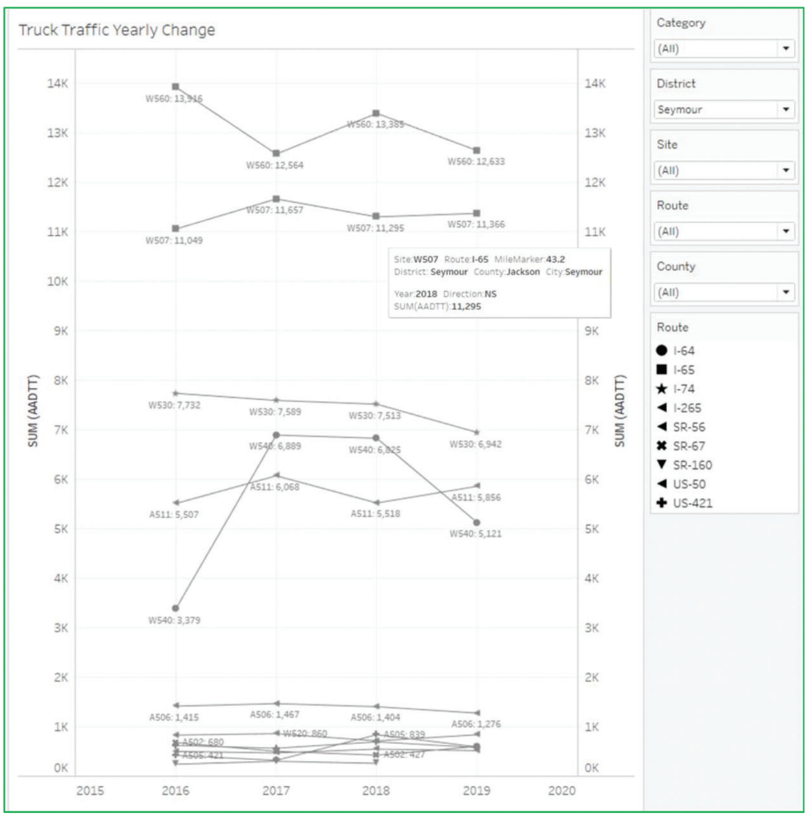


**Figure 10.6** Lane charts of AADTT.

A user can also select multiple sites to compare various features for specifc truck class or truck weight road category. For comparison of multiple sites, the truck traffic volumes are illustrated with stacked bar charts. The specific information related to the truck traffic volumes and distribitions is readily visible through tooltips.

*10.2.5 Boxplots*

Boxplots are used in the dashboard to show the difference ranges of traffic levels between sites in rual areas and sites in urban areas. As discussed in Chapter 8, boxplots are a standardized way of displaying the distribution of data based on a five number summary, including minimum, first quartile (Q1), median (second quartile: Q2), third quartile (Q3), and maximum. Figure 10.5 presents an example of boxplots showing the distributions of traffic volumes (AADT) and truck traffic volumes (AADTT) on roadway sections in rural and urban areas of several selected counties.

### *10.2.6 Line Charts*

Line charts are used in combination with tooltips to view truck traffic volumes in time series. An example of line charts is illustrated in Figure 10.6. In this example, demonstrated are the AADTT values of all ATR and WIM stations in District Seymour in the 4 years from 2016 to 2019. There are nine ATR and WIM stations on different roadway sections in the district. It can be seen that at ATR Site A510 the truck traffic volume in 2019 contains no values, indicating possible device malfunction.

## 11. CONCLUSIONS

The primary objective of this study was to update the traffic design input module, and thus to improve the current INDOT pavement design procedures. The traffic data recorded at 143 ATR and WIM stations over the most recent 3 years and annual traffic data maintained by INDOT were utilized in the analysis. The current truck traffic and the truck traffic in 2008 were compared and it was found that traffic volumes and truck traffic volumes had changes, mostly increased, considerably on the Indiana highway network. Truck traffic data in terms of Average Annual Daily Truck Traffic (AADTT) and axle load spectra were compiled and stored for MEPDG pavement design. Bus traffic data with respect of traffic volumes and axle load distributions were obtained through WIM and public transportation information.

The equivalent single axle load (ESAL) values were calculated based on the updated truck volumes and truck axle load data at WIM sites. New ESAL values were obtained using AASHTO equations and Axle Group Divisors. The ESAL values include annual ESAL values on roadway lanes, average annual ESALs per truck, average annual ESALs on different highways, and average annual ESALs on all roadways.

Analysis was performed to evaluate the shifts in truck traffic and axle load spectra for low and high truck volume roadways and more reasonable subcategories were determined.

Analysis was performed to better understand the traffic characteristics when they travel in groups with relative short headways between vehicles. The critical intervals were established to define vehicle platoons. Various types of platoons and their features were analyzed in terms of platoon lengths, leading vehicle types, and composition of vehicles.

Analysis of unclassified vehicles was performed with the ATR/WIM recorded data. A neural network model was established to determine the appropriate allocations of unclassified vehicles to truck classes. Since the number of unclassified vehicles is often fairly high at some ATR or WIM stations, the allocations will help to improve the accuracy of truck traffic data and thus improve pavement design. Video records of traffic on an interstate section and traffic data from a nearby WIM station were utilized to identify some causes for vehicle misclassifications.

A truck traffic data repository and visualization model and a Tableau interactive visualization dashboard model were developed for easy access, view, storage, and analysis of the updated MEPDG related traffic data.

All results and findings were included and combined to update the traffic variables in the current traffic design input module, including average annual daily truck traffic, truck volume monthly adjustment factors, truck volume lane distribution factors, truck volume directional distribution factors, truck volume class distributions, traffic volume hourly distribution factors, distributions of for single-, tandem-, tridem-, and quad-axle loads, average axle weight, average axle spacing, and average number of axle types.

The following recommendations are provided for future implementation of the research results:

- The updated truck traffic information should be used to replace the information produced from the last study for MEPDG pavement design. The information includes average annual daily truck traffic, truck volume monthly adjustment factors, truck volume lane distribution factors, truck volume directional distribution factors, truck volume class distributions, traffic volume hourly distribution factors, distributions of for single-, tandem-, tridem-, and quad-axle loads, average axle weight, average axle spacing, and average number of axle types.
- The subcategories for low truck volume roads (Group A) and high truck volume roads (Group D) should be utilized for pavement design to reflect more realistic traffic situations.
- Unclassified vehicles should not be discarded or arbitrarily assigned to truck classes. The developed allocation proportions should be applied to appropriately allocate unclassified vehicles to vehicle classes for pavement design.
- The updated ESAL values should be adopted for INDOT applications in the areas, such as pavement asset management and construction cost estimate.
- The truck traffic data repository and visualization model and a Tableau interactive visualization dashboard model can be used for easy access and analysis and for visualized view of the MEPDG related traffic data.
- It should be pointed out that the results of vehicle platoon analysis may not be implemented directly in MEPDG pavement design. However, the results and findings from the platoon analysis would provide a basis for future pavement structural analysis with respect to material fatigue under repeated loading.

The neural network model provided fairly good allocations of unclassified vehicles into the 13 classes of vehicles. As demonstrated in this study, with only limited traffic video records at one WIM site, some causes for misclassifying vehicles were able to be identified. It is believed that the accuracy of assigning unclassified vehicles to the correct vehicle classes can be considerably improved with sufficient amount of video data in combination of WIM data at more WIM stations. The combination of video/image and WIM data will provide key information and sources for further improving vehicle classification efficiency and quality. It is therefore proposed that future research to be conducted with the neural network algorithms and image processing techniques to further tackle the unclassified vehicle issues related to WIM data.

## REFERENCES


AASHTO. (1993). *AASHTO guide for design of pavement structures*. American Association of State Highway and Transportation Officials. https://habib00ugm.files.wordpress.com/2010/05/aashto1993.pdf

ARA. (2004). *Guide for mechanistic-empirical design of new and rehabilitated pavement structures*: *Part 2. Design Inputs* (NCHRP 1-37A). https://onlinepubs.trb.org/onlinepubs/archive/mepdg/Part2_Chapter4_Traffic.pdf

Aziza, R. S. R. A., Karim, M. R., Abdullahc, A. S., & Yamanaka H. (2014). *The effect of gross vehicle weight on platoon speed and size characteristics on two-lane road*. Full Paper Proceeding ITMAR-2014, Vol. 1, 708–724. https://www.globalilluminators.org/wp-content/uploads/2014/12/ITMAR-14-680.pdf

Bentley. (2020). *Modeling, documentation, and visualization software* [Webpage]. Retrieved June 27, 2020, from https://www.bentley.com/en/products/brands/microstation

Bhoopalam, A. K., Agatz, N., & Zuidwijk, R. (2018). Planning of truck platoons: A literature review and directions for future research. *Transportation Research Part B: Methodological*, *107*, 212–228. https://doi.org/10.1016/j.trb.2017.10.016

Bunnell, W. A., Li, H., Reed, M., Wells, T., Harris, D., Antich, M., Harney, S., & Bullock, D. M. (2018). *Implementation of weigh-in-motion data quality control and real-time dashboard development* (Joint Transportation Research Program Publication No. FHWA/IN/JTRP-2018/11). West Lafayette, IN: Purdue University. https://doi.org/10.5703/1288284316731

Castro-Neto, M., Jeong, Y., Jeong, M. K., & Han, L. D. (2009, March). *AADT prediction using support vector regression with data-dependent parameters*. Expert systems with application, *36*(2-2), 2979–2986. https://doi.org/10.1016/j.eswa.2008.01.073

Esri. (2020). *ArcGIS: The mapping and analytics platform*. Accessed June 5, 2020, from https://www.esri.com/en-us/arcgis/about-arcgis/overview

FHWA. (2016). *Traffic monitoring guide*. U.S. Department of Transportation Federal Highway Administration. https://www.fhwa.dot.gov/policyinformation/tmguide/tmg_fhwa_pl_17_003.pdf

Fryar, C. D., Kruszon-Moran, D., Gu, Q., & Ogden, C. L. (2018, December 20). Mean body weight, height, waist circumference, and body mass index among adults: United States, 1999–2000 through 2015–2016. *National Center for Health Statistics Report*, *122*, 1–16.

Google. (n.d.a). [Google Maps WIM Station 106 on I-70]. Retrieved February 12, 2021, https://www.google.com/maps/place/39%C2%B027’48.7%22N+87%C2%B004’12.3%22W/@39.4641089,-87.0697153,384m/data=!3m1!1e3!4m5!3m4!1s0x0:0x0!8m2!3d39.46354!4d-87.07009

Google. (n.d.b). [Google Maps WIM Station 315 on I-70]. Retrieved February 12, 2021, from https://www.google.com/maps/place/39%C2%B047’12.9%22N+86%C2%B008’03.5%22W/@39.7846036,-86.1382255,1230m/data=!3m1!1e3!4m5!3m4!1s0x0:0x0!8m2!3d39.786913!4d-86.134295

Gulen, S., Nagle, J., Weaver, J., & Gallivan, V. L. (2000). *Determination of practical ESALs per truck values on Indiana roads* (Joint Transportation Research Program. Publication No. FHWA/IN/JTRP-2000/23). West Lafayette, IN: Purdue University. https://doi.org/10.5703/1288284313175

Gungor, O. E., Al-Qadi, I. L., Gamez, A., & Hernandez, J. A. (2017). Development of adjustment factors for MEPDG pavement responses utilizing finite-element analysis. *Journal of Transportation Engineering, Part A: Systems*, 143(7). https://doi.org/10.1061/JTEPBS.0000040

Indiana Administrative Code. (2020). *105 Indiana Administrative Code 10-3-2*. Casetext. Retrieved June 11, 2020, from https://casetext.com/regulation/indiana-administrative-code/title-105-indiana-department-of-transportation/article-10-oversize-andor-overweight-vehicular-permits-for-highways/rule-105-iac-10-3-general-provisions-and-requirements-for-overweight-load-permits/section-105-iac-10-3-2-calculation-of-esal-values

INDOT. (2013). *Indiana design manual–2013*. Indiana Department of Transportation. https://www.in.gov/dot/div/contracts/design/IDM.htm

INDOT. (2019, June). *2018 Indiana public transit annual report*. Indiana Department of Transportation Office of Transit. https://www.in.gov/indot/files/INDOT%202018%20Transit%20Annual%20Report.pdf

Jiang, Y., Li, S., & Shamo, D. E. (2006). A platoon-based traffic signal timing algorithm for major-minor intersection types. *Journal of Transportation Research Part B: Methodological*, *40*(7), 543–562. https://doi.org/10.1016/j.trb.2005.07.003

Jiang, Y., Li, S., Nantung, T. E., & Chen, H. (2008). *Analysis and determination of axle load spectra and traffic input for the mechanistic-empirical pavement design guide* (Joint Transportation Research Program Publication No. FHWA/IN/JTRP-2008/07). West Lafayette, IN: Purdue University. https://doi.org/10.5703/1288284314325

Jiang, Y., Li, S., Nantung, T., Mangold, K., & MacArthur, S. A. (2008). Creation of truck axle load spectra using weigh-in-motion data. *Journal of the transportation Research Forum*, *47*(8), 45–61. https://doi.org/10.22004/ag.econ.206973

Karim, M. R., Saifizul, A. A., & Yamanaka, H. (2014, October). *The effect of gross vehicle weight on platoon speed and size characteristics on two-lane road* [Paper presentation]. International Conference on Innovative Trends in Multidisciplinary Academic Research, Istanbul, Turkey. http://eprints.um.edu.my/id/eprint/15738

Li, Q. J., Wang, K. C. P., Chen, C., Nguyen, V., & Zhang, Z. (2014). *Traffic loading spectra characterization for pavement ME design in a production environment*. Second Transportation & Development Congress 2014, Orlando, FL.

Li, S., Nantung, T., & Jiang, Y. (2005). Assessing issues, technologies, and data needs to meet traffic input requirements by mechanistic-empirical pavement design guide: Implementation initiatives. *Transportation Research Record*, 1917, 141–148.

Mesa-Arango, R., & Fabregas, A. (2017). Traffic impact of automated truck platoons in highway exits. In G. Dell'Acqua. & F. Wegman (Eds.), *Transport Infrastructure and Systems*. CRC Press.

Nantung, T. E. (2010, December). Implementing the mechanistic–empirical pavement design guide for cost savings in Indiana. *Transportation Research News 271*. http://onlinepubs.trb.org/onlinepubs/trnews/trnews271rpo.pdf

Neter, J., Wasserman, W., Kutmer, M., & Nachtsheim, C. (1996). *Applied linear statistical methods* (4th ed). Irwin.

Ng, J. Y.-H., Hausknecht, M., Vijayanarasimhan, S., Vinyals, O., Monga, R., & Toderici, G. (2015). Beyond short snippets: Deep networks for video classification. *2015 IEEE Conference on Computer Vision and Pattern Recognition (CVPR)* (pp. 4694–4702). Institute of Electrical and Electronics Engineers. https://doi.org/10.1109/CVPR.2015.7299101

Nichols, A. P., & Bullock, D. M. (2004). *Quality control procedures for weigh-in-motion data* (Joint Transportation Research Program Publication No. FHWA/IN/JTRP-2004/12). West Lafayette, IN: Purdue University. https://doi.org/10.5703/1288284313299

Papagiannakis, A. T., Bracher, M., & Jackson, N. C. (2006). Utilizing clustering techniques in estimating traffic input for pavement design. *Journal of Transportation Engineering*, *132*(11), 872–879. https://doi.org/10.1061/(ASCE)0733-947X(2006)132:11(872)

Paszke, A., Gross, S., Massa, F., Lerer, A., Bradbury, J., Chanan, G., Killeen, T., Lin, Z., Gimelshein, N., Antiga, L., Desmaison, A., Kopf, A., Yang, E., DeVito, Z., Raison, M, Tejani, A., Chilamkurthy, S., Steiner, B., Fang, L.… Chintala, S. (2019). Pytorch: An imperative style, high-performance deep learning library. In Wallach, H. Larochelle, H. Beygelzimer, A. d'Alché-Buc, F, Fox, E. & Garnett, R. (Eds.), *Advances in neural information processing systems*, *32* (pp. 8024–8035). Retrieved February 17, 2020, http://papers.neurips.cc/paper/9015-pytorch-an-imperative-style-high-performance-deep-learning-library

Pavement Interactive. (n.d.a). *Rigid pavement ESAL equation*. Retrieved June 11, 2020, from https://pavementinteractive.org/reference-desk/design/structural-design/rigid-pavement-esal-equation/

Pavement Interactive. (n.d.b). *Flexible pavement ESAL equation*. Retrieved June 11, 2020, from https://pavementinteractive.org/reference-desk/design/design-parameters/flexible-pavement-esal-equation/

Spencer, B. F., Jr., Hoskere, V., & Narazaki, Y. (2019). Advances in computer vision-based civil infrastructure inspection and monitoring. *Engineering*, *5*(2), 199–222. https://doi.org/10.1016/j.eng.2018.11.030

Subramanian, N. B. (2020). *Box and whiskers plot*. Aspirant. Retrieved May 25, 2020, from https://aiaspirant.com/box-plot/

Tableau. (2020). *Tableau desktop* [Webpage]. Retrieved June 27, 2020, from https://www.Tableau.com/products/desktop

TaghaviGhalesari, A., & Chang-Albitres, C. M. (2019). *Sustainable design of rigid pavements using a hybrid GP and OLS method*. Eighth International Conference on Case Histories in Geotechnical Engineering, Philadelphia, PA. American Society of Civil Engineers. https://doi.org/10.1061/9780784482124.033

Tarefder, R., & Rodriguez-Ruiz, J. (2013). WIM data quality and its influence on predicted pavement performance. *Transportation Letters*, *5*(3), 154–163. https://doi.org/10.1179/1942786713Z.00000000017

Titi, H. H., Coley, N. J., & Latifi, V. (2018). Evaluation of pavement performance due to overload single trip permit truck traffic in Wisconsin. *Journal of Advances in Civil Engineering*, *2018*(1070653). Hindawi Publishing Corporation.

Wang, K. C. P., Li, Q., Hall, K. D., Nguyen, V., & Xiao, D. X. (2011, December). Development of truck loading groups for the mechanistic-empirical pavement design guide. *Journal of Transportation Engineering*, *137*(12), 855–862. https://doi.org/10.1061/(ASCE)TE.1943-5436.0000277

Yang, X., & Wu, Z. (2012). *Effects of subgrade resilient modulus and climate inputs on MEPDG*. GeoCongress 2012, Oakland, CA. American Society of Civil Engineers. https://doi.org/10.1061/9780784412121.149

Yang, X., You, Z., Hiller, J., & Watkins, D. (2017, December). Correlation analysis between temperature indices and flexible pavement distress predictions using mechanistic-empirical design. *Journal of Cold Regions Engineering*, *31*(4). https://doi.org/10.1061/(ASCE)CR.1943-5495.0000135

Zhao, X., Chen, Y., & Zhao, H. (2018). Robust approximate constraint-following control for autonomous vehicle platoon systems. *Asian Journal of Control*, *20*(4), 1611–1623. https://doi.org/10.1002/asjc.1676

Ziedan, A., Onyango, M., Udeh, S., Wu, W., Owino, J., & Fomunung, I. (2017). *Analysis of site-specific MEPDG traffic inputs parameters for the state of Tennessee in comparison to national inputs*. International Conference on Highway Pavements and Airfield Technology 2017, Philadelphia, PA. American Society of Civil Engineers. https://doi.org/10.1061/9780784480922.002

# APPENDICES

**Appendix A. Axle Load Spectra and Annual ESAL Values**

**Appendix B. Complete Truck Traffic Input for the MEPDG at the I-70 WIM Site**

# APPENDIX A. AXLE LOAD SPECTRA AND ANNUAL ESAL VALUES

Table A.1 All-axle load distribution (percentage) for each truck class

| Axle Load Range (kips) | Vehicle Classes | | | | | | | | | |
|---|---|---|---|---|---|---|---|---|---|---|
| | C4 | C5 | C6 | C7 | C8 | C9 | C10 | C11 | C12 | C13 |
| 0–3 | 3.98 | 52.95 | 18.26 | 11.80 | 17.40 | 2.13 | 16.23 | 0.00 | 0.00 | 0.00 |
| 3–4 | 1.71 | 18.11 | 13.77 | 3.22 | 9.66 | 3.05 | 4.63 | 0.60 | 0.56 | 0.04 |
| 4–5 | 1.92 | 7.48 | 9.86 | 3.57 | 9.99 | 4.29 | 4.95 | 1.45 | 2.34 | 0.14 |
| 5–6 | 2.39 | 4.07 | 6.89 | 4.13 | 8.50 | 5.20 | 5.37 | 1.92 | 4.43 | 0.25 |
| 6–7 | 3.22 | 2.91 | 5.69 | 4.00 | 7.09 | 6.02 | 5.48 | 2.51 | 6.34 | 0.22 |
| 7–8 | 4.78 | 2.38 | 4.78 | 4.04 | 5.92 | 6.33 | 6.01 | 3.23 | 8.54 | 0.21 |
| 8–9 | 6.74 | 2.14 | 4.65 | 3.95 | 4.87 | 6.32 | 6.02 | 4.05 | 11.48 | 0.19 |
| 9–10 | 8.34 | 1.94 | 4.37 | 4.23 | 4.13 | 6.12 | 5.73 | 4.94 | 13.10 | 0.18 |
| 10–11 | 9.03 | 1.52 | 4.30 | 4.35 | 3.50 | 5.80 | 5.59 | 5.81 | 12.20 | 0.18 |
| 11–12 | 8.88 | 1.16 | 4.02 | 4.63 | 3.00 | 5.54 | 5.17 | 6.56 | 9.92 | 0.26 |
| 12–13 | 8.18 | 0.90 | 3.65 | 5.07 | 2.63 | 5.75 | 5.21 | 7.18 | 7.66 | 0.52 |
| 13–14 | 7.05 | 0.69 | 3.33 | 5.51 | 2.36 | 6.49 | 5.07 | 7.77 | 6.12 | 1.77 |
| 14–15 | 6.21 | 0.54 | 2.96 | 5.74 | 2.29 | 7.35 | 4.59 | 8.12 | 4.54 | 9.53 |
| 15–16 | 5.22 | 0.43 | 2.60 | 5.66 | 2.27 | 7.64 | 4.09 | 8.01 | 3.17 | 21.54 |
| 16–17 | 4.39 | 0.36 | 2.30 | 5.22 | 2.40 | 6.89 | 3.62 | 7.72 | 2.12 | 22.10 |
| 17–18 | 3.70 | 0.31 | 1.92 | 4.50 | 2.44 | 5.40 | 2.92 | 6.75 | 1.45 | 15.77 |
| 18–19 | 3.24 | 0.25 | 1.59 | 3.73 | 2.26 | 3.72 | 2.33 | 5.71 | 0.96 | 8.25 |
| 19–20 | 2.71 | 0.21 | 1.24 | 3.22 | 1.87 | 2.41 | 1.55 | 4.58 | 0.68 | 6.29 |
| 20–21 | 2.03 | 0.18 | 0.93 | 2.63 | 1.34 | 1.50 | 1.29 | 3.51 | 0.51 | 2.44 |
| 21–22 | 1.52 | 0.15 | 0.65 | 2.01 | 0.89 | 0.88 | 1.07 | 2.51 | 0.46 | 2.46 |
| 22–23 | 1.16 | 0.12 | 0.51 | 1.59 | 0.62 | 0.50 | 0.66 | 1.78 | 0.35 | 1.50 |
| 23–24 | 0.82 | 0.10 | 0.38 | 1.30 | 0.45 | 0.27 | 0.43 | 1.23 | 0.26 | 0.60 |
| 24–25 | 0.58 | 0.09 | 0.27 | 1.04 | 0.37 | 0.15 | 0.31 | 0.85 | 0.23 | 0.37 |
| 25–26 | 0.34 | 0.08 | 0.17 | 0.85 | 0.33 | 0.08 | 0.20 | 0.59 | 0.17 | 0.21 |
| 26–27 | 0.25 | 0.07 | 0.14 | 0.57 | 0.28 | 0.04 | 0.16 | 0.44 | 0.14 | 0.15 |
| 27–28 | 0.19 | 0.07 | 0.10 | 0.38 | 0.26 | 0.03 | 0.13 | 0.34 | 0.18 | 0.14 |
| 28–29 | 0.17 | 0.07 | 0.09 | 0.31 | 0.24 | 0.02 | 0.11 | 0.22 | 0.13 | 0.18 |
| 29–30 | 0.11 | 0.06 | 0.07 | 0.25 | 0.24 | 0.01 | 0.08 | 0.19 | 0.12 | 0.26 |
| 30–31 | 0.10 | 0.05 | 0.05 | 0.19 | 0.24 | 0.01 | 0.12 | 0.12 | 0.15 | 0.42 |
| 31–32 | 0.08 | 0.05 | 0.05 | 0.13 | 0.23 | 0.01 | 0.10 | 0.11 | 0.13 | 0.49 |
| 32–33 | 0.08 | 0.05 | 0.03 | 0.15 | 0.21 | 0.01 | 0.04 | 0.09 | 0.16 | 0.63 |
| 33–34 | 0.07 | 0.05 | 0.04 | 0.12 | 0.21 | 0.00 | 0.05 | 0.07 | 0.16 | 0.61 |
| 34–35 | 0.06 | 0.04 | 0.03 | 0.17 | 0.21 | 0.00 | 0.03 | 0.07 | 0.13 | 0.56 |
| 35–36 | 0.06 | 0.04 | 0.02 | 0.11 | 0.19 | 0.00 | 0.07 | 0.07 | 0.19 | 0.49 |
| 36–37 | 0.05 | 0.04 | 0.03 | 0.11 | 0.16 | 0.00 | 0.03 | 0.08 | 0.16 | 0.35 |
| 37–38 | 0.07 | 0.04 | 0.02 | 0.10 | 0.15 | 0.00 | 0.05 | 0.07 | 0.11 | 0.24 |
| 38–39 | 0.03 | 0.03 | 0.02 | 0.12 | 0.13 | 0.00 | 0.05 | 0.07 | 0.11 | 0.14 |
| 39–40 | 0.05 | 0.03 | 0.02 | 0.15 | 0.11 | 0.00 | 0.06 | 0.09 | 0.12 | 0.09 |
| >40 | 0.51 | 0.22 | 0.22 | 1.16 | 0.56 | 0.02 | 0.40 | 0.58 | 0.42 | 0.22 |

Table A.2 Single-axle load distribution (percentage) for each truck class

| Axle Load Range (kips) | Vehicle Classes | | | | | | | | | |
|---|---|---|---|---|---|---|---|---|---|---|
| | **C4** | **C5** | **C6** | **C7** | **C8** | **C9** | **C10** | **C11** | **C12** | **C13** |
| **0–3** | 4.16 | 52.95 | 16.67 | 11.33 | 3.23 | 8.68 | 52.82 | 0.00 | 0.00 | 0.00 |
| **3–4** | 1.16 | 18.11 | 8.33 | 3.71 | 8.08 | 5.49 | 4.60 | 0.30 | 0.57 | 0.26 |
| **4–5** | 0.90 | 7.48 | 16.67 | 5.11 | 11.48 | 4.58 | 3.93 | 0.75 | 2.43 | 0.55 |
| **5–6** | 1.19 | 4.07 | 8.33 | 5.63 | 9.41 | 3.99 | 3.48 | 1.34 | 4.50 | 0.71 |
| **6–7** | 1.87 | 2.91 | 8.33 | 4.25 | 7.07 | 3.67 | 3.41 | 2.18 | 5.41 | 0.61 |
| **7–8** | 3.57 | 2.38 | 8.33 | 2.99 | 5.88 | 3.51 | 2.65 | 3.12 | 6.05 | 0.54 |
| **8–9** | 6.04 | 2.14 | 8.33 | 2.41 | 5.21 | 3.44 | 3.59 | 4.10 | 6.85 | 0.47 |
| **9–10** | 8.08 | 1.94 | 0.00 | 2.13 | 4.84 | 3.45 | 2.58 | 5.09 | 8.79 | 0.51 |
| **10–11** | 9.29 | 1.52 | 8.33 | 3.20 | 4.45 | 3.48 | 2.44 | 6.04 | 11.00 | 0.35 |
| **11–12** | 9.28 | 1.16 | 0.00 | 2.94 | 4.00 | 3.59 | 1.78 | 6.86 | 12.02 | 0.38 |
| **12–13** | 8.92 | 0.90 | 0.00 | 3.38 | 3.62 | 4.15 | 1.85 | 7.53 | 11.09 | 0.62 |
| **13–14** | 7.85 | 0.69 | 16.67 | 4.50 | 3.23 | 5.04 | 2.30 | 8.11 | 9.42 | 1.80 |
| **14–15** | 6.85 | 0.54 | 0.00 | 5.08 | 2.99 | 6.09 | 2.12 | 8.48 | 6.93 | 8.65 |
| **15–16** | 5.73 | 0.43 | 0.00 | 4.85 | 2.74 | 7.23 | 1.74 | 8.33 | 4.86 | 13.97 |
| **16–17** | 4.75 | 0.36 | 0.00 | 4.85 | 2.65 | 7.56 | 1.36 | 8.00 | 3.15 | 11.20 |
| **17–18** | 4.00 | 0.31 | 0.00 | 4.09 | 2.57 | 7.27 | 1.29 | 7.03 | 2.09 | 12.96 |
| **18–19** | 3.62 | 0.25 | 0.00 | 3.72 | 2.40 | 5.87 | 1.01 | 5.94 | 1.28 | 11.06 |
| **19–20** | 3.14 | 0.21 | 0.00 | 3.70 | 2.19 | 4.33 | 1.08 | 4.75 | 0.82 | 7.01 |
| **20–21** | 2.32 | 0.18 | 0.00 | 3.61 | 1.76 | 2.99 | 0.59 | 3.63 | 0.54 | 5.91 |
| **21–22** | 1.79 | 0.15 | 0.00 | 2.99 | 1.34 | 1.92 | 0.77 | 2.56 | 0.43 | 7.56 |
| **22–23** | 1.36 | 0.12 | 0.00 | 2.65 | 1.08 | 1.20 | 0.59 | 1.80 | 0.35 | 4.36 |
| **23–24** | 0.93 | 0.10 | 0.00 | 2.80 | 0.87 | 0.76 | 0.66 | 1.22 | 0.22 | 1.95 |
| **24–25** | 0.66 | 0.09 | 0.00 | 2.21 | 0.75 | 0.49 | 0.21 | 0.83 | 0.18 | 1.20 |
| **25–26** | 0.38 | 0.08 | 0.00 | 1.84 | 0.68 | 0.29 | 0.17 | 0.55 | 0.12 | 0.49 |
| **26–27** | 0.27 | 0.07 | 0.00 | 1.09 | 0.61 | 0.18 | 0.24 | 0.41 | 0.09 | 0.30 |
| **27–28** | 0.20 | 0.07 | 0.00 | 0.81 | 0.56 | 0.12 | 0.17 | 0.29 | 0.08 | 0.29 |
| **28–29** | 0.20 | 0.07 | 0.00 | 0.79 | 0.55 | 0.09 | 0.10 | 0.18 | 0.08 | 0.48 |
| **29–30** | 0.12 | 0.06 | 0.00 | 0.57 | 0.54 | 0.07 | 0.21 | 0.14 | 0.04 | 0.47 |
| **30–31** | 0.12 | 0.05 | 0.00 | 0.37 | 0.55 | 0.06 | 0.35 | 0.07 | 0.07 | 0.73 |
| **31–32** | 0.11 | 0.05 | 0.00 | 0.29 | 0.52 | 0.05 | 0.35 | 0.06 | 0.05 | 0.44 |
| **32–33** | 0.09 | 0.05 | 0.00 | 0.24 | 0.48 | 0.04 | 0.14 | 0.04 | 0.05 | 0.65 |
| **33–34** | 0.09 | 0.05 | 0.00 | 0.22 | 0.48 | 0.04 | 0.10 | 0.02 | 0.03 | 0.56 |
| **34–35** | 0.08 | 0.04 | 0.00 | 0.21 | 0.47 | 0.03 | 0.14 | 0.02 | 0.03 | 0.61 |
| **35–36** | 0.08 | 0.04 | 0.00 | 0.15 | 0.42 | 0.04 | 0.17 | 0.02 | 0.04 | 0.54 |
| **36–37** | 0.06 | 0.04 | 0.00 | 0.12 | 0.37 | 0.02 | 0.03 | 0.03 | 0.04 | 0.37 |
| **37–38** | 0.09 | 0.04 | 0.00 | 0.08 | 0.33 | 0.02 | 0.00 | 0.02 | 0.03 | 0.24 |
| **38–39** | 0.04 | 0.03 | 0.00 | 0.10 | 0.28 | 0.02 | 0.17 | 0.02 | 0.04 | 0.20 |
| **39–40** | 0.05 | 0.03 | 0.00 | 0.10 | 0.24 | 0.02 | 0.21 | 0.02 | 0.03 | 0.11 |
| **>40** | 0.57 | 0.22 | 0.00 | 0.89 | 1.09 | 0.13 | 0.59 | 0.11 | 0.16 | 0.87 |

Table A.3 Tandem-axle load distribution (percentage) for each truck class

| **Axle Load Range (kips)** | **Vehicle Classes** | | | | | | | | | |
|---|---|---|---|---|---|---|---|---|---|---|
| | **C4** | **C5** | **C6** | **C7** | **C8** | **C9** | **C10** | **C11** | **C12** | **C13** |
| **0–6** | 15.63 | 0.00 | 48.77 | 30.33 | 54.85 | 14.01 | 22.81 | 13.30 | 7.50 | 2.21 |
| **6–8** | 13.56 | 0.00 | 10.46 | 9.40 | 13.10 | 12.63 | 11.14 | 8.55 | 20.93 | 1.57 |
| **8–10** | 17.15 | 0.00 | 9.03 | 9.20 | 8.30 | 12.75 | 11.66 | 7.46 | 39.50 | 0.98 |
| **10–12** | 16.45 | 0.00 | 8.32 | 8.54 | 5.16 | 11.59 | 11.09 | 6.12 | 22.62 | 0.63 |
| **12–14** | 11.87 | 0.00 | 6.98 | 9.19 | 3.72 | 12.44 | 11.84 | 4.96 | 4.65 | 1.81 |
| **14–16** | 8.95 | 0.00 | 5.56 | 9.29 | 3.75 | 15.13 | 11.13 | 6.93 | 1.31 | 21.40 |
| **16–18** | 6.62 | 0.00 | 4.22 | 8.08 | 4.58 | 12.21 | 8.83 | 7.18 | 0.78 | 37.59 |
| **18–20** | 4.22 | 0.00 | 2.83 | 5.64 | 3.82 | 5.95 | 5.27 | 4.71 | 0.53 | 13.80 |
| **20–22** | 2.33 | 0.00 | 1.59 | 3.64 | 1.63 | 2.26 | 2.88 | 4.29 | 0.38 | 1.99 |
| **22–24** | 1.30 | 0.00 | 0.88 | 2.05 | 0.45 | 0.71 | 1.16 | 3.73 | 0.19 | 0.92 |
| **24–26** | 0.67 | 0.00 | 0.44 | 1.39 | 0.18 | 0.20 | 0.65 | 3.24 | 0.18 | 0.88 |
| **26–28** | 0.36 | 0.00 | 0.24 | 0.73 | 0.10 | 0.06 | 0.31 | 3.10 | 0.19 | 1.01 |
| **28–30** | 0.18 | 0.00 | 0.15 | 0.44 | 0.06 | 0.02 | 0.19 | 2.88 | 0.12 | 1.94 |
| **30–32** | 0.08 | 0.00 | 0.11 | 0.32 | 0.04 | 0.01 | 0.20 | 2.57 | 0.17 | 3.75 |
| **32–34** | 0.09 | 0.00 | 0.07 | 0.22 | 0.04 | 0.01 | 0.10 | 2.57 | 0.13 | 3.60 |
| **34–36** | 0.05 | 0.00 | 0.05 | 0.28 | 0.04 | 0.00 | 0.11 | 2.15 | 0.13 | 2.27 |
| **36–38** | 0.06 | 0.00 | 0.05 | 0.18 | 0.03 | 0.00 | 0.10 | 2.50 | 0.14 | 1.49 |
| **38–40** | 0.06 | 0.00 | 0.04 | 0.23 | 0.04 | 0.00 | 0.11 | 3.24 | 0.14 | 1.00 |
| **40–42** | 0.07 | 0.00 | 0.04 | 0.17 | 0.03 | 0.00 | 0.07 | 3.24 | 0.11 | 0.48 |
| **42–44** | 0.07 | 0.00 | 0.05 | 0.17 | 0.02 | 0.00 | 0.11 | 3.27 | 0.10 | 0.28 |
| **44–46** | 0.06 | 0.00 | 0.04 | 0.16 | 0.02 | 0.00 | 0.10 | 1.72 | 0.07 | 0.17 |
| **46–48** | 0.10 | 0.00 | 0.04 | 0.22 | 0.02 | 0.00 | 0.04 | 1.72 | 0.09 | 0.12 |
| **48–50** | 0.08 | 0.00 | 0.04 | 0.13 | 0.02 | 0.00 | 0.12 | 0.60 | 0.06 | 0.11 |
| **>50** | 0.00 | 0.00 | 0.00 | 0.00 | 0.00 | 0.00 | 0.00 | 0.00 | 0.00 | 0.00 |

Table A.4 Tridem-axle load distribution (percentage) for each truck class

| **Axle Load Range (kips)** | **Vehicle Classes** | | | | | | | | | |
|---|---|---|---|---|---|---|---|---|---|---|
| | **C4** | **C5** | **C6** | **C7** | **C8** | **C9** | **C10** | **C11** | **C12** | **C13** |
| **0–12** | 0.00 | 0.00 | 0.00 | 38.36 | 34.07 | 97.05 | 74.54 | 62.88 | 9.75 | 1.07 |
| **12–15** | 0.00 | 0.00 | 0.00 | 20.16 | 3.40 | 0.55 | 12.80 | 3.70 | 15.52 | 12.37 |
| **15–18** | 0.00 | 0.00 | 0.00 | 19.14 | 6.17 | 0.39 | 6.55 | 5.31 | 13.40 | 60.97 |
| **18–21** | 0.00 | 0.00 | 0.00 | 11.27 | 6.74 | 0.49 | 3.08 | 3.98 | 10.11 | 17.04 |
| **21–24** | 0.00 | 0.00 | 0.00 | 5.13 | 7.05 | 0.45 | 1.79 | 3.66 | 9.59 | 4.71 |
| **24–27** | 0.00 | 0.00 | 0.00 | 2.26 | 4.91 | 0.18 | 0.36 | 2.75 | 6.04 | 0.61 |
| **27–30** | 0.00 | 0.00 | 0.00 | 0.80 | 4.22 | 0.13 | 0.31 | 2.57 | 6.44 | 0.29 |
| **30–33** | 0.00 | 0.00 | 0.00 | 0.34 | 4.28 | 0.10 | 0.11 | 2.06 | 6.88 | 0.92 |
| **33–36** | 0.00 | 0.00 | 0.00 | 0.37 | 3.90 | 0.07 | 0.08 | 2.20 | 9.30 | 1.36 |
| **36–39** | 0.00 | 0.00 | 0.00 | 0.38 | 5.23 | 0.10 | 0.07 | 2.38 | 6.67 | 0.54 |
| **39–42** | 0.00 | 0.00 | 0.00 | 0.54 | 5.48 | 0.13 | 0.11 | 3.55 | 3.20 | 0.07 |
| **42–45** | 0.00 | 0.00 | 0.00 | 0.40 | 6.80 | 0.09 | 0.11 | 2.63 | 2.02 | 0.01 |
| **45–48** | 0.00 | 0.00 | 0.00 | 0.54 | 5.60 | 0.14 | 0.05 | 1.72 | 0.89 | 0.02 |
| **48–51** | 0.00 | 0.00 | 0.00 | 0.30 | 2.14 | 0.13 | 0.05 | 0.63 | 0.18 | 0.01 |
| **>51** | 0.00 | 0.00 | 0.00 | 0.00 | 0.00 | 0.00 | 0.00 | 0.00 | 0.00 | 0.00 |

Table A.5 Annual ESAL values from AASHTO method (WIM Site 106)

| GVW (kips) | Vehicle Class | | | | | | | | | | | | | | |
|---|---|---|---|---|---|---|---|---|---|---|---|---|---|---|---|
| | **C0** | **C1** | **C2** | **C3** | **C4** | **C5** | **C6** | **C7** | **C8** | **C9** | **C10** | **C11** | **C12** | **C13** | **Total** |
| **3** | 0 | 1 | 30 | 1 | 0 | 0 | 0 | 0 | 0 | 0 | 0 | 0 | 0 | 0 | **31** |
| **6** | 4 | 2 | 1517 | 1548 | 0 | 37 | 0 | 0 | 0 | 0 | 0 | 0 | 0 | 0 | **3,108** |
| **9** | 60 | 4 | 94 | 2579 | 0 | 1059 | 1 | 0 | 4 | 0 | 0 | 0 | 0 | 0 | **3,801** |
| **12** | 270 | 6 | 23 | 730 | 5 | 1765 | 5 | 0 | 72 | 1 | 0 | 0 | 0 | 0 | **2,876** |
| **15** | 601 | 11 | 29 | 488 | 20 | 1874 | 39 | 1 | 270 | 5 | 0 | 0 | 0 | 0 | **3,339** |
| **18** | 1430 | 29 | 46 | 470 | 519 | 2464 | 430 | 2 | 574 | 17 | 0 | 0 | 0 | 0 | **5,981** |
| **21** | 2622 | 44 | 50 | 494 | 3150 | 3429 | 2220 | 5 | 757 | 53 | 1 | 0 | 0 | 0 | **12,824** |
| **24** | 4289 | 76 | 48 | 500 | 4976 | 4612 | 3602 | 7 | 929 | 226 | 2 | 4 | 0 | 0 | **19,271** |
| **27** | 6762 | 53 | 39 | 494 | 5327 | 5397 | 3260 | 21 | 1308 | 1068 | 4 | 23 | 0 | 0 | **23,756** |
| **30** | 10313 | 83 | 64 | 586 | 4910 | 5993 | 4111 | 36 | 2083 | 3243 | 10 | 42 | 0 | 0 | **31,474** |
| **33** | 14770 | 88 | 55 | 710 | 4398 | 5025 | 5079 | 78 | 3172 | 8228 | 27 | 43 | 1 | 0 | **41,675** |
| **36** | 22232 | 105 | 161 | 962 | 3209 | 4036 | 3607 | 83 | 4296 | 17848 | 46 | 75 | 5 | 0 | **56,665** |
| **39** | 25101 | 142 | 96 | 821 | 2260 | 3218 | 2791 | 142 | 5131 | 25671 | 75 | 232 | 25 | 0 | **65,705** |
| **42** | 28575 | 192 | 250 | 1070 | 2056 | 3206 | 4723 | 173 | 5833 | 34128 | 118 | 513 | 76 | 1 | **80,915** |
| **45** | 32766 | 269 | 151 | 1311 | 2012 | 3551 | 9899 | 205 | 6585 | 43780 | 154 | 623 | 147 | 2 | **101,453** |
| **48** | 37390 | 94 | 226 | 1266 | 2302 | 3885 | 17981 | 329 | 6221 | 54944 | 169 | 835 | 240 | 7 | **125,889** |
| **51** | 43193 | 80 | 245 | 1398 | 1968 | 5583 | 11233 | 512 | 5583 | 66857 | 235 | 1797 | 451 | 10 | **139,144** |
| **54** | 51015 | 148 | 435 | 1817 | 1823 | 4971 | 6618 | 661 | 5405 | 79006 | 240 | 3692 | 762 | 18 | **156,611** |
| **57** | 64174 | 0 | 9 | 398 | 1205 | 2536 | 4796 | 1228 | 5140 | 91160 | 286 | 7093 | 1299 | 39 | **179,363** |
| **60** | 75548 | 0 | 0 | 114 | 806 | 1348 | 3128 | 2266 | 4042 | 107167 | 335 | 12658 | 2277 | 83 | **209,774** |
| **63** | 89910 | 0 | 0 | 138 | 793 | 1231 | 1593 | 5212 | 3520 | 124585 | 403 | 20119 | 3735 | 149 | **251,389** |
| **66** | 98078 | 0 | 46 | 103 | 733 | 1025 | 1249 | 12888 | 3354 | 148433 | 444 | 30435 | 5680 | 154 | **302,622** |
| **69** | 116636 | 0 | 0 | 20 | 361 | 473 | 1373 | 24329 | 2502 | 183809 | 492 | 40413 | 8011 | 80 | **378,500** |
| **72** | 135247 | 0 | 0 | 109 | 389 | 950 | 1060 | 22513 | 2678 | 247704 | 596 | 48205 | 9823 | 54 | **469,329** |
| **75** | 174243 | 0 | 0 | 84 | 428 | 433 | 699 | 14220 | 2596 | 350763 | 621 | 49518 | 10720 | 75 | **604,400** |
| **78** | 195358 | 0 | 0 | 92 | 132 | 567 | 407 | 7530 | 1917 | 497324 | 875 | 46757 | 9968 | 96 | **761,022** |
| **81** | 211965 | 0 | 0 | 40 | 125 | 195 | 340 | 3867 | 1419 | 624396 | 996 | 40087 | 8083 | 91 | **891,603** |
| **84** | 272105 | 0 | 0 | 56 | 87 | 315 | 333 | 2096 | 1286 | 569122 | 1012 | 29662 | 5833 | 142 | **882,049** |
| **87** | 319005 | 0 | 0 | 111 | 74 | 287 | 371 | 1427 | 1229 | 435912 | 1025 | 21498 | 4022 | 114 | **785,073** |
| **90** | 386984 | 0 | 0 | 67 | 37 | 328 | 220 | 1075 | 1138 | 325876 | 841 | 16898 | 2571 | 102 | **736,137** |
| **93** | 415139 | 0 | 0 | 0 | 17 | 221 | 111 | 856 | 1055 | 196961 | 678 | 16176 | 1744 | 178 | **633,135** |
| **96** | 499601 | 0 | 0 | 0 | 103 | 88 | 205 | 587 | 817 | 101897 | 658 | 15119 | 1382 | 138 | **620,597** |
| **99** | 568428 | 0 | 0 | 0 | 57 | 95 | 171 | 688 | 1001 | 58780 | 555 | 15596 | 1043 | 187 | **646,601** |
| **102** | 648862 | 0 | 0 | 0 | 0 | 0 | 151 | 397 | 831 | 41695 | 589 | 16287 | 1111 | 240 | **710,163** |
| **105** | 775266 | 0 | 0 | 0 | 0 | 0 | 242 | 397 | 685 | 35551 | 708 | 17513 | 1129 | 311 | **831,802** |
| **108** | 925985 | 0 | 0 | 0 | 0 | 0 | 0 | 436 | 636 | 33542 | 493 | 19410 | 1298 | 290 | **982,091** |
| **111** | 1012106 | 0 | 0 | 0 | 37 | 0 | 37 | 231 | 275 | 32498 | 476 | 19938 | 878 | 324 | **1,066,800** |
| **114** | 1109419 | 0 | 0 | 0 | 45 | 0 | 36 | 145 | 424 | 27333 | 486 | 20905 | 875 | 316 | **1,159,984** |
| **117** | 1298624 | 0 | 0 | 0 | 0 | 0 | 362 | 365 | 506 | 23946 | 410 | 20548 | 902 | 479 | **1,346,141** |
| **120** | 1602297 | 0 | 0 | 0 | 50 | 0 | 49 | 258 | 436 | 18137 | 576 | 21811 | 869 | 445 | **1,644,927** |
| **123** | 1701198 | 0 | 0 | 0 | 0 | 0 | 0 | 326 | 389 | 12322 | 338 | 20919 | 918 | 461 | **1,736,871** |
| **126** | 1942633 | 0 | 0 | 0 | 0 | 0 | 56 | 345 | 333 | 7242 | 325 | 20882 | 733 | 464 | **1,973,012** |
| **Total** | **14920201** | **1428** | **3616** | **18580** | **44414** | **70195** | **92585** | **105935** | **86433** | **4631233** | **15299** | **596324** | **86611** | **5049** | **20,677,902** |

Table A.6 Annual ESAL values from axle group divisor method (WIM Site 106)

| GVW (kips) | Vehicle Class | | | | | | | | | | | | | |
|---|---|---|---|---|---|---|---|---|---|---|---|---|---|---|
| | C0 | C1 | C2 | C3 | C4 | C5 | C6 | C7 | C8 | C9 | C10 | C11 | C12 | C13 | Total |
| **3** | 0 | 1 | 19 | 0 | 0 | 0 | 0 | 0 | 0 | 0 | 0 | 0 | 0 | 0 | **20** |
| **6** | 3 | 2 | 1415 | 1583 | 0 | 40 | 0 | 0 | 0 | 0 | 0 | 0 | 0 | 0 | **3,043** |
| **9** | 66 | 5 | 104 | 2926 | 0 | 1232 | 1 | 0 | 4 | 0 | 0 | 0 | 0 | 0 | **4,338** |
| **12** | 313 | 6 | 26 | 853 | 5 | 2075 | 6 | 0 | 83 | 1 | 0 | 0 | 0 | 0 | **3,368** |
| **15** | 678 | 12 | 32 | 552 | 23 | 2113 | 44 | 1 | 316 | 6 | 0 | 0 | 0 | 0 | **3,775** |
| **18** | 1553 | 29 | 48 | 510 | 574 | 2673 | 466 | 2 | 670 | 20 | 0 | 0 | 0 | 0 | **6,546** |
| **21** | 2745 | 44 | 50 | 521 | 3359 | 3602 | 2353 | 5 | 866 | 61 | 1 | 0 | 0 | 0 | **13,606** |
| **24** | 4415 | 77 | 49 | 517 | 5160 | 4733 | 3803 | 8 | 1046 | 250 | 2 | 5 | 0 | 0 | **20,064** |
| **27** | 6963 | 55 | 40 | 506 | 5434 | 5480 | 3438 | 23 | 1432 | 1160 | 4 | 27 | 0 | 0 | **24,562** |
| **30** | 10713 | 89 | 68 | 602 | 4985 | 6090 | 4310 | 38 | 2222 | 3489 | 11 | 48 | 1 | 0 | **32,666** |
| **33** | 15505 | 97 | 60 | 735 | 4484 | 5154 | 5287 | 83 | 3339 | 8807 | 29 | 49 | 1 | 0 | **43,630** |
| **36** | 23674 | 118 | 180 | 1019 | 3306 | 4231 | 3737 | 89 | 4488 | 19047 | 49 | 83 | 5 | 0 | **60,028** |
| **39** | 27289 | 163 | 110 | 877 | 2365 | 3483 | 2883 | 152 | 5323 | 27392 | 80 | 255 | 27 | 0 | **70,399** |
| **42** | 31871 | 222 | 288 | 1179 | 2172 | 3568 | 4840 | 185 | 6019 | 36464 | 126 | 562 | 83 | 1 | **87,579** |
| **45** | 36966 | 311 | 174 | 1483 | 2097 | 4026 | 10058 | 218 | 6789 | 46763 | 164 | 673 | 161 | 2 | **109,884** |
| **48** | 42324 | 109 | 259 | 1441 | 2383 | 4429 | 18163 | 348 | 6397 | 58600 | 179 | 886 | 260 | 7 | **135,785** |
| **51** | 48817 | 92 | 279 | 1592 | 2043 | 6354 | 11349 | 548 | 5760 | 71065 | 251 | 1884 | 489 | 11 | **150,533** |
| **54** | 57337 | 168 | 493 | 2061 | 1937 | 5643 | 6692 | 693 | 5581 | 83559 | 253 | 3841 | 823 | 19 | **169,099** |
| **57** | 71519 | 0 | 9 | 448 | 1252 | 2873 | 4868 | 1301 | 5372 | 95802 | 300 | 7341 | 1396 | 42 | **192,524** |
| **60** | 83457 | 0 | 0 | 128 | 829 | 1523 | 3215 | 2376 | 4232 | 111905 | 352 | 13043 | 2431 | 90 | **223,580** |
| **63** | 97991 | 0 | 0 | 156 | 832 | 1401 | 1660 | 5438 | 3748 | 129188 | 425 | 20642 | 3958 | 160 | **265,599** |
| **66** | 105591 | 0 | 53 | 118 | 788 | 1166 | 1310 | 13410 | 3615 | 152967 | 469 | 31093 | 5969 | 165 | **316,712** |
| **69** | 123577 | 0 | 0 | 23 | 388 | 537 | 1449 | 25279 | 2706 | 188250 | 519 | 41164 | 8358 | 84 | **392,335** |
| **72** | 140860 | 0 | 0 | 126 | 422 | 1079 | 1139 | 23343 | 2934 | 252465 | 632 | 48996 | 10176 | 57 | **482,229** |
| **75** | 177873 | 0 | 0 | 95 | 473 | 493 | 753 | 14735 | 2842 | 356031 | 654 | 50336 | 11033 | 79 | **615,399** |
| **78** | 196398 | 0 | 0 | 104 | 147 | 649 | 447 | 7823 | 2104 | 503157 | 924 | 47593 | 10211 | 101 | **769,659** |
| **81** | 210033 | 0 | 0 | 46 | 139 | 223 | 376 | 4047 | 1591 | 630540 | 1052 | 41009 | 8252 | 94 | **897,404** |
| **84** | 264464 | 0 | 0 | 64 | 100 | 360 | 375 | 2222 | 1467 | 574597 | 1063 | 30642 | 5946 | 150 | **881,451** |
| **87** | 305114 | 0 | 0 | 128 | 83 | 329 | 419 | 1524 | 1409 | 440771 | 1087 | 22567 | 4123 | 118 | **777,672** |
| **90** | 361701 | 0 | 0 | 77 | 42 | 376 | 249 | 1158 | 1313 | 330400 | 887 | 18103 | 2659 | 107 | **717,072** |
| **93** | 385634 | 0 | 0 | 0 | 19 | 252 | 125 | 926 | 1231 | 200753 | 713 | 17678 | 1819 | 188 | **609,340** |
| **96** | 454488 | 0 | 0 | 0 | 118 | 100 | 234 | 644 | 970 | 104996 | 693 | 16795 | 1468 | 146 | **580,651** |
| **99** | 510884 | 0 | 0 | 0 | 66 | 107 | 194 | 758 | 1187 | 61696 | 583 | 17448 | 1126 | 199 | **594,248** |
| **102** | 576288 | 0 | 0 | 0 | 0 | 0 | 172 | 445 | 1004 | 44586 | 627 | 18299 | 1206 | 257 | **642,883** |
| **105** | 677080 | 0 | 0 | 0 | 0 | 0 | 275 | 449 | 829 | 38472 | 760 | 19750 | 1237 | 337 | **739,189** |
| **108** | 794278 | 0 | 0 | 0 | 0 | 0 | 0 | 491 | 784 | 36707 | 527 | 21958 | 1448 | 310 | **856,504** |
| **111** | 864251 | 0 | 0 | 0 | 43 | 0 | 42 | 263 | 349 | 35962 | 512 | 22685 | 967 | 345 | **925,419** |
| **114** | 933047 | 0 | 0 | 0 | 52 | 0 | 42 | 165 | 527 | 30503 | 522 | 23822 | 967 | 331 | **989,977** |
| **117** | 1074484 | 0 | 0 | 0 | 0 | 0 | 415 | 413 | 626 | 26803 | 443 | 23586 | 1002 | 510 | **1,128,282** |
| **120** | 1302161 | 0 | 0 | 0 | 58 | 0 | 57 | 296 | 539 | 20400 | 631 | 25079 | 980 | 479 | **1,350,679** |
| **123** | 1371058 | 0 | 0 | 0 | 0 | 0 | 0 | 374 | 495 | 13871 | 369 | 24233 | 1036 | 503 | **1,411,937** |
| **126** | 1545514 | 0 | 0 | 0 | 0 | 0 | 65 | 397 | 409 | 8151 | 357 | 24307 | 820 | 501 | **1,580,520** |
| **Total** | **12938978** | **1599** | **3756** | **20471** | **46180** | **76392** | **95310** | **110672** | **92616** | **4745656** | **16250** | **636484** | **90439** | **5391** | **18,880,191** |

## APPENDIX B. COMPLETE TRUCK TRAFFIC INPUT FOR THE MEPDG AT THE I-70 WIM SITE

**Truck Traffic and Axle Load Spectra**
WIM Site 950315, I-70, RP 83.44, Indianapolis
Five Lanes in One Direction

**AADTT: Two-way annual average daily truck traffic**
**MAF: Truck traffic monthly adjustment factors (note: twelve-month MAF total = 12.0)**
**DDF: Directional distribution factors, or percent trucks in the design direction**
**LDF: Truck lane distribution factors, or the percent trucks in the design lane**
**TCD: Truck class distribution (percent)**
**HDF: Hourly distribution factors (percent)**
**C4, C5, … C13: Class 4, Class 5, …, Class 13 of vehicle classifications**

| | AADTT Ln 1 | AADTT Ln 2 | AADTT Ln 3 | AADTT Ln 4 | AADTT Ln 5 | Total | MAF |
|---|---|---|---|---|---|---|---|
| AADTT Jan | 1807 | 3424 | 2280 | 1439 | 1336 | 10286 | 1.12 |
| AADTT Feb | 1400 | 2985 | 2123 | 1210 | 1440 | 9158 | 1.00 |
| AADTT Mar | 967 | 2621 | 1665 | 1637 | 1097 | 7987 | 0.87 |
| AADTT Apr | 971 | 1955 | 2866 | 1527 | 1568 | 8887 | 0.97 |
| AADTT May | 1053 | 1614 | 2346 | 431 | 971 | 6415 | 0.70 |
| AADTT Jun | 1126 | 2077 | 2622 | 591 | 1159 | 7575 | 0.83 |
| AADTT Jul | 900 | 2860 | 2050 | 333 | 544 | 6687 | 0.73 |
| AADTT Aug | 1142 | 3102 | 2321 | 1078 | 1398 | 9041 | 0.98 |
| AADTT Sep | 971 | 3430 | 3107 | 1923 | 1429 | 10860 | 1.18 |
| AADTT Oct | 1033 | 3239 | 3544 | 2318 | 1435 | 11569 | 1.26 |
| AADTT Nov | 941 | 3291 | 2574 | 2268 | 1573 | 10647 | 1.16 |
| AADTT Dec | 1013 | 3028 | 3261 | 1948 | 1813 | 11063 | 1.20 |
| Avg | 1110 | 2802 | 2563 | 1392 | 1314 | 9181 | |
| Sum | 13324 | 33626 | 30759 | 16703 | 15763 | 110175 | 12.00 |

| | C4 | C5 | C6 | C7 | C8 | C9 | C10 | C11 | C12 | C13 | All Truck |
|---|---|---|---|---|---|---|---|---|---|---|---|
| DDF | 0.58 | 0.59 | 0.57 | 0.55 | 0.54 | 0.58 | 0.70 | 0.64 | 0.61 | 0.98 | 0.57 |
| LDF- Ln 1 | 0.21 | 0.17 | 0.25 | 0.29 | 0.11 | 0.05 | 0.08 | 0.01 | 0.04 | 0.00 | 0.12 |
| LDF- Ln 2 | 0.31 | 0.22 | 0.37 | 0.33 | 0.28 | 0.47 | 0.34 | 0.27 | 0.38 | 0.00 | 0.31 |
| LDF- Ln 3 | 0.27 | 0.21 | 0.22 | 0.24 | 0.41 | 0.29 | 0.38 | 0.47 | 0.32 | 0.83 | 0.28 |
| LDF- Ln 4 | 0.12 | 0.16 | 0.11 | 0.09 | 0.12 | 0.17 | 0.13 | 0.22 | 0.22 | 0.02 | 0.15 |
| LDF- Ln 5 | 0.09 | 0.24 | 0.05 | 0.06 | 0.07 | 0.03 | 0.07 | 0.03 | 0.04 | 0.15 | 0.14 |

| All Lanes Combined AADTT | | | | | | | | | | | |
|---|---|---|---|---|---|---|---|---|---|---|---|
| | C4 | C5 | C6 | C7 | C8 | C9 | C10 | C11 | C12 | C13 | Total |
| Jan | 271 | 6205 | 221 | 39 | 568 | 2787 | 22 | 105 | 57 | 13 | 10288 |
| Feb | 262 | 5270 | 209 | 32 | 561 | 2664 | 16 | 89 | 52 | 5 | 9159 |
| Mar | 231 | 4380 | 214 | 43 | 550 | 2418 | 16 | 77 | 49 | 10 | 7987 |
| Apr | 272 | 4839 | 235 | 50 | 703 | 2604 | 13 | 107 | 56 | 9 | 8888 |
| May | 199 | 3668 | 167 | 35 | 503 | 1697 | 8 | 72 | 37 | 30 | 6414 |
| Jun | 232 | 3983 | 211 | 46 | 678 | 2264 | 8 | 88 | 44 | 22 | 7575 |

| | | | | | | | | | | | |
|---|---|---|---|---|---|---|---|---|---|---|---|
| Jul | 221 | 3011 | 216 | 59 | 602 | 2428 | 9 | 76 | 41 | 25 | 6687 |
| Aug | 281 | 4412 | 281 | 67 | 570 | 2923 | 16 | 94 | 55 | 50 | 8749 |
| Sep | 348 | 4839 | 376 | 84 | 608 | 4233 | 30 | 131 | 81 | 131 | 10861 |
| Oct | 395 | 4802 | 438 | 100 | 649 | 4654 | 33 | 156 | 93 | 249 | 11569 |
| Nov | 308 | 4680 | 347 | 84 | 454 | 3525 | 19 | 105 | 79 | 1046 | 10647 |
| Dec | 243 | 4685 | 235 | 51 | 316 | 2541 | 10 | 62 | 56 | 2863 | 11062 |
| Total | 3262 | 54774 | 3149 | 689 | 6761 | 34739 | 199 | 1161 | 699 | 4452 | 109885 |
| Average AADTT Yearly Decrease = 7.85% | | | | | | | | | | | |

| Monthly Adjustment Factor (MAF) | | | | | | | | | | | |
|---|---|---|---|---|---|---|---|---|---|---|---|
| | C4 | C5 | C6 | C7 | C8 | C9 | C10 | C11 | C12 | C13 | Total |
| Jan | 1.02 | 1.39 | 0.86 | 0.68 | 1.03 | 0.98 | 1.37 | 1.10 | 1.00 | 0.03 | 1.15 |
| Feb | 0.89 | 1.06 | 0.73 | 0.51 | 0.92 | 0.85 | 0.86 | 0.85 | 0.82 | 0.01 | 0.92 |
| Mar | 0.87 | 0.98 | 0.83 | 0.76 | 1.00 | 0.85 | 0.97 | 0.81 | 0.85 | 0.03 | 0.89 |
| Apr | 0.99 | 1.05 | 0.88 | 0.86 | 1.23 | 0.89 | 0.74 | 1.10 | 0.95 | 0.02 | 0.96 |
| May | 0.74 | 0.82 | 0.65 | 0.62 | 0.91 | 0.60 | 0.46 | 0.75 | 0.64 | 0.08 | 0.71 |
| Jun | 0.84 | 0.86 | 0.79 | 0.78 | 1.19 | 0.77 | 0.50 | 0.90 | 0.74 | 0.06 | 0.82 |
| Jul | 0.83 | 0.67 | 0.84 | 1.04 | 1.09 | 0.85 | 0.57 | 0.80 | 0.72 | 0.07 | 0.74 |
| Aug | 1.06 | 0.99 | 1.09 | 1.18 | 1.03 | 1.03 | 0.95 | 0.99 | 0.97 | 0.14 | 0.97 |
| Sep | 1.26 | 1.05 | 1.41 | 1.45 | 1.06 | 1.44 | 1.81 | 1.34 | 1.37 | 0.34 | 1.17 |
| Oct | 1.48 | 1.07 | 1.70 | 1.78 | 1.18 | 1.64 | 2.02 | 1.64 | 1.63 | 0.68 | 1.29 |
| Nov | 1.12 | 1.01 | 1.30 | 1.43 | 0.80 | 1.20 | 1.12 | 1.07 | 1.34 | 2.75 | 1.15 |
| Dec | 0.91 | 1.05 | 0.91 | 0.90 | 0.57 | 0.89 | 0.62 | 0.65 | 0.98 | 7.79 | 1.23 |
| Sum | 12.00 | 12.00 | 12.00 | 12.00 | 12.00 | 12.00 | 12.00 | 12.00 | 12.00 | 12.00 | 12.00 |

| | Hourly Volume | | | | | | | | | | |
|---|---|---|---|---|---|---|---|---|---|---|---|
| | Start Time | C4 | C5 | C6 | C7 | C8 | C9 | C10 | C11 | C12 | C13 | All Truck |
| **All Lanes Combined** | 0:00 | 5.67 | 168.40 | 6.05 | 0.88 | 18.82 | 120.50 | 0.47 | 3.44 | 2.35 | 20.24 | 346.83 |
| | 1:00 | 4.82 | 132.88 | 5.12 | 0.73 | 14.78 | 103.70 | 0.42 | 3.27 | 2.67 | 15.95 | 284.34 |
| | 2:00 | 3.76 | 104.62 | 4.46 | 0.55 | 12.54 | 91.61 | 0.32 | 3.86 | 2.65 | 11.24 | 235.61 |
| | 3:00 | 3.19 | 86.00 | 4.06 | 0.52 | 10.67 | 80.02 | 0.23 | 3.62 | 2.92 | 8.23 | 199.47 |
| | 4:00 | 2.87 | 62.01 | 3.76 | 0.41 | 9.22 | 70.88 | 0.22 | 3.59 | 2.86 | 6.08 | 161.90 |
| | 5:00 | 2.91 | 48.63 | 3.47 | 0.43 | 8.43 | 66.79 | 0.21 | 4.08 | 2.75 | 5.31 | 143.02 |
| | 6:00 | 4.15 | 44.38 | 4.17 | 0.56 | 9.36 | 66.67 | 0.26 | 4.78 | 2.75 | 5.59 | 142.65 |
| | 7:00 | 7.09 | 52.49 | 5.24 | 0.67 | 9.87 | 69.02 | 0.33 | 4.45 | 2.59 | 6.36 | 158.12 |
| | 8:00 | 10.11 | 85.68 | 8.53 | 1.04 | 13.06 | 75.22 | 0.45 | 4.59 | 2.64 | 11.77 | 213.10 |
| | 9:00 | 12.83 | 128.97 | 10.35 | 1.82 | 16.25 | 81.22 | 0.52 | 3.81 | 2.39 | 18.27 | 276.42 |
| | 10:00 | 14.64 | 182.45 | 13.34 | 2.71 | 22.76 | 98.14 | 0.77 | 4.07 | 2.29 | 20.47 | 361.63 |
| | 11:00 | 17.05 | 217.07 | 13.79 | 3.52 | 28.10 | 114.60 | 1.05 | 4.32 | 2.40 | 16.50 | 418.40 |
| | 12:00 | 16.82 | 231.98 | 14.94 | 4.06 | 31.10 | 128.50 | 1.05 | 3.78 | 2.10 | 18.72 | 453.06 |
| | 13:00 | 17.35 | 250.25 | 16.10 | 4.45 | 33.10 | 138.43 | 1.00 | 4.22 | 2.28 | 20.80 | 487.99 |
| | 14:00 | 17.15 | 250.88 | 16.78 | 5.33 | 34.49 | 150.79 | 1.05 | 4.25 | 2.15 | 20.93 | 503.79 |
| | 15:00 | 17.22 | 261.86 | 17.49 | 5.13 | 34.81 | 159.46 | 0.98 | 4.38 | 2.18 | 22.06 | 525.57 |
| | 16:00 | 18.25 | 275.74 | 18.39 | 5.05 | 37.22 | 170.07 | 1.17 | 4.68 | 2.30 | 17.14 | 550.02 |
| | 17:00 | 18.22 | 298.60 | 19.21 | 4.86 | 36.23 | 173.39 | 0.99 | 4.48 | 2.28 | 16.63 | 574.88 |
| | 18:00 | 18.21 | 313.85 | 18.52 | 4.36 | 36.87 | 171.42 | 1.06 | 4.92 | 2.43 | 17.40 | 589.03 |
| | 19:00 | 16.65 | 315.05 | 16.81 | 3.65 | 35.54 | 166.47 | 0.99 | 4.53 | 2.37 | 16.07 | 578.13 |
| | 20:00 | 14.32 | 303.82 | 14.22 | 2.57 | 31.81 | 163.30 | 0.89 | 3.85 | 2.31 | 17.88 | 554.97 |
| | 21:00 | 11.77 | 280.12 | 11.40 | 1.85 | 29.78 | 154.14 | 0.86 | 3.33 | 2.20 | 18.75 | 514.19 |
| | 22:00 | 8.99 | 250.42 | 9.28 | 1.30 | 25.69 | 147.31 | 0.72 | 3.18 | 2.10 | 22.65 | 471.65 |
| | 23:00 | 7.76 | 212.27 | 7.06 | 1.10 | 22.42 | 132.28 | 0.59 | 3.19 | 2.25 | 19.69 | 408.60 |
| AADTT | Sum | 271.76 | 4558.43 | 262.55 | 57.53 | 562.92 | 2893.95 | 16.62 | 96.67 | 58.23 | 374.74 | 9153.40 |
| TCD | Percent | 2.97 | 49.80 | 2.87 | 0.63 | 6.15 | 31.62 | 0.18 | 1.06 | 0.64 | 4.09 | 100.00 |

| Hourly Distribution Factor (HDF) (%) | | | | | | | | | | | |
|---|---|---|---|---|---|---|---|---|---|---|---|
| Start Time | C4 | C5 | C6 | C7 | C8 | C9 | C10 | C11 | C12 | C13 | All Truck |
| 0:00 | 2.08 | 3.69 | 2.31 | 1.54 | 3.34 | 4.16 | 2.85 | 3.55 | 4.04 | 5.40 | 3.79 |
| 1:00 | 1.77 | 2.91 | 1.95 | 1.26 | 2.63 | 3.58 | 2.55 | 3.38 | 4.59 | 4.26 | 3.11 |
| 2:00 | 1.38 | 2.30 | 1.70 | 0.95 | 2.23 | 3.17 | 1.94 | 4.00 | 4.55 | 3.00 | 2.57 |
| 3:00 | 1.18 | 1.89 | 1.55 | 0.91 | 1.89 | 2.77 | 1.40 | 3.74 | 5.02 | 2.20 | 2.18 |
| 4:00 | 1.06 | 1.36 | 1.43 | 0.71 | 1.64 | 2.45 | 1.32 | 3.71 | 4.91 | 1.62 | 1.77 |
| 5:00 | 1.07 | 1.07 | 1.32 | 0.75 | 1.50 | 2.31 | 1.29 | 4.23 | 4.72 | 1.42 | 1.56 |
| 6:00 | 1.53 | 0.97 | 1.59 | 0.97 | 1.66 | 2.30 | 1.55 | 4.94 | 4.73 | 1.49 | 1.56 |
| 7:00 | 2.61 | 1.15 | 2.00 | 1.17 | 1.75 | 2.38 | 1.96 | 4.61 | 4.45 | 1.70 | 1.73 |
| 8:00 | 3.72 | 1.88 | 3.25 | 1.81 | 2.32 | 2.60 | 2.74 | 4.75 | 4.54 | 3.14 | 2.33 |
| 9:00 | 4.72 | 2.83 | 3.94 | 3.16 | 2.89 | 2.81 | 3.12 | 3.94 | 4.10 | 4.88 | 3.02 |
| 10:00 | 5.39 | 4.00 | 5.08 | 4.71 | 4.04 | 3.39 | 4.63 | 4.21 | 3.93 | 5.46 | 3.95 |
| 11:00 | 6.27 | 4.76 | 5.25 | 6.11 | 4.99 | 3.96 | 6.35 | 4.46 | 4.13 | 4.40 | 4.57 |
| 12:00 | 6.19 | 5.09 | 5.69 | 7.05 | 5.52 | 4.44 | 6.33 | 3.91 | 3.61 | 4.99 | 4.95 |
| 13:00 | 6.38 | 5.49 | 6.13 | 7.74 | 5.88 | 4.78 | 6.02 | 4.37 | 3.92 | 5.55 | 5.33 |
| 14:00 | 6.31 | 5.50 | 6.39 | 9.26 | 6.13 | 5.21 | 6.33 | 4.39 | 3.69 | 5.59 | 5.50 |
| 15:00 | 6.34 | 5.74 | 6.66 | 8.91 | 6.18 | 5.51 | 5.88 | 4.53 | 3.75 | 5.89 | 5.74 |
| 16:00 | 6.71 | 6.05 | 7.00 | 8.78 | 6.61 | 5.88 | 7.05 | 4.84 | 3.95 | 4.57 | 6.01 |
| 17:00 | 6.70 | 6.55 | 7.32 | 8.44 | 6.44 | 5.99 | 5.97 | 4.64 | 3.91 | 4.44 | 6.28 |
| 18:00 | 6.70 | 6.89 | 7.05 | 7.58 | 6.55 | 5.92 | 6.36 | 5.09 | 4.17 | 4.64 | 6.44 |
| 19:00 | 6.13 | 6.91 | 6.40 | 6.34 | 6.31 | 5.75 | 5.95 | 4.69 | 4.07 | 4.29 | 6.32 |
| 20:00 | 5.27 | 6.66 | 5.42 | 4.47 | 5.65 | 5.64 | 5.37 | 3.98 | 3.96 | 4.77 | 6.06 |
| 21:00 | 4.33 | 6.15 | 4.34 | 3.22 | 5.29 | 5.33 | 5.18 | 3.44 | 3.78 | 5.00 | 5.62 |
| 22:00 | 3.31 | 5.49 | 3.54 | 2.25 | 4.56 | 5.09 | 4.30 | 3.29 | 3.60 | 6.04 | 5.15 |
| 23:00 | 2.86 | 4.66 | 2.69 | 1.90 | 3.98 | 4.57 | 3.56 | 3.30 | 3.86 | 5.25 | 4.46 |
| Sum | 100.00 | 100.00 | 100.00 | 100.00 | 100.00 | 100.00 | 100.00 | 100.00 | 100.00 | 100.00 | 100.00 |

**Single-Axle Load Distribution (Percentages) for Each Truck Class**

| Class | 4 | 5 | 6 | 7 | 8 | 9 | 10 | 11 | 12 | 13 |
|---|---|---|---|---|---|---|---|---|---|---|
| 3 kips | 4.16 | 52.95 | 16.67 | 11.33 | 3.23 | 8.68 | 52.82 | 0.00 | 0.00 | 0.00 |
| 4 kips | 1.16 | 18.11 | 8.33 | 3.71 | 8.08 | 5.49 | 4.60 | 0.30 | 0.57 | 0.26 |
| 5 kips | 0.90 | 7.48 | 16.67 | 5.11 | 11.48 | 4.58 | 3.93 | 0.75 | 2.43 | 0.55 |
| 6 kips | 1.19 | 4.07 | 8.33 | 5.63 | 9.41 | 3.99 | 3.48 | 1.34 | 4.50 | 0.71 |
| 7 kips | 1.87 | 2.91 | 8.33 | 4.25 | 7.07 | 3.67 | 3.41 | 2.18 | 5.41 | 0.61 |
| 8 kips | 3.57 | 2.38 | 8.33 | 2.99 | 5.88 | 3.51 | 2.65 | 3.12 | 6.05 | 0.54 |
| 9 kips | 6.04 | 2.14 | 8.33 | 2.41 | 5.21 | 3.44 | 3.59 | 4.10 | 6.85 | 0.47 |
| 10 kips | 8.08 | 1.94 | 0.00 | 2.13 | 4.84 | 3.45 | 2.58 | 5.09 | 8.79 | 0.51 |
| 11 kips | 9.29 | 1.52 | 8.33 | 3.20 | 4.45 | 3.48 | 2.44 | 6.04 | 11.00 | 0.35 |
| 12 kips | 9.28 | 1.16 | 0.00 | 2.94 | 4.00 | 3.59 | 1.78 | 6.86 | 12.02 | 0.38 |
| 13 kips | 8.92 | 0.90 | 0.00 | 3.38 | 3.62 | 4.15 | 1.85 | 7.53 | 11.09 | 0.62 |
| 14 kips | 7.85 | 0.69 | 16.67 | 4.50 | 3.23 | 5.04 | 2.30 | 8.11 | 9.42 | 1.80 |
| 15 kips | 6.85 | 0.54 | 0.00 | 5.08 | 2.99 | 6.09 | 2.12 | 8.48 | 6.93 | 8.65 |
| 16 kips | 5.73 | 0.43 | 0.00 | 4.85 | 2.74 | 7.23 | 1.74 | 8.33 | 4.86 | 13.97 |
| 17 kips | 4.75 | 0.36 | 0.00 | 4.85 | 2.65 | 7.56 | 1.36 | 8.00 | 3.15 | 11.20 |
| 18 kips | 4.00 | 0.31 | 0.00 | 4.09 | 2.57 | 7.27 | 1.29 | 7.03 | 2.09 | 12.96 |
| 19 kips | 3.62 | 0.25 | 0.00 | 3.72 | 2.40 | 5.87 | 1.01 | 5.94 | 1.28 | 11.06 |
| 20 kips | 3.14 | 0.21 | 0.00 | 3.70 | 2.19 | 4.33 | 1.08 | 4.75 | 0.82 | 7.01 |
| 21 kips | 2.32 | 0.18 | 0.00 | 3.61 | 1.76 | 2.99 | 0.59 | 3.63 | 0.54 | 5.91 |
| 22 kips | 1.79 | 0.15 | 0.00 | 2.99 | 1.34 | 1.92 | 0.77 | 2.56 | 0.43 | 7.56 |
| 23 kips | 1.36 | 0.12 | 0.00 | 2.65 | 1.08 | 1.20 | 0.59 | 1.80 | 0.35 | 4.36 |
| 24 kips | 0.93 | 0.10 | 0.00 | 2.80 | 0.87 | 0.76 | 0.66 | 1.22 | 0.22 | 1.95 |
| 25 kips | 0.66 | 0.09 | 0.00 | 2.21 | 0.75 | 0.49 | 0.21 | 0.83 | 0.18 | 1.20 |
| 26 kips | 0.38 | 0.08 | 0.00 | 1.84 | 0.68 | 0.29 | 0.17 | 0.55 | 0.12 | 0.49 |
| 27 kips | 0.27 | 0.07 | 0.00 | 1.09 | 0.61 | 0.18 | 0.24 | 0.41 | 0.09 | 0.30 |
| 28 kips | 0.20 | 0.07 | 0.00 | 0.81 | 0.56 | 0.12 | 0.17 | 0.29 | 0.08 | 0.29 |
| 29 kips | 0.20 | 0.07 | 0.00 | 0.79 | 0.55 | 0.09 | 0.10 | 0.18 | 0.08 | 0.48 |
| 30 kips | 0.12 | 0.06 | 0.00 | 0.57 | 0.54 | 0.07 | 0.21 | 0.14 | 0.04 | 0.47 |
| 31 kips | 0.12 | 0.05 | 0.00 | 0.37 | 0.55 | 0.06 | 0.35 | 0.07 | 0.07 | 0.73 |
| 32 kips | 0.11 | 0.05 | 0.00 | 0.29 | 0.52 | 0.05 | 0.35 | 0.06 | 0.05 | 0.44 |
| 33 kips | 0.09 | 0.05 | 0.00 | 0.24 | 0.48 | 0.04 | 0.14 | 0.04 | 0.05 | 0.65 |
| 34 kips | 0.09 | 0.05 | 0.00 | 0.22 | 0.48 | 0.04 | 0.10 | 0.02 | 0.03 | 0.56 |
| 35 kips | 0.08 | 0.04 | 0.00 | 0.21 | 0.47 | 0.03 | 0.14 | 0.02 | 0.03 | 0.61 |
| 36 kips | 0.08 | 0.04 | 0.00 | 0.15 | 0.42 | 0.04 | 0.17 | 0.02 | 0.04 | 0.54 |
| 37 kips | 0.06 | 0.04 | 0.00 | 0.12 | 0.37 | 0.02 | 0.03 | 0.03 | 0.04 | 0.37 |
| 38 kips | 0.09 | 0.04 | 0.00 | 0.08 | 0.33 | 0.02 | 0.00 | 0.02 | 0.03 | 0.24 |
| 39 kips | 0.04 | 0.03 | 0.00 | 0.10 | 0.28 | 0.02 | 0.17 | 0.02 | 0.04 | 0.20 |
| 40 kips | 0.05 | 0.03 | 0.00 | 0.10 | 0.24 | 0.02 | 0.21 | 0.02 | 0.03 | 0.11 |
| 41 kips | 0.57 | 0.22 | 0.00 | 0.89 | 1.09 | 0.13 | 0.59 | 0.11 | 0.16 | 0.87 |

**Tandem-Axle Load Distribution (Percentages) for Each Truck Class**

| Class | 4 | 5 | 6 | 7 | 8 | 9 | 10 | 11 | 12 | 13 |
|---|---|---|---|---|---|---|---|---|---|---|
| 6 kips | 15.63 | 0.00 | 48.77 | 30.33 | 54.85 | 14.01 | 22.81 | 13.30 | 7.50 | 2.21 |
| 8 kips | 13.56 | 0.00 | 10.46 | 9.40 | 13.10 | 12.63 | 11.14 | 8.55 | 20.93 | 1.57 |
| 10 kips | 17.15 | 0.00 | 9.03 | 9.20 | 8.30 | 12.75 | 11.66 | 7.46 | 39.50 | 0.98 |
| 12 kips | 16.45 | 0.00 | 8.32 | 8.54 | 5.16 | 11.59 | 11.09 | 6.12 | 22.62 | 0.63 |
| 14 kips | 11.87 | 0.00 | 6.98 | 9.19 | 3.72 | 12.44 | 11.84 | 4.96 | 4.65 | 1.81 |
| 16 kips | 8.95 | 0.00 | 5.56 | 9.29 | 3.75 | 15.13 | 11.13 | 6.93 | 1.31 | 21.40 |
| 18 kips | 6.62 | 0.00 | 4.22 | 8.08 | 4.58 | 12.21 | 8.83 | 7.18 | 0.78 | 37.59 |
| 20 kips | 4.22 | 0.00 | 2.83 | 5.64 | 3.82 | 5.95 | 5.27 | 4.71 | 0.53 | 13.80 |
| 22 kips | 2.33 | 0.00 | 1.59 | 3.64 | 1.63 | 2.26 | 2.88 | 4.29 | 0.38 | 1.99 |
| 24 kips | 1.30 | 0.00 | 0.88 | 2.05 | 0.45 | 0.71 | 1.16 | 3.73 | 0.19 | 0.92 |
| 26 kips | 0.67 | 0.00 | 0.44 | 1.39 | 0.18 | 0.20 | 0.65 | 3.24 | 0.18 | 0.88 |
| 28 kips | 0.36 | 0.00 | 0.24 | 0.73 | 0.10 | 0.06 | 0.31 | 3.10 | 0.19 | 1.01 |
| 30 kips | 0.18 | 0.00 | 0.15 | 0.44 | 0.06 | 0.02 | 0.19 | 2.88 | 0.12 | 1.94 |
| 32 kips | 0.08 | 0.00 | 0.11 | 0.32 | 0.04 | 0.01 | 0.20 | 2.57 | 0.17 | 3.75 |
| 34 kips | 0.09 | 0.00 | 0.07 | 0.22 | 0.04 | 0.01 | 0.10 | 2.57 | 0.13 | 3.60 |
| 36 kips | 0.05 | 0.00 | 0.05 | 0.28 | 0.04 | 0.00 | 0.11 | 2.15 | 0.13 | 2.27 |
| 38 kips | 0.06 | 0.00 | 0.05 | 0.18 | 0.03 | 0.00 | 0.10 | 2.50 | 0.14 | 1.49 |
| 40 kips | 0.06 | 0.00 | 0.04 | 0.23 | 0.04 | 0.00 | 0.11 | 3.24 | 0.14 | 1.00 |
| 42 kips | 0.07 | 0.00 | 0.04 | 0.17 | 0.03 | 0.00 | 0.07 | 3.24 | 0.11 | 0.48 |
| 44 kips | 0.07 | 0.00 | 0.05 | 0.17 | 0.02 | 0.00 | 0.11 | 3.27 | 0.10 | 0.28 |
| 46 kips | 0.06 | 0.00 | 0.04 | 0.16 | 0.02 | 0.00 | 0.10 | 1.72 | 0.07 | 0.17 |
| 48 kips | 0.10 | 0.00 | 0.04 | 0.22 | 0.02 | 0.00 | 0.04 | 1.72 | 0.09 | 0.12 |
| 50 kips | 0.08 | 0.00 | 0.04 | 0.13 | 0.02 | 0.00 | 0.12 | 0.60 | 0.06 | 0.11 |

**Tridem-Axle Load Distribution (Percentages) for Each Truck Class**

| Class | 4 | 5 | 6 | 7 | 8 | 9 | 10 | 11 | 12 | 13 |
|---|---|---|---|---|---|---|---|---|---|---|
| 12 kips | 0.00 | 0.00 | 0.00 | 38.36 | 34.07 | 97.05 | 74.54 | 62.88 | 9.75 | 1.07 |
| 15 kips | 0.00 | 0.00 | 0.00 | 20.16 | 3.40 | 0.55 | 12.80 | 3.70 | 15.52 | 12.37 |
| 18 kips | 0.00 | 0.00 | 0.00 | 19.14 | 6.17 | 0.39 | 6.55 | 5.31 | 13.40 | 60.97 |
| 21 kips | 0.00 | 0.00 | 0.00 | 11.27 | 6.74 | 0.49 | 3.08 | 3.98 | 10.11 | 17.04 |
| 24 kips | 0.00 | 0.00 | 0.00 | 5.13 | 7.05 | 0.45 | 1.79 | 3.66 | 9.59 | 4.71 |
| 27 kips | 0.00 | 0.00 | 0.00 | 2.26 | 4.91 | 0.18 | 0.36 | 2.75 | 6.04 | 0.61 |
| 30 kips | 0.00 | 0.00 | 0.00 | 0.80 | 4.22 | 0.13 | 0.31 | 2.57 | 6.44 | 0.29 |
| 33 kips | 0.00 | 0.00 | 0.00 | 0.34 | 4.28 | 0.10 | 0.11 | 2.06 | 6.88 | 0.92 |
| 36 kips | 0.00 | 0.00 | 0.00 | 0.37 | 3.90 | 0.07 | 0.08 | 2.20 | 9.30 | 1.36 |
| 39 kips | 0.00 | 0.00 | 0.00 | 0.38 | 5.23 | 0.10 | 0.07 | 2.38 | 6.67 | 0.54 |
| 42 kips | 0.00 | 0.00 | 0.00 | 0.54 | 5.48 | 0.13 | 0.11 | 3.55 | 3.20 | 0.07 |
| 45 kips | 0.00 | 0.00 | 0.00 | 0.40 | 6.80 | 0.09 | 0.11 | 2.63 | 2.02 | 0.01 |
| 48 kips | 0.00 | 0.00 | 0.00 | 0.54 | 5.60 | 0.14 | 0.05 | 1.72 | 0.89 | 0.02 |
| 51 kips | 0.00 | 0.00 | 0.00 | 0.30 | 2.14 | 0.13 | 0.05 | 0.63 | 0.18 | 0.01 |

**All-Axle Load Distribution (Percentages) for Each Truck Class**

| Class | 4 | 5 | 6 | 7 | 8 | 9 | 10 | 11 | 12 | 13 |
|---|---|---|---|---|---|---|---|---|---|---|
| 3 kips | 3.98 | 52.95 | 18.26 | 11.80 | 17.40 | 2.13 | 16.23 | 0.00 | 0.00 | 0.00 |
| 4 kips | 1.71 | 18.11 | 13.77 | 3.22 | 9.66 | 3.05 | 4.63 | 0.60 | 0.56 | 0.04 |
| 5 kips | 1.92 | 7.48 | 9.86 | 3.57 | 9.99 | 4.29 | 4.95 | 1.45 | 2.34 | 0.14 |
| 6 kips | 2.39 | 4.07 | 6.89 | 4.13 | 8.50 | 5.20 | 5.37 | 1.92 | 4.43 | 0.25 |
| 7 kips | 3.22 | 2.91 | 5.69 | 4.00 | 7.09 | 6.02 | 5.48 | 2.51 | 6.34 | 0.22 |
| 8 kips | 4.78 | 2.38 | 4.78 | 4.04 | 5.92 | 6.33 | 6.01 | 3.23 | 8.54 | 0.21 |
| 9 kips | 6.74 | 2.14 | 4.65 | 3.95 | 4.87 | 6.32 | 6.02 | 4.05 | 11.48 | 0.19 |
| 10 kips | 8.34 | 1.94 | 4.37 | 4.23 | 4.13 | 6.12 | 5.73 | 4.94 | 13.10 | 0.18 |
| 11 kips | 9.03 | 1.52 | 4.30 | 4.35 | 3.50 | 5.80 | 5.59 | 5.81 | 12.20 | 0.18 |
| 12 kips | 8.88 | 1.16 | 4.02 | 4.63 | 3.00 | 5.54 | 5.17 | 6.56 | 9.92 | 0.26 |
| 13 kips | 8.18 | 0.90 | 3.65 | 5.07 | 2.63 | 5.75 | 5.21 | 7.18 | 7.66 | 0.52 |
| 14 kips | 7.05 | 0.69 | 3.33 | 5.51 | 2.36 | 6.49 | 5.07 | 7.77 | 6.12 | 1.77 |
| 15 kips | 6.21 | 0.54 | 2.96 | 5.74 | 2.29 | 7.35 | 4.59 | 8.12 | 4.54 | 9.53 |
| 16 kips | 5.22 | 0.43 | 2.60 | 5.66 | 2.27 | 7.64 | 4.09 | 8.01 | 3.17 | 21.54 |
| 17 kips | 4.39 | 0.36 | 2.30 | 5.22 | 2.40 | 6.89 | 3.62 | 7.72 | 2.12 | 22.10 |
| 18 kips | 3.70 | 0.31 | 1.92 | 4.50 | 2.44 | 5.40 | 2.92 | 6.75 | 1.45 | 15.77 |
| 19 kips | 3.24 | 0.25 | 1.59 | 3.73 | 2.26 | 3.72 | 2.33 | 5.71 | 0.96 | 8.25 |
| 20 kips | 2.71 | 0.21 | 1.24 | 3.22 | 1.87 | 2.41 | 1.55 | 4.58 | 0.68 | 6.29 |
| 21 kips | 2.03 | 0.18 | 0.93 | 2.63 | 1.34 | 1.50 | 1.29 | 3.51 | 0.51 | 2.44 |
| 22 kips | 1.52 | 0.15 | 0.65 | 2.01 | 0.89 | 0.88 | 1.07 | 2.51 | 0.46 | 2.46 |
| 23 kips | 1.16 | 0.12 | 0.51 | 1.59 | 0.62 | 0.50 | 0.66 | 1.78 | 0.35 | 1.50 |
| 24 kips | 0.82 | 0.10 | 0.38 | 1.30 | 0.45 | 0.27 | 0.43 | 1.23 | 0.26 | 0.60 |
| 25 kips | 0.58 | 0.09 | 0.27 | 1.04 | 0.37 | 0.15 | 0.31 | 0.85 | 0.23 | 0.37 |
| 26 kips | 0.34 | 0.08 | 0.17 | 0.85 | 0.33 | 0.08 | 0.20 | 0.59 | 0.17 | 0.21 |
| 27 kips | 0.25 | 0.07 | 0.14 | 0.57 | 0.28 | 0.04 | 0.16 | 0.44 | 0.14 | 0.15 |
| 28 kips | 0.19 | 0.07 | 0.10 | 0.38 | 0.26 | 0.03 | 0.13 | 0.34 | 0.18 | 0.14 |
| 29 kips | 0.17 | 0.07 | 0.09 | 0.31 | 0.24 | 0.02 | 0.11 | 0.22 | 0.13 | 0.18 |
| 30 kips | 0.11 | 0.06 | 0.07 | 0.25 | 0.24 | 0.01 | 0.08 | 0.19 | 0.12 | 0.26 |
| 31 kips | 0.10 | 0.05 | 0.05 | 0.19 | 0.24 | 0.01 | 0.12 | 0.12 | 0.15 | 0.42 |
| 32 kips | 0.08 | 0.05 | 0.05 | 0.13 | 0.23 | 0.01 | 0.10 | 0.11 | 0.13 | 0.49 |
| 33 kips | 0.08 | 0.05 | 0.03 | 0.15 | 0.21 | 0.01 | 0.04 | 0.09 | 0.16 | 0.63 |
| 34 kips | 0.07 | 0.05 | 0.04 | 0.12 | 0.21 | 0.00 | 0.05 | 0.07 | 0.16 | 0.61 |
| 35 kips | 0.06 | 0.04 | 0.03 | 0.17 | 0.21 | 0.00 | 0.03 | 0.07 | 0.13 | 0.56 |
| 36 kips | 0.06 | 0.04 | 0.02 | 0.11 | 0.19 | 0.00 | 0.07 | 0.07 | 0.19 | 0.49 |
| 37 kips | 0.05 | 0.04 | 0.03 | 0.11 | 0.16 | 0.00 | 0.03 | 0.08 | 0.16 | 0.35 |
| 38 kips | 0.07 | 0.04 | 0.02 | 0.10 | 0.15 | 0.00 | 0.05 | 0.07 | 0.11 | 0.24 |
| 39 kips | 0.03 | 0.03 | 0.02 | 0.12 | 0.13 | 0.00 | 0.05 | 0.07 | 0.11 | 0.14 |
| 40 kips | 0.05 | 0.03 | 0.02 | 0.15 | 0.11 | 0.00 | 0.06 | 0.09 | 0.12 | 0.09 |
| 41 kips | 0.51 | 0.22 | 0.22 | 1.16 | 0.56 | 0.02 | 0.40 | 0.58 | 0.42 | 0.22 |

**Average Axle Weight (kip) and Average Axle Spacing (feet)**

| Class | 4 | 5 | 6 | 7 | 8 | 9 | 10 | 11 | 12 | 13 |
|---|---|---|---|---|---|---|---|---|---|---|
| W1 | 11.86 | 4.90 | 12.50 | 14.61 | 9.16 | 11.96 | 12.16 | 11.46 | 12.17 | 18.32 |
| W2 | 12.92 | 4.29 | 8.40 | 11.17 | 10.81 | 12.29 | 11.40 | 16.63 | 10.18 | 17.59 |
| W3 | 10.63 | 0.00 | 7.82 | 13.10 | 8.29 | 11.75 | 11.29 | 16.02 | 9.81 | 19.99 |
| W4 | 0.00 | 0.00 | 0.00 | 13.77 | 7.8 | 11.68 | 7.58 | 13.28 | 12.46 | 17.69 |
| W5 | 0.00 | 0.00 | 0.00 | 1.37 | 0.00 | 11.39 | 9.73 | 13.20 | 12.39 | 17.66 |
| W6 | 0.00 | 0.00 | 0.00 | 10.46 | 0.00 | 0.00 | 9.41 | 0.00 | 11.36 | 18.48 |
| W7 | 0.00 | 0.00 | 0.00 | 10.83 | 0.00 | 0.00 | 6.25 | 0.00 | 0.00 | 17.89 |
| W8 | 0.00 | 0.00 | 0.00 | 0.00 | 0.00 | 0.00 | 8.77 | 0.00 | 0.00 | 17.20 |
| W9 | 0.00 | 0.00 | 0.00 | 0.00 | 0.00 | 0.00 | 0.00 | 0.00 | 0.00 | 17.17 |
| W10 | 0.00 | 0.00 | 0.00 | 0.00 | 0.00 | 0.00 | 0.00 | 0.00 | 0.00 | 16.97 |
| W11 | 0.00 | 0.00 | 0.00 | 0.00 | 0.00 | 0.00 | 0.00 | 0.00 | 0.00 | 16.49 |
| W12 | 0.00 | 0.00 | 0.00 | 0.00 | 0.00 | 0.00 | 0.00 | 0.00 | 0.00 | 15.87 |
| S1-2 | 22.68 | 12.57 | 16.83 | 11.45 | 14.53 | 16.69 | 16.45 | 12.95 | 15.48 | 3.31 |
| S2-3 | 4.45 | 0.00 | 4.34 | 9.35 | 19.49 | 4.58 | 4.59 | 21.09 | 4.51 | 3.25 |
| S3-4 | 0.00 | 0.00 | 0.00 | 4.29 | 11.08 | 32.99 | 23.48 | 9.35 | 19.80 | 3.50 |
| S4-5 | 0.00 | 0.00 | 0.00 | 4.33 | 0.00 | 4.70 | 8.47 | 20.97 | 9.11 | 3.28 |
| S5-6 | 0.00 | 0.00 | 0.00 | 4.07 | 0.00 | 0.00 | 4.31 | 0.00 | 21.12 | 3.32 |
| S6-7 | 0.00 | 0.00 | 0.00 | 0.00 | 0.00 | 0.00 | 4.80 | 0.00 | 0.00 | 3.34 |
| S7-8 | 0.00 | 0.00 | 0.00 | 0.00 | 0.00 | 0.00 | 4.41 | 0.00 | 0.00 | 3.27 |
| S8-9 | 0.00 | 0.00 | 0.00 | 0.00 | 0.00 | 0.00 | 0.00 | 0.00 | 0.00 | 3.20 |
| S9-10 | 0.00 | 0.00 | 0.00 | 0.00 | 0.00 | 0.00 | 0.00 | 0.00 | 0.00 | 3.18 |
| S10-11 | 0.00 | 0.00 | 0.00 | 0.00 | 0.00 | 0.00 | 0.00 | 0.00 | 0.00 | 3.12 |
| S11-12 | 0.00 | 0.00 | 0.00 | 0.00 | 0.00 | 0.00 | 0.00 | 0.00 | 0.00 | 3.04 |

**Average Axle Spacing (feet) and Average Number of Axle Types**

| Class | 4 | 5 | 6 | 7 | 8 | 9 | 10 | 11 | 12 | 13 |
|---|---|---|---|---|---|---|---|---|---|---|
| S1-2 | 22.68 | 12.57 | 16.83 | 11.45 | 14.53 | 16.69 | 16.45 | 12.95 | 15.48 | 3.31 |
| S2-3 | 0.84 | 0.00 | 4.34 | 9.35 | 19.49 | 4.58 | 4.59 | 21.09 | 4.51 | 3.25 |
| S3-4 | 0.00 | 0.00 | 0.00 | 4.28 | 9.32 | 32.99 | 23.48 | 9.35 | 19.80 | 3.50 |
| S4-5 | 0.00 | 0.00 | 0.00 | 0.57 | 0.00 | 4.70 | 8.47 | 20.97 | 9.11 | 3.28 |
| S5-6 | 0.00 | 0.00 | 0.00 | 0.06 | 0.00 | 0.00 | 4.31 | 0.00 | 21.12 | 3.32 |
| S6-7 | 0.00 | 0.00 | 0.00 | 0.00 | 0.00 | 0.00 | 0.12 | 0.00 | 0.00 | 3.34 |
| S7-8 | 0.00 | 0.00 | 0.00 | 0.00 | 0.00 | 0.00 | 0.04 | 0.00 | 0.00 | 3.22 |
| S8-9 | 0.00 | 0.00 | 0.00 | 0.00 | 0.00 | 0.00 | 0.00 | 0.00 | 0.00 | 3.07 |
| S9-10 | 0.00 | 0.00 | 0.00 | 0.00 | 0.00 | 0.00 | 0.00 | 0.00 | 0.00 | 2.83 |
| S10-11 | 0.00 | 0.00 | 0.00 | 0.00 | 0.00 | 0.00 | 0.00 | 0.00 | 0.00 | 2.23 |
| S11-12 | 0.00 | 0.00 | 0.00 | 0.00 | 0.00 | 0.00 | 0.00 | 0.00 | 0.00 | 1.10 |
| Single | 1.81 | 2.00 | 1.00 | 1.22 | 2.14 | 1.19 | 1.47 | 4.75 | 3.79 | 0.26 |
| Tandem | 0.37 | 0.00 | 2.00 | 1.66 | 1.69 | 3.80 | 2.82 | 0.09 | 1.99 | 1.25 |
| Tridem | 0.00 | 0.00 | 0.00 | 1.27 | 0.01 | 0.01 | 1.74 | 0.16 | 0.21 | 9.41 |
| Quad | 0.00 | 0.00 | 0.00 | 0.00 | 0.00 | 0.00 | 0.00 | 0.00 | 0.00 | 0.00 |
| Quinate | 0.00 | 0.00 | 0.00 | 0.00 | 0.00 | 0.00 | 0.00 | 0.00 | 0.00 | 0.00 |
| Hexad | 0.00 | 0.00 | 0.00 | 0.00 | 0.00 | 0.00 | 0.01 | 0.00 | 0.00 | 0.00 |

## About the Joint Transportation Research Program (JTRP)

On March 11, 1937, the Indiana Legislature passed an act which authorized the Indiana State Highway Commission to cooperate with and assist Purdue University in developing the best methods of improving and maintaining the highways of the state and the respective counties thereof. That collaborative effort was called the Joint Highway Research Project (JHRP). In 1997 the collaborative venture was renamed as the Joint Transportation Research Program (JTRP) to reflect the state and national efforts to integrate the management and operation of various transportation modes.

The first studies of JHRP were concerned with Test Road No. 1—evaluation of the weathering characteristics of stabilized materials. After World War II, the JHRP program grew substantially and was regularly producing technical reports. Over 1,600 technical reports are now available, published as part of the JHRP and subsequently JTRP collaborative venture between Purdue University and what is now the Indiana Department of Transportation.

Free online access to all reports is provided through a unique collaboration between JTRP and Purdue Libraries. These are available at http://docs.lib.purdue.edu/jtrp.

Further information about JTRP and its current research program is available at http://www.purdue.edu/jtrp.

## About This Report

An open access version of this publication is available online. See the URL in the citation below.

Bao, J., Hu, X., Peng, C., Jiang, Y., Li, S., & Nantung, T. (2020). *Truck traffic and load spectra of Indiana roadways for the mechanistic-empirical pavement design guide* (Joint Transportation Research Program Publication No. FHWA/IN/JTRP-2020/21). West Lafayette, IN: Purdue University. https://doi.org/10.5703/1288284317227